SSEN Annual Postgraduate Research Symposium 2024

Saif, Alasoul; Nwigwe, Johnpaul; Miller, Jonathan; Din, Amin; Samuel, Oluwafemi; Jovanovic, Filip

DOI:
10.20933/100001314

Publication date:
2024

Document Version
Publisher's PDF, also known as Version of record

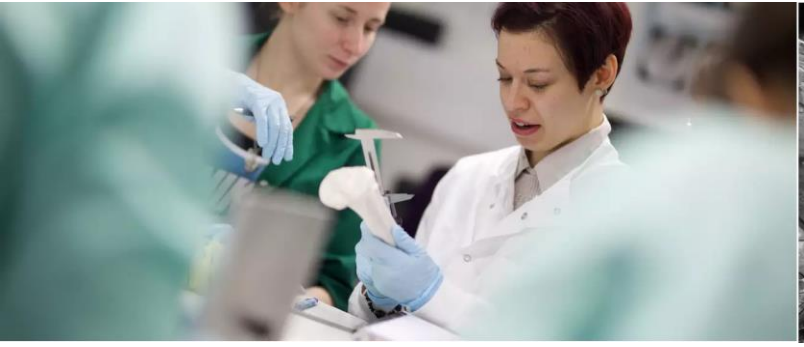
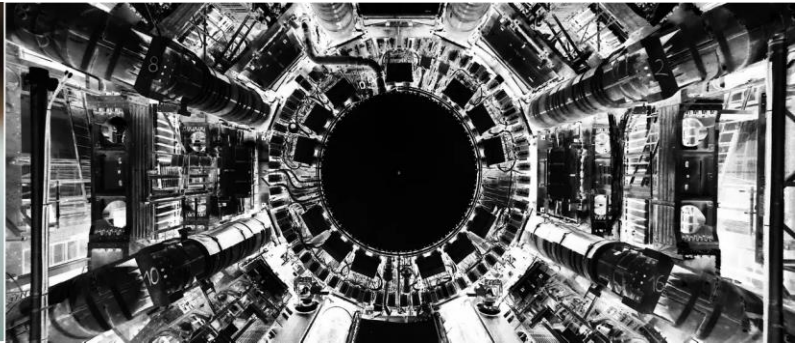

University of Dundee

SCHOOL OF SCIENCE AND ENGINEERING

Annual Postgraduate Research Symposium 2024

21-22 May 2024




SSEN Postgraduate Research Symposium 2024 – Final Programme

Tuesday 21st May 2024

Time	Presenter	Title
09:00 – 09:15	**Registration and coffee** (Dalhousie Foyer)	
09:15 – 09:30	**Welcome & Introductions (Fordyce Davidson, Alan Cuthbertson)**	
09:30 – 10:15	**Michael Macdonald**	**Keynote Lecture:** Laser worms and their adventures in the rhizosphere: Plant Root Environment Microscopy
Session 1	Chair: Vladimir Janjic (Dalhousie Lecture Theatre 2)	
10:25 – 10:45	**Alasoul Saif** *(LRCFS)*	*Drug characterization & impurity mapping using R*
10:45 – 11:05	**Johnpaul Nwigwe** *(Computing)*	*Enhancing Packet Switching: Traffic Prediction & Congestion Control Performance Evaluation with Feed Forward Neural Network & Recurrent Neural Network*
11:05 – 11:25	**Jonathan Miller** *(Mathematics)*	*Space & time on the membrane & in the population: modelling T6SS dynamics at multiple scales*
11:25 – 11:40	**Coffee break** (Dalhousie Foyer)	
Session 2	Chair: Tom Jones (Dalhousie Lecture Theatre 2)	
11:40 – 12:00	**Amin Din** *(Mechanical Engineering)*	*Modelling Electron Response on Laser Engineered Surface Structures*
12:00 – 12:20	**Oluwafemi Samuel** *(Computing)*	*Fingerprint Recognition: How Far from Perfection?*
12:20 – 12:40	**Filip Jovanovic** *(Civil Engineering)*	*Optimisation of average quantities in a forced Lorenz system: Influence of periodic orbits*
12:40 – 13:00	**Poster presentations 1**	11 posters (2 mins per poster – see list)
13:00 – 14:15	**Lunch, poster viewings and group photograph** (Dalhousie Foyer)	
Session 3	Chairs: Julieta Gomez Garcia-Donas & Corrina Wilson (Dalhousie Lecture Theatre 2)	
14:15 – 14:35	**Ruhee Kahar** *(Physics)*	*What Time Can Tell Us About Space: Mapping Accretion in Intermediate Mass YSOs*
14:35 – 14:55	**Han Li** *(Biomedical Engineering)*	*Enhancing Transcranial Focused Ultrasound: Performance Analysis Based on Reconstructed CT -Derived Skull Acoustical Properties*
14:55 – 15:15	**Poster presentations 2**	10 posters (2 mins per poster – see list)
15:15 – 15:30	**3 Minute Thesis (3MT)**	Amin Din *(Physics)*; Kirstie Gray & Daryna Kostiuchyk *(LRCFS)*
15:30 – 15:45	**Coffee break** (Dalhousie Foyer)	
Session 4	Chairs: Tom Vettenburg & Amin Din (Dalhousie Lecture Theatre 2)	
15:45 – 16:05	**Nader Alharbi** *(Mathematics)*	*The Effectiveness of Blended Learning in Mathematics using the Madrasati Platform: Secondary School Teachers' Perceptions in Saudi Arabia*
16:05 – 16:25	**Thomas Riccio** *(Civil Engineering)*	*Seeing through the rock – insights on geotechnical behaviour via XCT*
16:25 – 16:45	**Yazeed Almalaq** *(Computing)*	*Energy and Performance Optimisation for Embedded Systems*
1645	**Concluding remarks (Day 1) (Alan Cuthbertson)**	

Wednesday 22nd May 2024

Time	Presenter	Title
09:15 – 09:20	**Welcome Day 2 (Alan Cuthbertson)**	
09:20 – 09:35	**Tom Curtin (LLC)**	*Introduction to the Discovery Research Portal*
09:35 – 09:50	**Jillian Findlay (RIS)**	*Trusted Research*
Session 5	Chair: Dumitru Trucu & Daniel Norman (Dalhousie Lecture Theatre 2)	
09:50 – 10:10	**Jinpeng Liao** *(Biomedical Engineering)*	*A Deep-Learning Method for Single-Scan Optical Coherence Tomography Angiography Generation*
10:10 – 10:30	**Kayode Oyinola** *(LRCFS)*	*Electrochemical detection and profiling of 3,4-methylenedioxypyrovalerone on screen-printed carbon electrodes using nanostructured functionalized quantum dots*
10:30 – 10:50	**Olusegun Adebayo** *(Mathematics)*	*Modeling and Analysis of Non-local Interactions in Wound Healing: Numerical Simulations, Analytical Investigations, and Machine-Learning Approaches*
10:50 – 11:10	**Sarah Higgins** *(Mechanical Engineering)*	*A Selective Coating Deposition Technique for Gas Turbine Components*
11:10 – 11:25	**Coffee break** (Dalhousie Foyer)	
Session 6	Chair: Jonathan Knappett (Dalhousie Lecture Theatre 2)	
11:25 – 11:45	**Struan Robertson** *(LRCFS)*	*Retrieving shoeprint images using convolutional neural networks*
11:45 – 12:05	**Hussam Namanqani** *(Civil Engineering)*	*Understanding communication practices amongst practitioners on mega projects in Saudi Arabia*
12:05 – 12:25	**Yimeng Wang** *(Mechanical Engineering)*	*Novel hybrid antibacterial surfaces for medical implants*
12:25 – 12:45	**Daniel Norman** *(Mathematics)*	*Operator Learning for Solar Physics*
12:45 – 13:45	**Lunch and poster viewing** (Dalhousie Foyer)	
Session 7	Chair: Alan Cuthbertson (Dalhousie Lecture Theatre 2)	
13:45 – 14:05	**Eszter Somjai** *(CAHID)*	*A validation study of newly established ear morphology prediction guidelines in facial approximation*
14:05 – 14:25	**Zhenyi Zhao** *(Computing)*	*Optic disk segmentation based on a retinal foundation model*
14:25 – 14:45	**Zhihao Tao** *(Mathematics)*	*A non-local spatio-temporal cancer invasion process with cross-diffusion and cross-adhesion*
14:45 – 15:05	**Euan Mackay** *(Physics/Life Sciences)*	*Modelling of Actomyosin Dynamics as an Active Elastomer*
15:05 – 15:20	**Coffee break** (Dalhousie Foyer)	
Session 8	Chair: Herve Menard (Dalhousie Lecture Theatre 2)	
15:20 – 15:40	**Nicole Orr** *(Computing)*	*Protocol Switching in Argumentative Dialogue*
15:40 – 16:00	**Yunpeng Zhao** *(Physics)*	*Planet Formation in Wind-Driven Accretion Discs via Pebble Accretion*
16:00 – 16:20	**Martin Sanner** *(Mathematics)*	*An explainable model for solar active regions*
16:20	**Concluding remarks and close (Day 2) (Alan Cuthbertson)**	
16:30 onwards	**Optional visit to Dukes Bar**	

Poster Presentations 1: 12:40 – 13:00, Tuesday 21st May 2024

Presenter	Title
Alzahra Altalib *(Biomedical Engineering)*	*Synthetic high-quality Computed Tomography (CT) Image generation from low-quality Cone-Beam CT*
Amirhossein Pourali *(Biomedical Engineering)*	*Photoacoustic imaging with endogenous contrast (biomarkers)*
Danial Kordbacheh *(Biomedical Engineering)*	*Sonodynamic Therapy for glioblastoma*
Jasmine Usher *(Biomedical Engineering)*	*Assessing and quantifying the relationship between spasticity, proprioception, and movement post-stroke*
Saeed Charbenny *(Biomedical Engineering)*	*Skull Exposure to Various Ultrasound Wave Propagation*
Thomas Zhang *(Biomedical Engineering)*	*Oral Soft Tissue Angiography Imaging Using a Hand-held Intraoral Probe*
Zhengshuyi Feng *(Biomedical Engineering)*	*Multi-Functional Imaging Optical Coherence Tomography (OCT) for Monitoring Acne Development in Human Facial Skin In-Vivo*
Nick Deane *(Biomedical Engineering)*	*Novel sensor development for an improved muscle movement detection and classification*
Shirooza Mubarak *(Life Sciences)*	*Building and optimizing light-sheet microscope to analyse the coordination and control of critical cell behaviours driving gastrulation in the chick embryo*
Yuhang Dong *(Mechanical Engineering)*	*Antimicrobial ZnO nanoparticle embedded Polyethersulfone synthesis using green chemistry*
Ferdinand Hollauf *(Physics)*	*North PHASE observations of the young cluster Tr37*

Poster Presentations 2: 15:00 – 15:20, Tuesday 21st May 2024

Presenter	Title
Anderson You *(Computing)*	*How can subtitled media be adapted for People with Aphasia?*
Nawaf Alajlani *(Computing)*	*Investigating the degree of inclusion of educators in the development of Adaptive Learning system*
Corrina Wilson *(CAHID)*	*A brief investigation into the relationships of macroscopic and microscopic bone traits in the elderly clavicle*
Kelly Watson *(CAHID)*	*Intracortical porosity in the clavicle of an elderly Scottish sample: exploring sampling areas within the cross-section*
Kirstie Gray *(LRCFS)*	*Electropolymerized InZnSe@PtAg quantum dots@molecularly imprinted polymer on screen-printed carbon electrodes for the ultrasensitive detection of NS1 dengue virus protein with smartphone-based sensing in saliva*
Steven Baginski *(LRCFS)*	*The Metabolic Profile of the Synthetic Cannabinoid Receptor Agonist ADB-HEXINACA using Human Hepatocytes, LC-QTOF-MS and Synthesized Reference Standards*
Liqun Fang *(Civil Engineering)*	*Experimental study on the effects of installation parameters on vibratory driving performance of monopiles*
Yi Yuan *(Civil Engineering)*	*Fluid-Solid Flow Transition in Mixed (Sand-Mud) Sediment: Enhanced Modelling of Sedimentation in Estuarine and Coastal Waters*
Wadhhah Aldehani *(Medicine)*	*Feasibility of Polyvinyl Chloride's as a breast ultrasound phantom*
Muteb Alrashdi *(Medicine)*	*Advancing Prostate Cancer Treatment: The Role of Focused Ultrasound and Sonodynamic Therapy*

University of Dundee

Oral Presentations

(In order of Sessions)

University of Dundee

Drug characterization and impurity mapping using R.

Alasoul Saif[1], Herve Menard[2], Lorna Nisbet[3]

[1] Leverhulme Research Centre for Forensic Science, 2606048@dundee.ac.uk
[2] Leverhulme Research Centre for Forensic Science, h.menard@dundee.ac.uk
[3] Leverhulme Research Centre for Forensic Science, lnisbet001@dundee.ac.uk

Abstract

Background & Aims:

Illicit drug markets continue to experience significant growth, and while there is a continuous need to determine the main pharmacologically active substances, the detection and characterisation of minor compounds is starting to receive significant interest for providing strategic, tactical, and public health intelligence. Limited research has been conducted to examine the presence of inactive compounds or other substances in illicit drug samples. These chemicals, known as adulterants or cutting agents, can be impurities. As they are typically present in small concentrations, their observation in analytical results a challenge and requires significant manual effort. The aim of this work is to directly analyse gas chromatography -mass spectrometry (GC-MS) data to systematically detect and assign minority substances in all processed samples using an R script to speed up analysis.

Methods:

Samples included in this study were part of an ongoing non-judicial seizures drug monitoring project. These samples were analysed by GC-MS in full scan mode, and the output data were converted in a format suitable for long term preservation. The data are processed in R to (i) detect the presence of minor peaks and (ii) compare them to already known substances present in a self-built reference library. The R script compares mass spectra between the peaks of interest and the ones available in the library using vectors and indexing similarity.

Results & Discussion:

107 samples were analysed by GC-MS. With the developed R code set to extract peaks that are three times the signal-to-noise ratio of the baseline, using the total ion chromatogram, a total of 3,825 peaks of interest were detected throughout the entire series. Among these, 119 peaks were identified as distinct. The analysis of the data revealed that all 119 peaks can be accounted for by examining 27 samples out of 107, and that a mere 10 of these samples were sufficient to cover 102 of the identified peaks.

Peak assignment was carried out by comparing peaks between samples using the MS data. The comparison and matching of each detected peak were done by the measure of similarity (and the use of angular vectors) from which a matching factor is returned, with 0 being an opposite match and 1 being a perfect match to the reference peak. Additional analysis can be carried out using the matching factors and the individual peak retention time to establish groups and relationships between samples, and thus facilitating the identification of compounds.

Conclusion:

The research demonstrates the feasibility of developing a facile method to systematically detect chemicals present in a large series of samples. With careful consideration, a list of peaks of interest present in one or more samples can be established by using a targeted number of samples. Such an approach is of great interest for facilitating and expediting data analysis, as well as determining commonalities between samples. The outcomes of this approach could significantly enhance forensic intelligence in drug profiling for investigation and operational work, providing additional information to aid in establishing possible relationships between batches of seized drugs.

Enhancing Packet Switching: Traffic prediction and Congestion Control Performance Evaluation with Feed Forward Neural Network and Recurrent Neural Network

Johnpaul Nwigwe [1], Iain Martin [2], Craig Ramsay [3]

[1] School of Science and Engineering (Computing), jnwigwe@dundee.ac.uk
[2] School of Science and Engineering (Computing), I.martin@dundee.ac.uk
[3] School of Science and Engineering (Computing), c.d.ramsay@dundee.ac.uk

Abstract

Internet network traffic is on the rise due to the proliferation of smart technology applications, such as smart cars, smart houses, smart mobile devices. Network traffic prediction and congestion analyses is important for optimum utilization of the network resource and maximizing throughput. However, numerous classical and machine learning algorithms have been proposed to solve this problem but not without limitations. Network prediction and congestion control is a process of capturing and analysing network characteristics with the aim of optimizing resource allocation. In this study, we introduce a new network traffic prediction and congestion control algorithm using a feed forward neural network (FFNN) with a multi-channel routing control system (MCRCCS) to predict network traffic and control congestion. The significance of the study is to improve on the limitations of previous work which uses an FFNN with an active queue management - algorithms (FFNN-AQM) and then evaluate the performance against other recent work using a recurrent neural network (LSTM_RNN). The experiment was run using Python discrete simulation techniques with two distinct datasets. The simulation results showed that our proposed feedforward multi-channel routing congestion control model outperformed both the previously published results using active queue management and a network traffic prediction model using the long-short term memory of a recurrent neural network. with a mean square error of 0.0935, mean absolute error of 0.0625 and relative error of 18%. Also, the self- similarity behaviour of our model shows good quality of service (QoS) and promises better quality of experience (QoE) for end-users.

Model Congestion Prediction and Congestion Control Mechanism.

The neural network is designed to generate and transmit signals from the channel with minimum congest threshold to the micro-controller for transmission of packet to the destination. The channel with the smallest congestion threshold is the control parameter that determines the firing of the neuron and if the input signal exceeds the minimum threshold, the neural network will update its weight to select the next channel with the minimum congestion threshold as an alternative route using a recursively square method. Fig 1 illustrates the traffic prediction and congestion control mechanism of our proposed model.

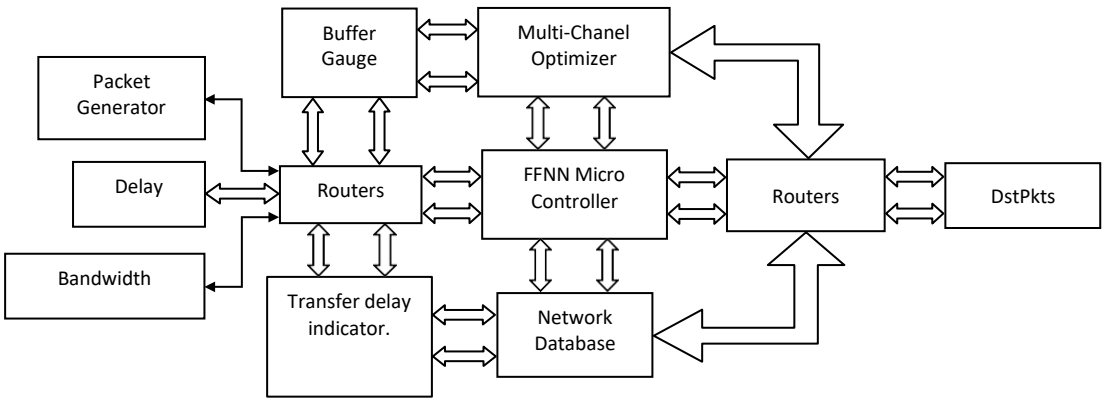

Fig 1 Model schematic diagram

University of Dundee

Space and time on the membrane and in the population: modelling T6SS dynamics at multiple scales

Jonathan Miller[1], Philip Murray, Fordyce Davidson[3]

[1] School of Science and Engineering (Mathematics), jpmiller@dundee.ac.uk
[2] p.murray@dundee.ac.uk
[3] f.a.davidson@dundee.ac.uk

Abstract

Bacterial competition plays a pivotal role in species dominance and pathogenicity. Species exploit diverse sets of tools to ensure an advantage is gained. The gram-negative facultative anaerobe Serratia Marcescens is an adaptive and highly effective bacteria capable of establishing competitive niches and causing a multitude of hospital acquired infections, commonly regarded as multidrug resistant [2]. A key tool used is the Type IV Secretion System (T6SS), a dynamic transmembrane molecular machine found in many other gram-negative bacterial species.

The T6SS can be delineated at three structures, membrane complex, baseplate, and tube/sheath complex. It undergoes a dynamic and repeated assembly and disassembly process. Beginning at the outer membrane and nucleating inwards, the T6SS erects a structure to house a firing spike tipped with toxin proteins for specialised attacks. Prior to assembly, the membrane complex reorientates about the cell surface, once assembly has commenced, the baseplate connects to the membrane complex, fixing position and becoming the basal complex. The tube/sheath complex is then constructed surrounding the spike and at completion contracts rapidly, the spike is expelled out of the cell. Target cells hit by the T6SS react often in cell death and friendly fire is negated through immunity. Disassembly returns the membrane complex to a reorientation state until assembly and the firing process is repeated. Varied behavioural modes, such as being responsive and aggressive in cell-to-cell interactions have been observed, S. marcescens wields an aggressive T6SS [2].

The core component proteins of the T6SS are relatively conserved across species with greater variability occurring in regulation facilities operating the firing process [3]. Whilst the primary functionality is well established, how the firing process dynamics on the single cell scale affects population dynamics is less so. Observations detail that perturbations in the T6SS regulation network governing the firing kinetics such as reduced reorientation leads to a reduction in its competitive edges and an overproduction of various proteins leads to an increase in firing rates and so an increase in competitive edges [2]. The observed perturbation effects raise questions about T6SS dynamics. How exactly do the firing kinetics and spatial reorientation dynamics drive intracellular characteristics and what if any effect does this have on population behaviour and competitive capabilities.

In this study I develop a mathematical model to simulate the firing kinetics, spatial reorientation, and the number of machines at the single cell level to explore T6SS behaviours. I employ Markov processes and state-dependent random walks to represent the T6SS states as assembly, attack, and disassembly, with spatial reorientation. I then incorporate these single cell models into multi-cell-agent-based mechanistic population models for the analysis and prediction of long-term effects. I show that through variations in parameter space single-cell T6SS behaviours characterise spatiotemporal description, namely how fast or slow a machine can attack and kill a target cell. Further I show that where some topological assumptions are made, targeted population will have a critical population size needed for survival to occur. Finally, I derive theoretical estimates to validate and contrast with synthetics data generation. The study concludes that T6SS intracellular behaviour is indicative of intercellular population survival in specific topological assumptions.

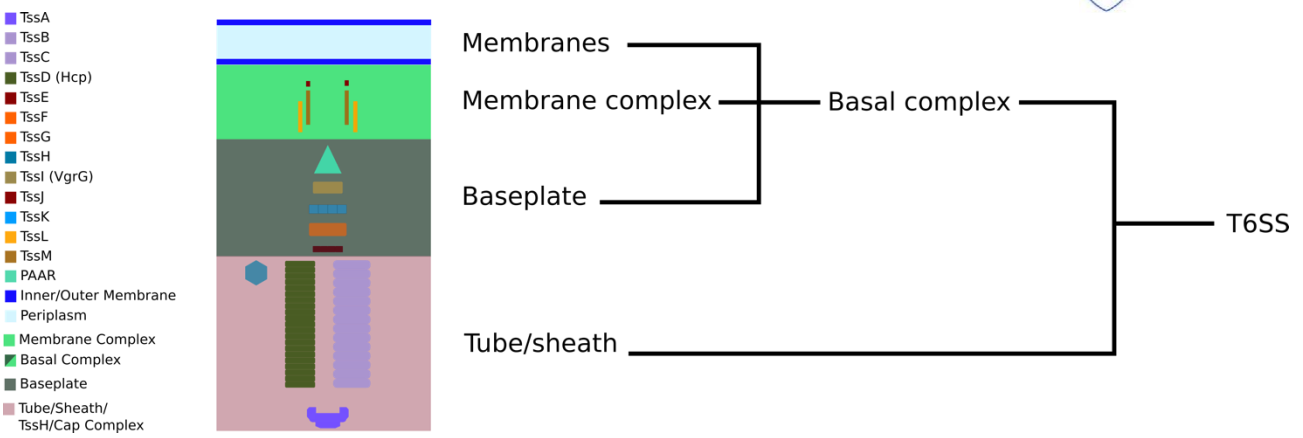

Figure 1: Core protein components of the T6SS with heirarchical references to complexes. The T6SS core proteins form the make the membrane complex, the baseplate (together with the membrane complex these two items form the basal complx) and the tupe/sheath complex all form the T6SS.

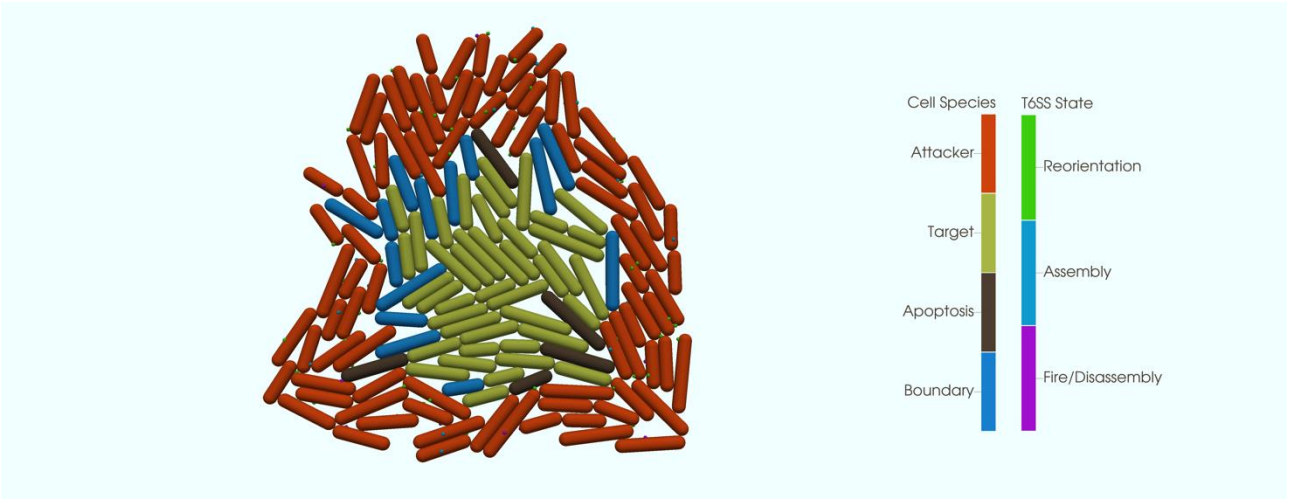

Figure 2: Simulated population of rod-shaped bacteria. Two populations are present. The attacking population (red) carry T6SS machines are invading the targets whom they surround. Targets (yellow, blue – on boundary between attackers, and brown – undergoing cell death) are surrdounded. This simulation explores the ability of the targets to survive given parameters of both the populations and the T6SS parmaters.

References

[1] Tavares-Carreon F, De Anda-Mora K, Rojas-Barrera IC, Andrade A. *Serratia marcescens* antibiotic resistance mechanisms of an opportunistic pathogen: a literature review. PeerJ. 2023 Jan 5;11:e14399. doi: 10.7717/peerj.14399. PMID: 36627920; PMCID: PMC9826615.

[2] Ostrowski A, Cianfanelli FR, Porter M, Mariano G, Peltier J, et al. (2018) Killing with proficiency: Integrated post-translational regulation of an offensive Type VI secretion system. PLOS Pathogens 14(7): e1007230. https://doi.org/10.1371/journal.ppat.1007230

[3] Zoued, A., Brunet, Y. R., Durand, E., Aschtgen, M.-S., Logger, L., Douzi, B., Journet, L., Cambillau, C., & Cascales, E. (2014). Architecture and assembly of the Type VI secretion system. Biochimica et Biophysica Acta (BBA) - Molecular Cell Research, 1843(8), 1664-1673. https://doi.org/10.1016/j.bbamcr.2014.03.018

University of Dundee

Modelling Electron Response on Laser Engineered Surface Structures

Amin Din[1], Amin Abdolvand[2], Svetlana Zolotovskaya[3]

[1] School of Science and Engineering, a.din@dundee.ac.uk
[2] a.abdolvand@dundee.ac.uk

Abstract

Surfaces, when bombarded by electrons exhibit secondary electron emission (SEE). Whereby incident electrons liberate atomically bound electrons. This process is quantified by scientists through the measurement of the secondary electron yield (SEY), which describes the ratio of emitted electrons to those incident on the material. The implications of SEE are particularly significant in the context of particle accelerators, namely the large hadron collider, where electrons can arise in the vacuum chambers triggering SEE. The presence of secondary electrons directly impacts the performance of the LHC, even today. Consequently, research has been devoted to reducing the SEY of materials used in the LHC. Dundee has pioneered laser engineered surface structures which has been demonstrated to reduce the SEY of metals used in the LHC [1]. The resulting complex surfaces exhibit multi-scale geometrical features, often with altered chemical compositions [2], depicted in Figure 1, left. At present, this solution is highly experimental which requires both time and recourses. To address this, we derive a model capable of reproducing these complex laser-produced surfaces to support the design of low SEY reducing surfaces. Through simulation, we subject these geometries to incident electrons and compare the SEY to samples made in the laboratory.

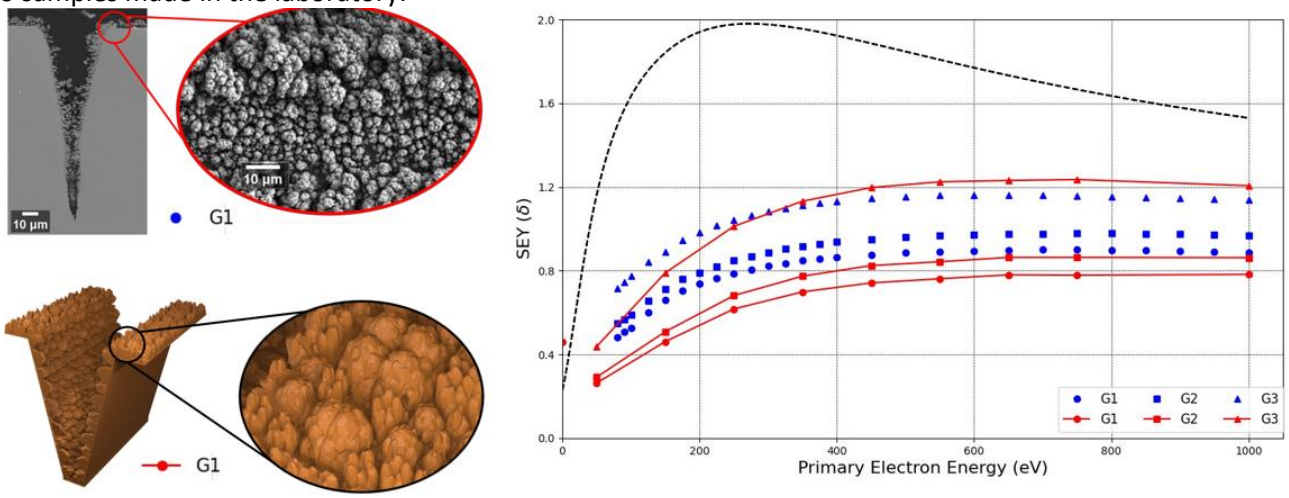

Figure 1: Left presents the surface topography of a laser produced sample measured using scanning electron microscopy. Below is the modelled counterpart. Right plots the measured, blue, and simulated data, red.

Presented in Figure 1, right, are the measured and modelled SEY data, with the model accurately calculating the electron response of surfaces subjected to laser ablation. Insights from this model reveal that the conventional idea of high aspect ratio structures are not required to reduce the SEY. Modelling indicates that laser ablation modifies the surface composition which assists the geometrical features in reducing the SEY. In summary, we present an advanced comprehensive model including multi-scale surface topography and surface chemistry, capturing the SEY response of laser modified surfaces serving as predictive tool for producing low SEY surfaces. This has significant implications, especially at CERN, where in addition to the low SEYs, material removal depth and processing speeds are of paramount importance.

References

[1] Bajek, D., Wackerow, & Abdolvand,… A. (2020). Role of surface microgeometries on electron escape probability and secondary electron yield of metal surfaces. Scientific Reports, 10(1), 1–8.

[2] Calatroni, S., Garcia-Tabares Valdivieso,… & Abdolvand, A. (2020). Optimization of the secondary electron yield of laser-structured copper surfaces at room and cryogenic temperature. Physical Review Accelerators and Beams, 23(3)

Fingerprint Recognition: How Far from Perfection?

Oluwafemi Samuel[1], Iain Martin[2], Ludovic Magerand[3]

[1] School of Science and Engineering (Computing), o.a.samuel@dundee.ac.uk
[2] i.matin@dundee.ac.uk
[3] l.magerand@dundee.ac.uk

Abstract

Biometric recognition has become ubiquitous in practically every society with a variety of applications such as access control, judicious delivery of social benefits, national identification, elections, security and more. The face, fingerprint, voice, DNA, and gait are some of the popular biometrics in use. Of these, the fingerprint is arguably the most widely used, particularly because of the relative stability of its unique characteristics, i.e. the ridge (and valley) patterns as well as minutiae (bifurcations and ridge endings – as shown in Figure 1) and lower cost of implementation. This is not to say that fingerprint recognition is not without its challenges which might vary depending on the area of application and demography of users. The performance of fingerprint recognition algorithms is only as good as the quality of the fingerprint images that they are presented with, albeit the state-of-the-art can achieve an accuracy of over 99%. Various application and user-specific factors can affect the quality of fingerprints, and by implication, their suitability for recognition. Some of these factors are age, ambient conditions, human-biometric-sensor-interaction (HBSI), occupational requirements (e.g. manual work), genetics and medical conditions.

Fingerprint recognition is largely a feature representation and classification problem, a field that is dominatedby deep learning algorithms as is applicable in most comparable fields today. Given that the performance ofthese algorithms could be biased towards the data on which they are trained, it is ideal to test them widely in various operating settings and populations to assess how well they generalise. This research presents oneof such opportunities by using a dataset that replicates the possible scenarios of an African election. The dataset called MASIVE consists of 12403 fingerprint images. In an initial experiment, the NFIQ quality assessment tool was used to analyse the quality of the fingerprints based on most of the factors listed above.Follow-up experiments have also been conducted to assess the extent to which recognition algorithms are able to correctly match each fingerprint to its corresponding mated sample and how this varies with the different factors. In doing so, two algorithms were used: MinutiaeNet + Minutia Cylinder Code (MCC) and VeriFinger. The open source MinutiaeNet + MCC is a baseline and a bit older while VeriFinger is the state-of-the-art, commercial, off-the-shelf tool.

A comparison of the performance of these algorithms (Figure 2) is indicative of the significant improvement that has been achieved in fingerprint recognition within the last few years, even when deployed in operating settings. The experiments also reveal some consistency between the fingerprint image quality assessment and matching rate. For instance, they are both dependent on age and HBSI. In the immediate future, the useof some soft biometrics (comprising of metadata from MASIVE) will be explored to achieve an even better matching performance to help improve the credibility of elections in African countries where fingerprint Verification has been adopted.

Figure 1: Unique features of a fingerprint [1]

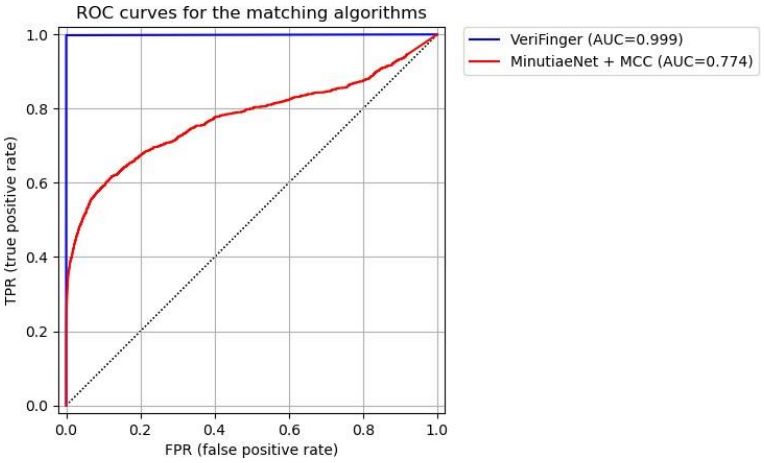

Figure 2: Reciever Opertor Characteristic (ROC) curve indicating the performance of fingerprint matching algorithm – VeriFinger and MinutiaeNet + MCC

References

[1] Ju, Seunghwan & Seo, Hee-Suk. (2011). Password Based User Authentication Methodology Using Multi-Input on Multi-Touch Environment. Journal of the Korea Society for Simulation. 20. 10.9709/JKSS.2011.20.1.039.

Optimisation of Average Quantities in a Forced Lorenz System: Influence of Periodic Orbits

Filip Jovanovic[1] & Dr Tom S. Eaves[2]

[1] School of Science and Engineering, University of Dundee, [1] f.jovanovic@dundee.ac.uk,
[2] teaves001@dundee.ac.uk

Abstract

Surface drag (skin friction) gives rise to significant levels of energy loss throughout a wide range of transport systems. One approach which proved effective in drag reduction was to oscillate the surfaces of the flow transversely to the flow direction, where through simulations and experiment it was demonstrated that this approach can achieve a drag reduction of up to 25% (Quadrio, 2011) at moderate Reynolds numbers. It is clear that this reduction occurs as a result of structural changes within the flow in the near-wall region. However, what specifically happens to the structures and the way in which they evolve throughout the periodic forcing remains unknown.

One approach to understanding how periodic forcing impacts averages of turbulent motion is to focus on how it does so for simple chaotic systems as a preliminary step, such as the Lorenz system of equations (Lorenz, 1963). In this talk, we demonstrate how periodic forcing impacts averages in this system and relate this with structural changes in the Lorenz system's unstable periodic orbits. These orbits are known to act as the only components needed for the computation of averages in the Lorenz system (Eckhardt & Ott, 1994), and this talk will demonstrate to what extent this holds for a periodically forced Lorenz system. Periodic forcing imposes a frequency on the system which is not necessarily commensurate with the frequencies of its periodic orbits, leading to the emergence of invariant tori. Whilst averages may be computed using invariant tori (Parker et al., 2023), they are challenging to compute. Instead, we approximate invariant tori via 'pseudo periodic orbits' (PPOs, see figure 1) which repeat once only in space, and that are embedded within the tori. We investigate the performance of these PPOs in predicting system averages.

Additionally, we go on to explore optimal forcing methods within Lorenz, outlining a methodology with which to analyse a wider range of chaotic systems, with the aim of designing optimised strategies for drag reduction.

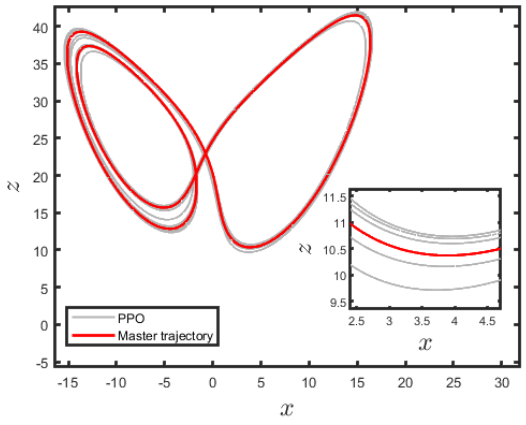

Figure 1: A collection of pseudo periodic orbits (PPOs) embedded within an invariant torus in a periodically forced Lorenz system (grey) along with an averaged 'master trajectory' which approximates this collection of PPOs (red).

References

B. Eckhardt & G. Ott (1994). Periodic orbit analysis of the Lorenz attractor. *Z. Phys*, B 93: 259–266.

E. N. Lorenz (1963). Deterministic nonperiodic flow. *J. Atmos. Sci*. 20: 130–141.

M. Quadrio (2011). Drag reduction in turbulent boundary layers by in-plane wall motion. *Philos.T. R. Soc*, A 369: 1428–1442.

J. P. Parker, O. Ashtari, T. M. Schneider (2023). Predicting chaotic statistics with unstable invariant tori. *Chaos*, 33: 083111.

What Time Can Tell Us About Space: Mapping Accretion in Intermediate Mass YSOs

Ruhee Kahar[1], Aurora Sicilia-Aguilar[2]

[1] SUPA, School of Science and Engineering, University of Dundee, 2475089@dundee.ac.uk
[2] SUPA, School of Science and Engineering, University of Dundee, a.siciliaaguilar@dundee.ac.uk

Abstract

Although substantial effort has been put into understanding the formation of low-mass stars and their planetary system, the knowledge of their intermediate mass counterparts is still lacking. For instance, accretion mechanisms on intermediate mass stars are unknown as their magnetic fields are too weak to sustain magnetospheric accretion.

I will present the primary stages in my study of time variability of accretion-related lines in young intermediate-mass stars, using the novel STAR-MELT code (Campbell-White et al., 2021), combined with long- and short-cadence spectroscopic and photometric data. The STAR-MELT code was developed to facilitate the analysis of time-resolved emission line spectroscopy of young stellar objects and can automatically extract, identify, and fit emission lines.

The 25 targets chosen for study comprise of spectral types B-K, which includes HAeBe stars as well as massive T Tauri stars that will eventually evolve into A or B type. These objects have well-known protoplanetary discs, and evidence of extinction by circumstellar material. The analysis data is newly received from CARMENES as well as being supplemented by archival data, to assist us in distinguishing rotational modulation from accretion rate variations.

Emission and absorption lines with broad and narrow components, including metallic ones, are detected in these stars in a similar way to what is found in their lower-mass counterparts. The STAR-MELT code measures the variability in velocity and relative intensity for different lines and we aim to trace the structure of accretion columns and distinguish between different accretion mechanisms as they evolve over time. Our first results are that we observe rapid changes in the emission lines consistent with some degree of rotational modulation. The profiles are wind-dominated and could be related to non-axisymmetric winds.

We have also found, using TESS data, that in some cases we find periodic modulations, suggesting somewhat stable spots in intermediate mass-stars. The periods are shorter than in T Tauri stars, which is expected since we assume higher mass stars to be faster rotators. We determined whether the accretion is rotationally modulated, which would indicate that the accretion columns are discrete and non-axisymmetric.

By the end of this project, our plan is to have analysed the time-resolved spectroscopy so that the data can be used to explore the 3-D structure of accretion columns and unveil the planet-disc connection and the inner structure of protoplanetary discs.

I will also present a brief overview of some of the first results of the young stellar cluster NGC 2264 from the North-PHASE Legacy Survey. We have been investigating the stellar variability of the young stars distributed within the cluster with an aim to find new YSO, characterise accretion and study inner disk evolution within the cluster.

Reference

Justyn Campbell-White, Aurora Sicilia-Aguilar, Carlo F. Manara, Soko Matsumura, Min Fang, Antonio Frasca, and Veronica Roccatagliata (2021). The STAR-MELT PYTHON package for emission-line analysis of YSOs, *Monthly Notices of the Royal Astronomical Society*, 507(3):3331–3350

Enhancing Transcranial Focused Ultrasound: Performance Analysis Based on Reconstructed CT-Derived Skull Acoustical Properties

Han Li[1], Zhihong Huang[2], Tom Gilbertson[3]

[1] School of Science and Engineering, University of Dundee, hwli@dundee.ac.uk
[2] School of Science and Engineering, University of Dundee, z.y.huang@dundee.ac.uk
[3] School of Medicine, University of Dundee

Abstract

Background and Introduction: Focused ultrasound (FUS) is increasingly recognized for its potential in neuromodulation by targeting specific brain areas with acoustic energy. However, the complex anatomy of the skull introduces significant uncertainties in transmission efficiency and targeting accuracy, thus reducing the efficacy in the in-vivo applications. This study introduces a comprehensive framework using computed tomography (CT) imaging to analyse and reconstruct skull acoustical properties, thereby evaluating the impact on acoustic transmission and enhancing the precision of FUS applications at the sub-MHz frequency domain.
Methods: CT data from 20 skulls were analysed using a proprietary segmentation method developed in-house to reconstruct parameters such as skull thickness, radiodensity ratio, and mass density. Acoustic speeds were measured at 84 distinct locations, facilitating a correlation between skull bulk density and the speed of sound. The skull scattering effect was quantified by evaluating the difference between the radius of curvature between the transducer and the skull. The attenuation inside the skull was calculated based on the skull porosity. These acoustical properties informed a mathematical model emulating continuous wave propagation through three distinct skull layers. And a k-Wave simulations model to calculate the transmission efficiency. Both results were empirically validated through 3D acoustic field mapping experiments.
Results: The reconstruction framework highlighted the contrast between the cortical bone and trabecular bone. The reconstructed images of skull acoustical properties distinguished the variations in porosity and vascular structures within the trabecular bone, critical for understanding ultrasound transmission. The transmission efficiency of the skull region showed an exponential decrease along the increase in frequency. The transmission efficiencies calculated and simulated showed strong concordance with experimental measurements, confirming the model's reliability across frequencies ranging from 100kHz to 1000kHz. Notably, fluctuations in transmission efficiency were attributed to wave interactions influenced by variations in skull thickness and transducer-skull spacing. Our analysis framework effectively identifies optimal FUS transmission locations and appropriate thresholds for transmitted acoustic energy, providing invaluable insights for in vivo neuromodulation research. By leveraging detailed CT-based reconstructions of skull acoustical properties, this study significantly advances the precision of transcranial focused ultrasound for therapeutic neuromodulation, offering a robust methodological framework for future clinical research and application.

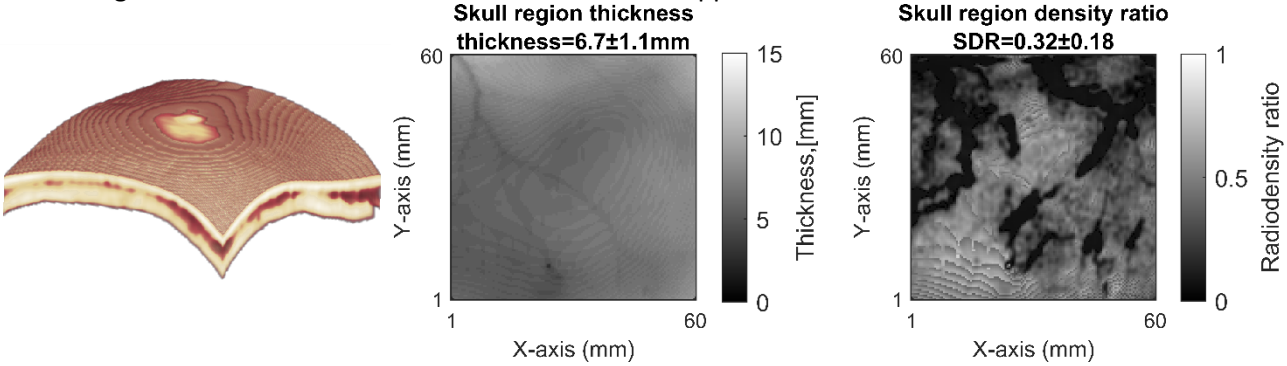

Figure 1: segmented and reconstrcuted skull region and its acoustical propeties analysis.

The Effectiveness of Blended Learning in Mathematics using the Madrasati Platform: Secondary School Teachers' Perceptions in Saudi Arabia

Nader Alharbi[1], Dr John McDermott[2], Prof. Keith Topping[3]

[1] School of Science and Engineering (Mathematics), University of Dundee, nalharbi@dundee.ac.uk
[2] j.z.mcdermott@dundee.ac.uk
[3] k.j.topping@dundee.ac.uk

Abstract

Using technology and integrating digital platforms in education has become increasingly significant, particularly in enhancing blended learning approaches. Madrasati, meaning 'My School,' is an e-learning management system introduced by Saudi Arabia's Ministry of Education (MOE) to support distance learning through electronic educational tools designed to enhance the teaching and learning processes. This study focuses on the effectiveness of the Madrasati platform in facilitating blended learning, specifically for mathematics teachers in secondary schools within the Qassim region of Saudi Arabia. This study uses a mixed-methods research design to analyse mathematics teachers' perceptions, acceptance, and engagement with the Madrasati platform. Through the utilisation of the Analysis of Moment Structures (AMOS) and the Statistical Package for the Social Sciences (SPSS), the research examines teachers' responses based on the Technology Acceptance Model (TAM). The Technology Acceptance Model (TAM) was employed to analyse the data and test hypotheses related to perceived usefulness (PU), perceived ease of use (PEU), and mathematics information quality (IQ) regarding the Madrasati platform.

A comprehensive survey was conducted among 204 mathematics teachers in Qassim City to explore the perceived usefulness, ease of use, and quality of mathematics information provided by the Madrasati platform. The results revealed a significant positive relationship between the quality of mathematics content in the platform and perceived ease of use, suggesting that high-quality content enhances its ease of use among teachers and students. However, the quality of content did not significantly influence teachers' perceptions of its usefulness. Perceived ease of use was positively related to perceived usefulness but not to behavioural intentions to use the platform for teaching, indicating that while ease of use contributes to recognising the platform's utility, it does not directly influence teachers' intentions to adopt it.

Semi-structured interviews with twelve teachers further revealed a preference for traditional classroom teaching, with the Madrasati platform augmenting this primary mode of instruction. Teachers highlighted the platform's role in enhancing teacher-student communication, providing unconventional learning materials, and ensuring continuity of learning regardless of students' physical attendance. However, the teachers also identified barriers to effective platform use, including economic challenges, increased teacher workload, and infrastructure issues.

This study contributes to understanding blended learning's effectiveness in the Saudi Arabian educational context, emphasising the critical role of digital platforms like Madrasati in supporting mathematics education. The findings are instrumental in the MOE and learning institutions considering technology integration in teaching and learning processes. It highlights the need to address infrastructure and support issues to maximise the benefits of digital platforms for educational enhancement.

Seeing through the rock – insights on geotechnical behaviour via XCT

Thomas Riccio, Matteo Ciantia[2], Michael Brown[3]

[1] School of Science and Engineering (Civil engineering), University of Dundee, 140007677@dundee.ac.uk
[2] m.o.ciantia@dundee.ac.uk
[3] m.j.brown@dundee.ac.uk

Abstract

The use of X-ray computed tomography (XCT) in geotechnical engineering has enabled insights into the micro and macro in-situ behaviour of soil and rock. Researchers have used this technique to observe sub-surface characteristics of various small-scale soil/rock-foundation challenges. For example, pile foundations which are used to support offshore structures (Figure 1) have been studied at small-scale using XCT. Examples include observing the pile installation behaviour in sand (Doreau-Malioche et al., 2018; Riccio et al., 2024) and in soft rock (Alvarez-Borges et al., 2021; Riccio et al., 2023), the latter posing challenges in geotechnical design - a result of its unique hydro-mechanical behaviour (Ciantia, 2022).

XCT in lab-based geotechnical studies is typically conducted after a test/event, and few examples exist of 'live' (during the event) CT and radiography use due to space limitations within a CT bay. As part of the ICE-PICK project (Ciantia, 2021), Riccio et al. (2024) developed a new loading frame apparatus which was operable from within an XCT bay (see Figure 1a). The system, instrumented with high-capacity load cells and displacement sensors, enabled application of vertical and horizontal displacement/load allowing for small-scale geotechnical tests to be performed. Chiefly, it was used to study and further understand the installation, lateral and cyclic performance of small-scale pile foundations in soft rock. This material is of interest to researchers as it exhibits a unique hydro-mechanical behaviour, degrading to a soft-low strength material when subjected to mechanical action. These attributes contribute to poor pile foundation performance in the field (Buckley, 2018; Jardine et al., 2023) and in numerical simulations (Ciantia, 2022; Jardine et al., 2023; Zheng et al., 2023).

In this instance, tests performed using the new multi-axis frame paired with XCT are shared. First, an overview is given of the small-scale cone penetration tests (CPT) used to characterise the soft rock. Thereafter, some of the small-scale open-ended pile tests, also performed using the frame, are discussed. The tests, paired with live radiography and post-test XCT (in this example), offered new sub-surface insights into the rock-damage/porosity evolution of both the piles and CPTs during and after installation/loading (see e.g. Figure 1b and c). These insights have aided the understanding of certain mechanisms which occur during pile installation and lateral loading in soft rock. They have also contributed to the development of new simple design approaches for pile foundations which capture more efficiently the unique material behaviour.

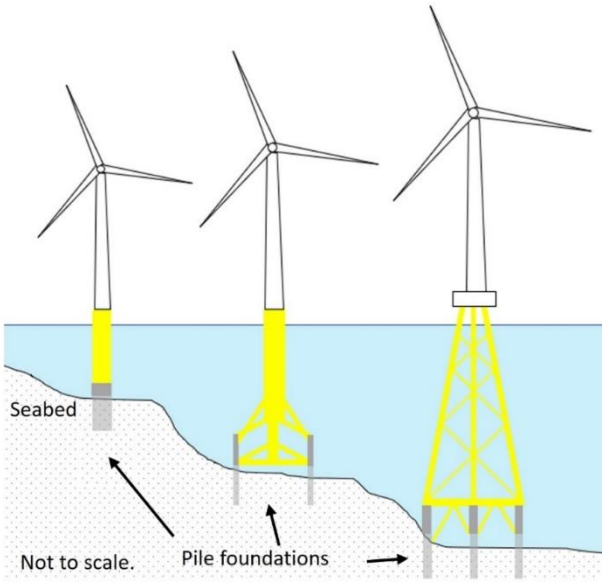

Figure 1: Examples of pile foundations used to support various offshore structures

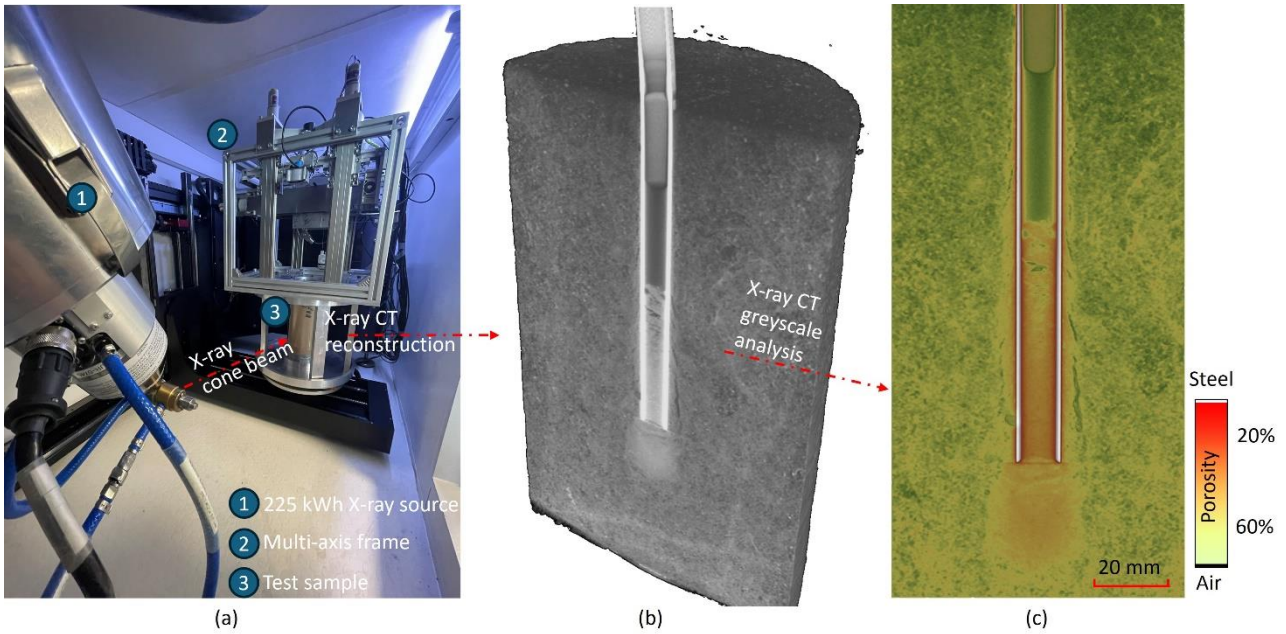

Figure 2: (a) X-ray CT bay and multi-axis frame at the University of Dundee (b) Post-test X-ray CT reconstruction of small-scale pile jacked into calcarenite soft rock and (c) Grey-scale analysis on centre-slice through pile to observe porosity changes during testing. Note. c sourced from (Riccio et al., 2024).

References

Alvarez-Borges, F., Ahmed, S., Madhusudhan, B. N., & Richards, D. (2021). Investigation of pile penetration in calcareous soft rock using X-ray computed tomography. *International Journal of Physical Modelling in Geotechnics*. https://doi.org/10.1680/jphmg.20.00031

Buckley, R. (2018). *The Axial Behaviour of Displacement Piles in Chalk* (Issue February) [Doctoral thesis, Imperial College London]. https://doi.org/https://doi.org/10.25560/78617

Ciantia, M. (2021). *ICE-PICK: Installation effects on cyclic axial and lateral performance of displacement piles in chalk*.

Ciantia, M. O. (2022). Installation Effects on Axial Performance of Monopiles in Chalk for Offshore Renewables. *Proceedings of the 2nd Vietnam Symposium on Advances in Offshore Engineering*, 424–432. https://doi.org/https://doi.org/10.1007/978-981-16-7735-9_47

Doreau-Malioche, J., Combe, G., Viggiani, G., & Toni, J. B. (2018). Shaft friction changes for cyclically loaded displacement piles: An X-ray investigation. *Geotechnique Letters*, *8*(1), 66–72. https://doi.org/10.1680/jgele.17.00141

Jardine, R. J., Buckley, R. M., Liu, T., Andolfsson, T., Byrne, B. W., Kontoe, S., McAdam, R. A., Schranz, F., & Vinck, K. (2023). The axial behaviour of piles driven in chalk. *Géotechnique*, *19(6)*, 1–45. https://doi.org/10.1680/jgeot.22.00041

Riccio, T., Ciantia, M. O., Previtali, M., Brown, M. J., & Csetenyi, L. (2024). A 4D investigation of model pile installation. *Proceedings of the XVII ECSMGE 2024*, 1–4.

Riccio, T., Previtali, M., Ciantia, M. O., & Brown, M. J. (2023). P-y response in porous rock: numerical derivation with experimental validation. *9th International SUT OSIG Conference "Innovative Geotechnologies for Energy Transition,"* 1357–1362. https://sut.org/event/osig2023/

Riccio, T., Romero, T., Mánica, M., Previtali, M., & Ciantia, M. (2024). A 4D soil-structure interaction model testing apparatus. *Submitted to Geotechnical Testing Journal*, *1*(1), 1–12.

Zheng, J., Previtali, M., Ciantia, M., & Knappett, J. (2023). Comparison of continuum (PFEM) and discrete (DEM) approaches for large insertion BVPs in soft rocks. *VIII International Conference on Particle-Based Methods*, 1–9. https://doi.org/10.23967/c.particles.2023.037

Energy and Performance Optimisation for Embedded Systems

Yazeed Almalaq[1], Vladimir Janjic[2]

[1] School of Science and Engineering (Computing), 2480402@dundee.ac.uk
[2] VJanjic001@dundee.ac.uk

Abstract

Modern mobile devices such as smartphones and tablets, have become very popular due to many reasons, including portability, flexibility, and performance. These devices offer powerful computing, which makes them very appealing for running different types of applications. By leveraging these computing capabilities and artificial intelligence (AI), user experiences have improved such as facial print and voice dictation. Using such features and algorithms will result in higher energy consumption due to their high-performance demands. Therefore, there is a need to manage and control the resources of these devices for each application to adopt this development in performance and use optimal energy. To achieve this, resource allocation (assigning available resources including CPU and memory, to particular tasks) is one of the techniques that can enhance system performance and energy efficiency by reducing inefficient resource usage. For instance, having eight cores in a device leads to the possibility of splitting eight tasks (for example background music, email refreshing, and browsing) one per core at a time. Optimal management of such a technique helps to save more energy. Additionally, using the existing technique in the latest mobile phones, like battery saver mode (reducing background tasks like email refreshing, location services, and a darker screen), showed a noticeable amount of energy savings when running social media and video game applications of about 27% compared with the default setting on an Android Google Pixel 6a. This indicates that there is a huge waste of energy. Thus, the aim of this thesis is to reduce energy consumption while maintaining the quality of performance of applications on embedded systems. This can be done by developing a system that should be able to make decisions, such as deciding what number of cores and what type to allocate to each of the running applications. This will go in four steps, as shown in Figure 1, starting with identifying and extracting parameters, then the profiling step, which is collecting data from measurements, then the modeller, which is the process of filtering, and finally the optimisations and decision step.

University of Dundee

A Deep-Learning Method for Single-Scan Optical Coherence Tomography Angiography Generation

Jinpeng Liao[1], Zhihong Huang[2], Chunhui Li[3]

[1] School of Science and Engineering (Biomed. Eng.), University of Dundee, UK, jyliao@dundee.ac.uk
[2] z.y.huang@dundee.ac.uk
[3] C.Li@dundee.ac.uk

Background, Motivation and Objective

Optical coherence tomography angiography (OCTA) is a non-invasively imaging modality that extends the functionality of OCT by extracting the signal of moving red blood cells from the surrounding static biological tissues. OCTA has emerged as a valuable tool for analyzing skin microvasculature, allowing for more accurate diagnosis and treatment monitoring. Most existing OCTA extraction (e.g., speckle variance (SV)) algorithms implement a larger number of the repeat (NR) OCT scans at the same position to produce high-quality angiography images. However, a higher NR requires a longer data acquisition time, resulting in more unpredictable motion artifacts. In this study, we aim to leverage the power of neural networks to extract vascular signals from a single-repeated OCT signal, thereby generating high-quality OCTA images.

Methods

In this study, we proposed an angiography extraction pipeline based on a single-repeat OCT scan utilizing a trained U-Net. The pipeline can facilitate the data acquisition speed and reduce the motion artifacts in OCTA imaging. Regarding data collection, a swept-source OCT system with a 200kHz sweeping rate was used to acquire skin data from 14 healthy volunteers (The data acquisition was approved by an institutional review board).

A twelve-repeated scanning protocol with a 5.16 mm^2 field of view and ~8.6 µm spatial sample rate was used to acquire data. The high-quality OCTA images generated by twelve-repeated OCT scans served as ground truth, while the input was structural images from the first single-repeated OCT scan. Supervised training was used to reduce the mean square error between the network output and ground truth.

Results/Discussion

In contrast to the reference OCTA image obtained via the SV algorithm on four NR OCT scans, the vascular image extracted by U-Net exhibits higher contrast and more vascular texture details, resulting in a higher PSNR of 17.28. Conversely, the denoising convolution neural network (DnCNN) outcomes perform inadequately compared to the reference OCTA image and U-Net. We believe that the encoder-decoder architecture network can perform better in angiography extraction. The results show that the U-Net can facilitate the data acquisition speed by extracting OCTA images from a one-repeated OCT scan, enabling a fast OCTA scan and accurate diagnosis to be achieved for patients.

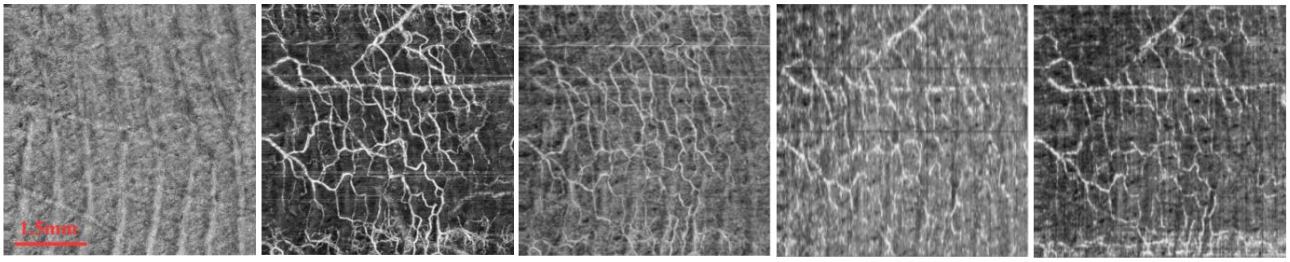

Figure 1: Visual comparison in skin palm area. (A) is the enface image of the model input structural image; (B) is the enface image of the valid image from a twelve-repetitions OCT scan; (C) is the enface image of the reference image from a four-repetitions OCT scan; (D) and (E) are the enface single-scan OCTA images generated by DnCNN and U-Net.

Electrochemical detection and profiling of 3,4-methylenedioxypyrovalerone on screen-printed carbon electrodes using nanostructured functionalized quantum dots

Kayode Oyinlola[1], Oluwasesan Adegoke[2], Niamh Nic Daeid[3]

[1] Leverhulme Research Centre for Forensic Science, School of Science and Engineering, University of Dundee, Dundee, DD1 4HN, UK.

[1]2358940@dundee.ac.uk, [2]o.adegoke@dundee.ac.uk, [3]n.nicdaeid@dundee.ac.uk

Abstract

The increasing prevalence of new psychoactive substances, particularly synthetic cathinones (SCs) is becoming a major concern for law enforcement and public health professionals due to their potential for addiction, overdose, and negative mental and physical health effects. Identifying samples containing controlled substances is important for public health and safety. However, the lack of routine screening tools has hindered efforts to address the rising prevalence of modified synthetic cathinone compounds such as 3,4-methylenedioxypyrovalerone (MDPV) in communities. Conventional methods for MDPV detection including liquid chromatography-mass spectrometry (LC-MS), gas chromatography-mass spectrometry (GC-MS), and nuclear magnetic resonance (NMR) spectroscopy are expensive and require the use of bulky and sophisticated equipment, making them unsuitable for routine onsite testing. This work reports on the development of a low-cost and simple-to-use electrochemical nanosensor for the rapid and ultrasensitive detection of MDPV. The nanosensor was fabricated using MnInPSeS quantum dots (QDs) and molecularly imprinted polymer (MIP) modified on screen-printed carbon electrodes (SPCEs). Dopamine was electropolymerized on the modified alloyed MnInPSeS QDs SPCE surface in the presence of MDPV (as the template), forming the SPCE/MnInPSeS QDs@-MIP nanosensor. The SPCE/QDs@MIP nanosensor had a wider linear concentration range for MDPV detection and a lower limit of detection compared to the previously reported methods. Differential pulse voltammetry was used for the electrochemical profiling study, where a fingerprint of MDPV was obtained in drug mixtures that mimicked adulterated samples. MDPV was successfully detected in 8 out of 10 drug mixtures, giving the SPCE/MnInPSeS QDs@-MIP nanosensor an 80% detection efficiency.

Modeling and Analysis of Non-local Interactions in Wound Healing: Numerical Simulations, Analytical Investigations, and Machine-Learning Approaches

Olusegun E. Adebayo[1], Raluca Eftimie[1,2], Dumitru Trucu[2]

[1] Laboratoire de mathématiques de Besançon, UMR CNRS 6623, University of Franche-Comté, Besançon 25000, France

[2] Division of Mathematics, University of Dundee, Dundee, DD1 4HN, United Kingdom

Abstract

The movement of cells during (normal and abnormal) wound healing results from biomechanical interactions that combine cell responses with growth factors as well as cell-cell and cell-matrix interactions (adhesion and remodelling). In this talk, we consider a non-local partial differential equation model for the interactions between fibroblasts, macrophages, and the extracellular matrix via a growth factor in the context of wound healing. We first investigate numerically the dynamics of this non-local model and the dynamics of the localised versions of this model. The results suggest the following: (i) local models explain normal wound healing and non-local models could also explain abnormal wound healing (although the results are parameter- dependent); (ii) the models can explain two types of wound healing, i.e., by primary intention, when the wound margins come together from the side, and by secondary intention when the wound heals from the bottom up.

Following up on numerical simulations showing the solutions of this class of models approaching either spatially homogeneous steady states or spatially heterogenous states with overgrown cell densities, we start by investigating the linear stability of the steady states and further prove the local in-time existence and uniqueness of solutions for this class of non-local models using the framework of the analytic semi-groups of operators.

Finally, since clinical misdiagnosing skin disorders (e.g., keloids) leads to the administration of wrong treatments with life-impacting consequences, in this study we use different CNN models to classify various images of skin disorders as either malignant or benign; or as malignant, benign or keloid.

References

1. **O.E. Adebayo**, S. Urcun, G. Rolin, S. Bordas, D. Trucu and R. Eftimie, Mathematical investigation of normal and abnormal wound healing dynamics: local and non-local models. *Mathematical biosciences and engineering*, 20 (2023): 17446–17498.
2. R. Eftimie, G. Rolin, **O.E. Adebayo**, S. Urcun, F. Chouly and S. Bordas, Modelling Keloids Dynamics: A Brief Review and New Mathematical Perspectives, *Bulletin of Mathematical biology*, 85 (2023):117.
3. **O.E**. **Adebayo**, R. Eftimie, D. Trucu, Analysis of a non-local model for normal and abnormal wound healing [*submitted*].
4. **O.E**. **Adebayo**, R. Eftimie, D. Trucu, Machine learning and deep learning approaches for classifying images of keloids in the context of malignant and benign skin disorders *[In preparation]*

A Selective Coating Deposition Technique for Gas Turbine Components

Sarah Higgins[1,2], Thomas D.A. Jones[3], Qi Zhao[3]

[1] University of Dundee, 140007687@dundee.ac.uk
[2] ATL Turbine Services, s.higgins@atlturbineservices.co.uk
[3] University of Dundee, t.d.a.jones@dundee.ac.uk, q.zhao@dundee.ac.uk

Abstract

ATL Turbine Services are funding this PhD and are an organisation specialising in the refurbishment of late lifecycle turbine parts. The failure of gas turbine components is often from high temperature oxidation, erosion, corrosion, or a combination. To achieve higher performance and longer life for these high-cost, critical components, additional protection is required due to the high temperatures, stresses, and wear that they encounter during use. This additional protection can come in the form of the application of a protective coating.

The overall aim of the PhD research project is to develop a coating method that can minimise the current limitations of the coating application processes and allow for a more selective, protective, and environmentally friendly methodology. To be investigated first was the environmental impact of a new protective coating.

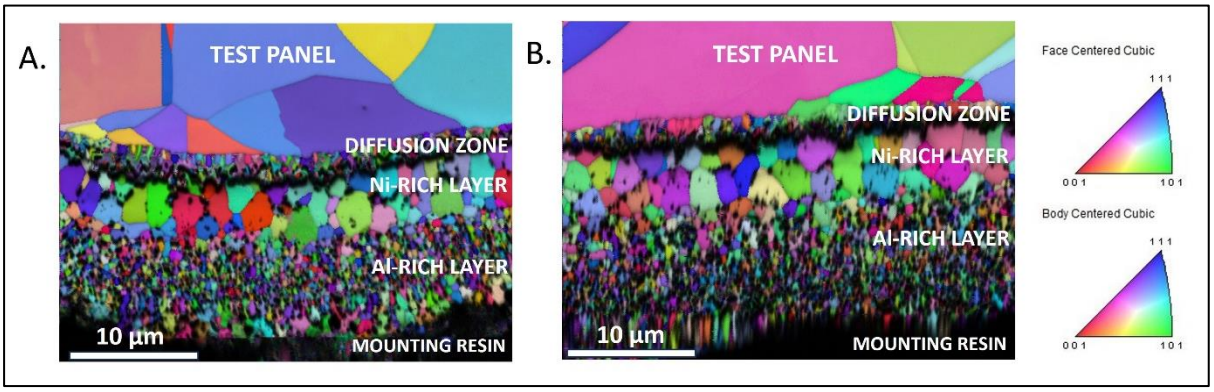

Figure 1: A) CFIPAL EBSD IPF map. B) IP1041 EBSD IPF map.

Gas turbine hot end components have been protected for over 30 years against sulphidation, oxidation and hot corrosion attacks by the application of a diffused aluminide slurry coating [1]. UK REACH (registration, evaluation, authorisation, and restriction of chemicals) is ruling out the use of hexavalent chromium due to health and safety reasons, which renders the industry favourite sulphidation protection coatings, unusable [2].

A hexavalent chromium-free replacement has been developed by Indestructible Paint Ltd (CFIPAL) and it is critical to understand if this replacement coating will protect the parts to the same extent as its predecessor (IP1041). Quantification of the coating's metallurgical structure (figure 1), composition, physical properties and corrosion resistance were evaluated. From the testing it was concluded that CFIPAL was physically and chemically sufficient to become the industry replacement for IP1041.

Moving forward, the PhD aim is to utilise the more environmentally friendly, CFIPAL, in developing a deposition technique to allow for the application of thermal sprayed coatings to be selectively applied to gas turbine components.

References

[1] P. Holder, 'CF Ipal – a case study of the chrome-free drop in replacement for IP1041 hexavalent chrome coating', Transactions of the IMF, vol. 101, no. 2, pp. 60–63, Mar. 2023, doi: 10.1080/00202967.2023.2182946.
[2] 'Reach - applications for authorisation AFA037-01 chromium trioxide', Health and Safety Executive (https://consultations.hse.gov.uk/crd-reach/reach-afa-037-01/) Accessed 21/12/23).

University of Dundee

Retrieving shoeprint images using convolutional neural networks

Struan Robertson[1], Roberto Puch-Solis[2], Stephen McKenna[3]

[1] Leverhulme Research Center for Forensic Science, sjyrobertson@dundee.ac.uk
[2] Leverhulme Research Center for Forensic Science, rpuchsolis001@dundee.ac.uk
[3] School of Science and Engineering (Computing), s.j.z.mckenna@dundee.ac.uk

Abstract

Footwear marks are commonly found at crime scenes and can be used for investigation to identify potential suspects, and as evidence in court once a suspect has been charged with a crime. For investigation, a shoemark can be used to link crime scenes (when a shoemark from one crime scene matches a shoemark from another) and for identifying potential suspects who may have left the shoemark. A shoe impression from a crime scene is referred to as a *shoemark* whereas an impression taken under controlled conditions isreferred to as a *shoeprint*. Shoeprint image retrieval refers to searching a database of shoeprint images taken from suspects for matches to a shoemark from a crime scene, to identify potential suspects that could have left the shoemark. Recently, this task has been addressed with pre-trained convolutional neural networks.

The current objectives of this project are to improve the performance of shoeprint retrieval algorithms on real world data. A further goal would be to describe a framework to allow for automatic quantitative analysisof shoemark evidence. Processing shoemark evidence is a labour-intensive process requiring trained individuals to manually find the make and model of the shoe responsible for the mark. An automated processwould allow for this evidence to be investigated more easily, potentially expediting, and reducing the cost ofinvestigation.

Wen et al. proposed using a convolutional neural network (CNN) to extract a representation from a shoemark image which could then be compared to representations similarly extracted from a database of reference shoeprints using template matching. This project improves upon the results obtained by Wen et al by using a more modern CNN architecture and by comparing images over a set of scale and rotation transformations, allowing for potential misalignment between shoemark and shoeprint images. We achieved state of the art retrieval results on the FID-300 dataset (Kortylewski et al.), with the matching reference shoeprint for a shoemark present in the top 1% of returned potential matches 87.3% of the time. This was a 5.3% improvement on Wen et al., who scored 82% on the same test.

Several avenues for future work will be explored. Firstly, we plan to gain access to (and perhaps collect) larger datasets of shoeprint and shoemark images. Advanced machine learning models will then be trained for the task of shoeprint image retrieval. Over time, footwear acquires localised damage, known as randomly acquired characteristics (RACs). Machine learning models could be used to identify RACs and thus uniquely identify shoes from shoemarks, somewhat analogously to fingerprint recognition. Shoemark evidence oftenfeatures multiple overlapping shoemarks. Therefore, an automatic method for separating overlappingshoemarks is a further interesting avenue for research.

References

Wen, Curran, Wevers (2023). Shoeprint image retrieval and crime scene shoeprint image linking by usingconvolutional neural network and normalized cross correlation. *Science & Justice, 63*(4): 439-450.

Kortylewski, Albrecht, Vetter (2015). Unsupervised Footwear Impression Analysis and Retrieval from Crime SceneData. *Computer Vision – ACCV 2014 Workshops, 9008*: 644-658.

Understanding communication practices amongst practitioners on mega projects in Saudi Arabia

Hussam Namanqani[1], Mr. Andrew Munns[2]
PGR, School of Science and Engineering (Civil Engineering), 2410561@dundee.ac.uk
Senior Lecturer, School of Science and Engineering (Civil Engineering), a.k.munns@dundee.ac.uk

Abstract

Saudi Arabia has been transferring its economy to a new era where knowledge-based practices and sustainability will become the country's priority, with mega projects forming a major element of this transition. The construction industry is a major participant in this transition, but as an industry it continues to be conventional in its practices in which quality, cost and time are the main constructs to consider. However, human factors such as knowledge sharing, and communication practices are less prominent. This study aims to explore the communication practices within construction mega-projects in Saudi Arabia, exploring the existing opportunities and challenges the industry encounters with these projects. Based on the literature review, a conceptual framework was developed to facilitate potential communication practices, identifying two main dimensions. First, transformational aspects move from explicit into implicit knowledge, whilst the second dimension includes three communication practices: individual, teamwork and leadership interventions. For the individual, their intention in communicating is facilitated by identifying both seeking understanding and matching the needs. Combining them may assist in promoting knowledge-sharing and communication practices. In the context of teamwork, communication and knowledge sharing are more likely to occur only when task coordination is considered through an agreed-developed level of trustworthiness and transparency. Construction leaders and managers are more likely to communicate through data evaluation and a shared decision-making framework. The three identified levels of individuals, teamwork and leadership should predict knowledge sharing as the main construct associated with communication practices in construction mega projects. Using this conceptual framework of communication on construction mega projects, the study collected data through a self-administered questionnaire, which included eight main constructs. 202 participants working as construction managers, engineers and technicians in Saudi Arabia completed the questionnaire. Data was analyzed via two main phases: a) descriptive data analysis was conducted to present demographic data using IBM-SPSS, whereas b) association between constructs was analyzed by conducting Structured Equation Modeling (SEM) using Smart PLS software. Findings show a significant association in individual communication practices, particularly between seeking understanding and willingness to share knowledge. The construct of matching the needs is a mediator variable that facilitates the association between seeking understanding and knowledge-sharing. Knowledge sharing is, on the other hand, significantly associated with establishing effective communication. The teamwork and leadership practices were not associated with effective communication practices in this study. This would imply that the communication practices of the individual has a greater impact on the practices of construction mega-projects than teamwork or leadership.

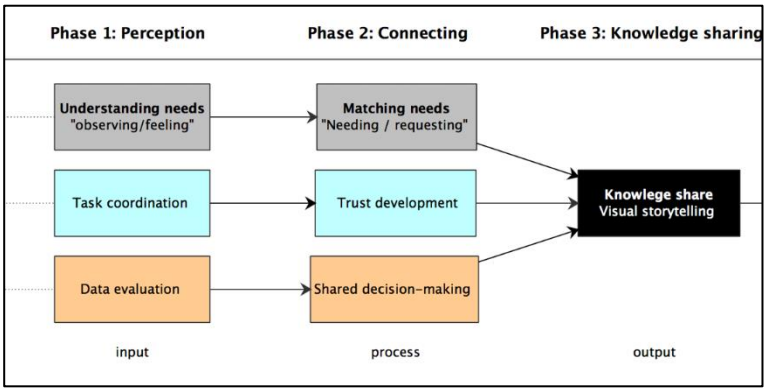

Figure 1: Conceptual Framework (Float model)

Novel hybrid antibacterial surfaces for medical implants

Yimeng Wang[1], Qi Zhao[2] and Svetlana Zolotovskaya[3]

[1] School of Science and Engineering, email: yzzvwang@dundee.ac.uk
[2] q.zhao@dundee.ac.uk
[3] s.a.zolotovskaya@dundee.ac.uk

Abstract

With the advent of the “post-antibiotic era”, the development of antibacterial surfaces for medical devices has a more significant impact than previously believed. The medical implant infections caused by bacterial colonisation and subsequent biofilm formation have reached 52% [1]. Almost 70% of all medical implants are made of metallic materials. A number of antimicrobial strategies have been proposed for metal surfaces including release-based chemical coating with antimicrobial agents such as silver ions (Ag^+). Prof Qi Zhao and his group proposed the “optimal surface energy” theory and provided a model for developing a "2 in 1" antibacterial nanocomposite surface by combining Ag nanoparticles with bactericidal properties with "non-stick" PTFE coating [2]. Recently, it has been shown that the micro/nano-structured surfaces are important for promoting osteoblast integration and preventing initial bacterial attachment [3]. In our work, we employed laser-induced periodic surface structuring (LIPSS) in combination with chemical coating, based on polydopamine-chitosan-Ag nanoparticles (PDA-CS-AgNPs), to achieve deterministic surface structures with precisely defined surface chemistry on medical grade titanium to boost the antimicrobial performance and expand functional space. This novel hybrid surface exhibited an improved antibacterial efficacy against Gram-negative *Escherichia coli* (WT F1693) and Gram-positive *Staphylococcus aureus* (ATCC 12600) by 96.6 % and 91.9 %, respectively (Fig. 1). Extended DLVO theory was used to model different bacterium-surface interaction scenarios after the surface modifications. This novel antimicrobial strategy has the potential to widen the scope of clinical therapy and significantly improve patient outcome circumventing the development of bacterial resistance.

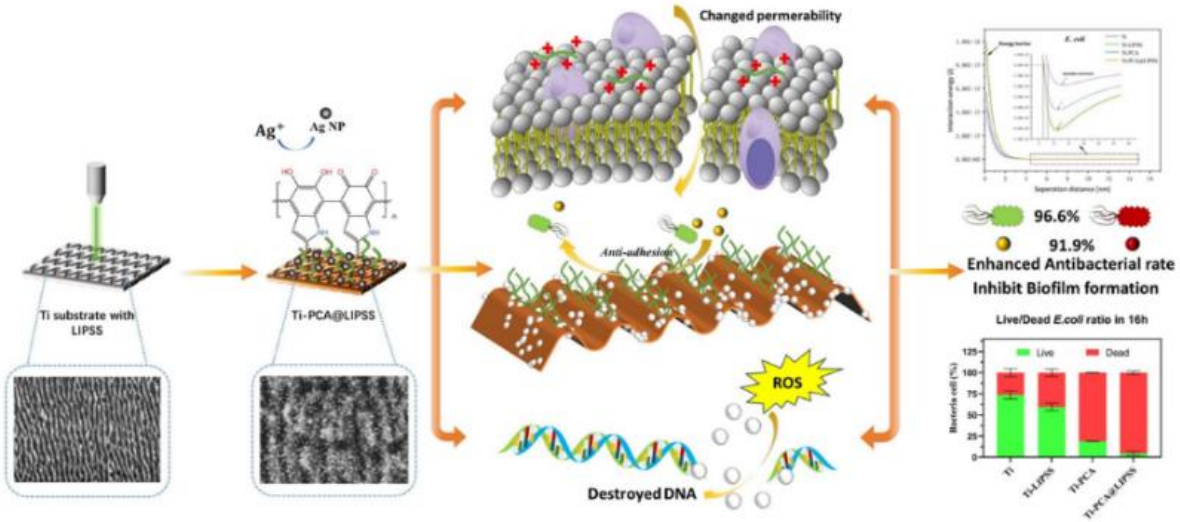

Fig. 1 Schematic of hybrid antibacterial surface fabrication and antibacterial results.

References:

1. Jiang, P., Zhang, Y., Hu, R., Shi, B., Zhang, L., Huang, Q., Yang, Y., Tang, P. and Lin, C. (2023). Advanced surface engineering of titanium materials for biomedical applications: From static modification to dynamic responsive regulation. *Bioactive Materials*, 27, pp.15-57.
2. Wang, L. & Zhao, Q et al (2019) In-vitro antibacterial and anti-encrustation performance of silver-polytetrafluoroethylene nanocomposite coated urinary catheters, *Journal of Hospital Infection*, 103(1):56-63
3. K. Schwibbert, A. M. Richter, J. Krüger, J. Bonse (2024). Laser-Textured Surfaces: A Way to Control Biofilm Formation?, *Laser & Photonics Reviews*, 18(1): 2300753.

Operator Learning for Solar Physics

Daniel Norman[1], Eric Hall[2], Karen Meyer[3]

[1] School of Science and Engineering (Mathematics), dznorman@dundee.ac.uk
[2] ehall001@dundee.ac.uk
[3] kmeyer001@dundee.ac.uk

Abstract

A problem we in a modern society face today is the threat of severe solar weather. This difficult to predict phenomena can cause power grid outages, disrupts GPS and damages expensive and critical satellites in orbit, further details on how the government rates this danger can be found in the UK Risk Register [1]. The severe solar weather my research focuses on is solar flares, caused by highly active regions of the Sun sending out large quantities of plasma, some of which can travel down the earth's magnetic field lines causing the damage talked about above and simulations of active regions are an important part of space weather forecasting. An active region is an area on the Sun that has an especially intense magnetic field over a period of time, shown in figure 1 the white regions indicate a positive region with black indicating a negative region. Simulations of these regions can indicate when a region is going to flare and how strongly it may do so but simulations can also be impractical as they take time to run and are computationally heavy. The research I am undertaking will use neural networks to create a statistical surrogate for the simulations by learning an operator which can take the input data we get from satellites such as the Solar and Heliospheric observatory (SOHO) satellite shown in figure 1 and output the simulated coronal magnetic field shown in figure 2. To use supervised operator learning techniques requires a large database of training data, this will be both input data in the form of magnetograms shown in figure 1 and output data of coronal magnetic fields shown in figure 2. In this talk, I will review the methodology I am using for generating this database, from obtaining the raw data through to simulating the magnetofrictional field using the universities supercomputer. Currently we have finished simulating AR10977 (active region 10977) and have obtained a list of some 20 more that are intended to also be simulated. This work will inform the selection of an appropriate operator learning method will be carried out to get a working and computationally efficient system that can predict the likelihood of active regions flaring. Being able to make these predictions potentially hours ahead of being hit by severe solar weather is the main goal of this research, to help be more prepared when bad weather comes our way.

References

[1] UK risk register (2023) https://www.gov.uk/government/publications/national-risk-register-2023

University of Dundee

A validation study of newly established ear morphology prediction guidelines in facial approximation

Eszter Maja Somjai[1], Tobias Houlton[2], Clare Lamb[3]

[1]Master's by Research student, University of Dundee, emsomjai@dundee.ac.uk
[2] Primary supervisor, thoulton001@dundee.ac.uk
[3] Secondary supervisor, c.z.lamb@dundee.ac.uk

Abstract

Forensic facial approximation and superimposition methods rely on understanding soft and hard tissue anatomical correlations. Guyomarc'h and Stephan investigated eight previously published ear prediction methods, finding that computed tomography scans of 78 living adults did not support any of these recommendations; however, correlations between ear features, sex, age, and facial height led to the development of four validated prediction methods, though accuracy remains a challenge due to significant error. Utilising an independent sample, this study aimed to test these existing protocols and trail newly proposed regression equations.

This study utilised 38 computed tomography scans from the New Mexico Decedent Database (deceased) and the University of Science and Technology Hospital Yemen database (living). Observations were performed in 3D Slicer. Skull placement and linear measurement definitions were standardised via Python scripting. All statistical tests were performed using SPSS.

Following an assessment of normal distribution, potential sexual dimorphism, asymmetry, and mean differences in population affinities were examined using independent t-tests for normally distributed variables and Mann-Whitney U tests for non-parametric variables. Correlations between measurements and chronological ages were determined using Pearson's r and Spearman's correlation. Stepwise multiple regression was used to devise new prediction protocols.

This project largely supported Guyomarc'h and Stephan's findings. In contrast, guidelines proposing only slight differences between the height of the nose and height of the ear (c.2 mm) was found to be unreliable (explains only 13.47% of variation); no correlation was found between the supramastoid crest and auricle (p=0.149), and that lobe morphology correlated (r=0.487) with mastoid lateral angle.

Comparably high standard errors of the estimates for regression equations established in this study (especially for ear height) were comparable to those of Guyomarc'h and Stephan. Future research should focus on expanding ear approximation guidelines, potentially incorporating additional landmarks, investigating interlandmark distances and semilandmarks, or adopting a geometric-morphometric approach to enhance reliability. Furthermore, the wider implementation of deep learning in forensic anthropology could prove beneficial in identifying associations between hard and soft tissue features in the auriculotemporal region, especially when established relationships are deemed unreliable with limited alternative options.

	Guyomarc'h & Stephan's finding	Common ground	This study
Rule 1	Posterior jaw line (mandible ramus angle) is not parallel to the ear angle, and they are not correlated.	There was a no statistically significant correlation between the ear angle and mandibular ramus angle	agrees: r(37) = .140, p = .410, with the coefficient of determination of r2=0.0196
Rule 2	Soft nose height 1 underestimates ear height; hard nose height 2 overestimates it. Positive but weak correlations exist between ear height		
	N/A	soft nose height 1 estimate error	underestimates by 10.314 mm
	6.688 mm	soft nose height 2 estimate error	overestimates by 6.688 mm
		hard nose height 1 estimate error	underestimates by 6.296 mm
		hard nose height 2 estimate error	overestimates by 4.961 mm
	r = 0.30	correlation coefficients (nose height vs ear height)	higher; r = 0.367
Rule 3	Adding 2 mm to the measurement of g'-sn (soft nose height 2) will decrease precision of ear height prediction.		explains 13.47% variation, equally unreliable
Rule 4	Mediolateral orientation of the mastoid process (mastoid lateral angle) does not correlate with the size and orientation of the outer ear (ear		
Rule 5	r = 0.41	correlation between mastoid height and ear width	r=0.453
	Ear width is not equal to half of its height.		
	r= 0.6	Ear height and ear width are correlated.	r=0.444.
	approximately 0.6.	Mean ration of ear width/ear height is…	0.573873863 in this study
Rule 6	Supramastoid crest development does not correlate with ear protrusion but is significantly linked to the ear height (sa-sba and obs-obi) and orientation at its insertion (EIA). No left/right asymmetry is present.	ear protrusion did not correlate to development of supramastoid crest; the means of supramastoid crest morphology for left and right side were not significantly different therefore no asymmetry in the population was observed.	ear protrusion vs supramastoid crest: (r=+/-0.242; p=0.149). No correlations found between supramastoid crest, ear width, ear height or ear insertion height
Rule 7	The lobe morphology (free or attached) is not related to the mastoid form or other ear measurements.	ear lobe morphology did not correlate with auricular metrics (ear protrusion, ear angle, ear insertion angle, ear height, ear width, ear insertion height). No left/right asymmetry is present.	showed a statistically significant moderate correlation between the lobe morphology and mastoid lateral angle (r=+/-0.487, p=0.002), but showed no correlations regarding other measurements of the mastoid process (mastoid height, mastoid anterior angle)
Rule 8	23°	ear angle - hard nose angle difference	18.37207061°
	18°	ear angle-soft nose angle difference	17.14357412°
	Ear angle is not parallel to soft nose angle or hard nose angle. Ear orientation and nose orientation does not correlate.	The ear angles were not parallel to either nasal root angle or hard nose angle	agrees

Figure 1: Summary of rule testing findings of the current study compared to the results of Guyomarc'h and Stephan (2012)

Reference

Guyomarc'h P, Stephan CN (2012). The validity of ear prediction guidelines used in facial approximation. *J Forensic Sci.*, 57(6):1427-41. doi: 10.1111/j.1556-4029.2012.02181.x.

University of Dundee

Optic disk segmentation based on a retinal foundation model

Zhenyi Zhao[1], Emanuele Trucco[2]

[1] VAMPIRE, Computing, School of Science and Engineering, 2578745@dundee.ac.uk
[2] VAMPIRE, Computing, School of Science and Engineering, e.trucco@dundee.ac.uk

Abstract

Research has shown that Transformers perform better than Convolutional Neural Networks (CNN) after training on large-scale datasets. In computer vision, researchers have begun to develop foundation models (FM) based on Transformers and large-scale datasets. FM are generally trained with self-supervised tasks and can be adapted to diverse downstream tasks after fine-tuning; e.g., in computer vision, image classification or segmentation. RETFound [1] is a FM trained on 904,170 colour fundus photography (CFP) retinal images (Figure 1). Excellent performance has been proven in disease detection tasks, namely image-level classification tasks.

Our research investigates the performance of RETFound in optic disc segmentation. We plan to compare results obtained with RETFound with the baseline network developed in our group, VAMPIRE's DUNet [2], which is a CNN-based network trained on 129 CFP retinal images with augmentation. Image segmentation aims to partitioning digital images into foreground and background regions, namely pixel-level classification tasks; in our case, the foreground is the optic disk (Figure 1). The area and shape of the optic disk are important diagnostic indicators of many eye diseases such as glaucoma.

In the image-level classification task, the RETFound classification model contains an encoder and a classification head. However, a segmentation model requires inserting a decoder between the encoder and the segmentation head (Figure 2). Developing such a decoder and adapting RETFound to segment images is the target of our current research. We reviewed the related work and adopted the decoders of Segmenter [3] and MedSAM [4], which are segmentation models containing the same encoder backbone as RETFound. In detail, we combine the models in two ways: RETFound with the decoder of Segmenter, and RETFound with the decoder of MedSAM. Then we freeze the model weights of RETFound and train the model to the latter contain our own VAMPIRE datasets as well as public datasets. We assess the segmentation performance with the Dice loss. Besides, as MedSAM is trained on multimodal medical images (e.g., X-ray and CT), we also fine-tune the whole MedSAM on optic disk segmentation training datasets as the second baseline work. Finally, we use testing datasets to test four architectures: RETFound + Segmenter decoder, RETFound + MedSAM decoder, and two baseline architectures (DUNet and fine-tuned MedSAM). Currently, we are still in the process of training models and results are forthcoming. Given that RETFound was trained on large-scale real (clinical) datasets, we believe that 'RETFound + Segmenter decoder' or 'RETFound + MedSAM decoder' will give the best performance.

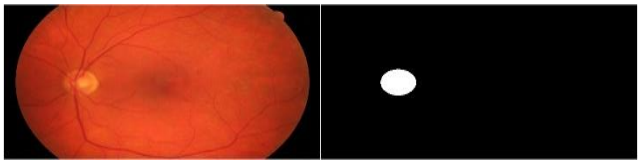

Figure 1: CFP retinal image and OD segmentation mask

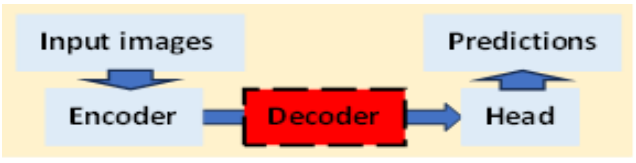

Figure 2: Classification and segmentation model

References

[1] Zhou, Y., Chia, M. A., Wagner, S. K., Ayhan, M. S., Williamson, D. J., Struyven, R. R., ... & Keane, P. A. (2023). A foundation model for generalizable disease detection from retinal images. Nature, 622(7981), 156-163.

[2] Mookiah, M. R. K., Hogg, S., MacGillivray, T., & Trucco, E. (2021). On the quantitative effects of compression of retinal fundus images on morphometric vascular measurements in VAMPIRE. Computer Methods and Programs in Biomedicine, 202, 105969.

[3] Strudel, R., Garcia, R., Laptev, I., & Schmid, C. (2021). Segmenter: Transformer for semantic segmentation. In Proceedings of the IEEE/CVF international conference on computer vision (pp. 7262-7272).

[4] Ma, J., He, Y., Li, F., Han, L., You, C., & Wang, B. (2024). Segment anything in medical images. Nature Communications, 15(1), 654.

A non-local spatio-temporal cancer invasion process with cross-diffusion and cross-adhesion

Zhihao Tao[1] , Dumitru Trucu[2], Raluca Eftimie[2,3]

[1] Division of Mathematics, University of Dundee, Dundee, DD1 4HN, United Kingdom, zytao@dundee.ac.uk
[2] Division of Mathematics, University of Dundee, Dundee, DD1 4HN, United Kingdom
[3] Laboratoire de Mathématiques de Besançon, Université Franche-Comté, Besançon, 25000, France

Abstract

In this talk we focus on establishing an extensive computational modelling and analysis framework for the invasion of a solid tumour in the human body that accounts for the interplay between the cross-adhesion and cross-diffusion cells sub-populations processes that are involved within the underlying cancer cells migration. Specifically, we will explore the non-local spatio-temporal evolution of an invading tumour that assumes two cancer cells sub-populations (namely, a primary cancer cell population as well as a mutated one) that proliferate and at the same time exercise both random movement and directed migration. In particular, the directed movement is assumed to be driven here by the naturally arising interplay between cell-adhesion and cross-diffusion cells populations processes, and in this context, this talk will explore three cell migration scenarios. These will be accompanied by numerical simulation (based on finite volume) as well as a novel functional analysis approach for the cross-diffusion parameters sensitivity.

Modelling of Actomyosin Dynamics as an Active Elastomer

Euan Mackay[1], Rastko Sknepnek[1,2], Jens Januschke[3]

[1] Computational Biology, School of Life Sciences, University of Dundee
[2] School of Science and Engineering, University of Dundee
[3] Molecular, Cell and Developmental Biology, School of Life Sciences, University of Dundee

Abstract

The cytoskeleton is a cellular structure present in most types of eukaryotic cells. It is made up of several types of filaments. The cytoskeleton allows cells to move, as well as change or maintain their shape. The smallest of the main types of filaments are actin filaments, which play a role in helping cells maintain their surface level structure as well as perform whole cell movement. These are long fibrous polymers, made up of smaller actin subunits, with a diameter of around 5-9 nm (Chugh and Paluch,2018; Lewis et al., 2008; Svitkina, 2020) and a persistence length in the tens of microns.

Another important class of proteins with regards to controlling cellular shape change and movementis myosin, a family of motor proteins. These motors can create contractile forces using ATP hydrolysis (Chugh and Paluch, 2018; Lewis et al., 2008; Svitkina, 2020). Actomyosin networks are the name given to large networks formed from many crosslinked actin filaments and many myosin proteins. These networks perform a wide variety of tasks such as muscle contraction, wound healing, cell migration, and cell division (Lewis et al., 2008; Miao and Blankenship, 2020; Salbreux et al., 2012).

Actomyosin networks play an important role in tissue development across a wide variety of species(Salbreux et al., 2012). In particular, when many cells are seen to move collectively, the actomyosin network is often seen to pulse periodically, with highly dense regions of actin or myosin forming and dissipating in a continuous cycle. While these pulsations have been seen a wide variety of tissue types from species as diverse as mice, flies, and frogs, their exact origin and purpose is not yet known (Miao and Blankenship, 2020).

A theoretical description of these pulsations has been developed in the form of an active elastomermodel for the actomyosin cortex (Banerjee et al., 2017, 2011). However while there is some excellent work on the linear stability analysis (Banerjee et al., 2011; Banerjee and Marchetti, 2011)and one-dimensional simulations of this model (Alonso et al., 2016; Banerjee et al., 2017), missing from the literature is a comprehensive set of two-dimensional simulations based on this model. Thegoal of my research is to use the Finite Element Method to be able to perform 2D simulations of this model based in realistic cellular geometries such as the one shown below.

So far, we have been able to show that using this approach we are able to produce qualitatively similar actomyosin dynamics to those seen in experiments on files. We have also been able to show a similar scaling in the number of actomyosin pulses with cell size, to the ones seen in experiments.

In future, we hope to extend our model to three dimensions. As well as being more biologically realistic we also hope to be able to explain the symmetry breaking behaviour in the neural stem cells found in files. We hypothesis that actomyosin oscillations in this system break the symmetryin the cell which allows for cellular division.

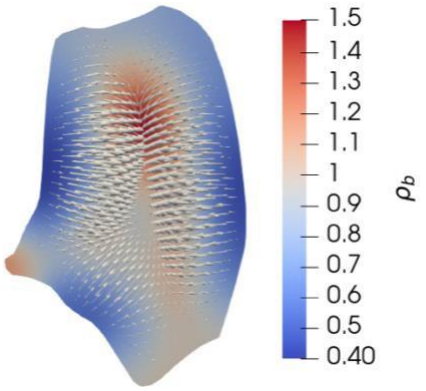

Figure 1: Snapshot of simulation on realistic cellular geometry. Colour shows myosin density at each point inthe cell. Arrows show velocity of actomyosin mesh at each point in the cell.

References

1. Lewis, J. *et al. Molecular Biology of the Cell*. (Garland Science, 2008).
2. Chugh, P. & Paluch, E. K. The actin cortex at a glance. *Journal of Cell Science* **131**, jcs186254 (2018).
3. Svitkina, T. M. Actin Cell Cortex: Structure and Molecular Organization. *Trends in Cell Biology* **30**,556–565 (2020).
4. Salbreux, G., Charras, G. & Paluch, E. Actin cortex mechanics and cellular morphogenesis. *Trends inCell Biology* **22**, 536–545 (2012).
5. Miao, H. & Blankenship, J. T. The pulse of morphogenesis: actomyosin dynamics and regulation in epithelia. *Development* **147**, dev186502 (2020).
6. Banerjee, S., Liverpool, T. B. & Marchetti, M. C. Generic phases of cross-linked active gels: Relaxation, oscillation and contractility. *EPL* **96**, 58004 (2011).
7. Banerjee, D. S., Munjal, A., Lecuit, T. & Rao, M. Actomyosin pulsation and flows in an active elastomer with turnover and network remodeling. *Nat Commun* **8**, 1121 (2017).
8. Banerjee, S. & Marchetti, M. C. Instabilities and oscillations in isotropic active gels. *Soft Matter* **7**,463–473 (2011).
9. Alonso, S., Strachauer, U., Radszuweit, M., Bär, M. & Hauser, M. J. B. Oscillations and uniaxial mechanochemical waves in a model of an active poroelastic medium: Application to deformation patternsin protoplasmic droplets of Physarum polycephalum. *Physica D: Nonlinear Phenomena* **318–319**, 58–69 (2016).

Protocol Switching in Argumentative Dialogue

Nicole Orr[1], John Lawrence[2], Chris Reed

[1] University of Dundee, 170010591@dundee.ac.uk
[2] j.lawrence@dundee.ac.uk

Abstract

Dialogue protocols define how a dialogue may proceed and the moves its participants can make within it. Over the course of a dialogue the participants' goals and strategies may change in response to the other participants within the dialogue. Enabling agents to switch between dialogue protocols gives them the flexibility to address these changes and make use of them. The focus of my work is on the development of Dialogue as a Service (DaaS), a platform for building multi-agent dialogue systems, and, in particular, the theoretical research challenges around how protocol switching occurs in real-world dialogues and how this can be handled in such multi-agent dialogue systems. DaaS can be used to create a wide range of multi-agent dialogue systems due to its few restrictions and inherent flexibility, which can be illustrated through the use of two examples from literature. Protocol switches can be both licit and illicit; however, current research has only focused on implementing licit protocol switches.

Protocol switching, also referred to as dialectical shift (Walton and Krabbe, 1995) can be either licit or illicit. They define dialectical shift as a change from one type of dialogue to another, a change in the context and "flavour" of the dialogue. Licit protocol switches are constructive shifts to the dialogue that have been openly made and agreed to by all of the dialogue's participants. In contrast, illicit protocol switches are those that are inappropriate or concealed from one or more of the dialogue's participants. Often in natural language conversations several protocol switches will occur over the course of the dialogue.

There has been limited research into how licit protocol switches can be implemented and managed within argumentation-based dialogue systems. Illicit protocol switches are often associated with fallacies. Walton and Krabbe state that many fallacies are caused by the occurrence of an illicit shift from one type of dialogue to another. The difference between the same utterance being fallacious or non-fallacious is dependent upon the context of the dialogue in which it has occurred. Several utterances are valid moves within the context of one protocol but become fallacious when misused in a different type of protocol. One of the examples is how an illicit protocol switch from a persuasive protocol to a negotiation protocol can cause the fallacy of bargaining to occur.

Reference

Walton D, Krabbe EC (1995). Commitment in dialogue: Basic concepts of interpersonal reasoning. SUNY press.

Planet Formation in Wind-Driven Accretion Discs via Pebble Accretion

Yunpeng Zhao[1], Soko Matsumura[2]

[1]University of Dundee, 2440931@dundee.ac.uk
[2]University of Dundee, s.matsumura@dundee.ac.uk

Abstract

In the dynamic realm of astrophysics, understanding the formation and evolution of planetary systems is a fundamental question. Our research investigates the processes governing these systems, with a particular focus on the role of wind-driven accretion discs. Conventional planet formation models have largely relied on the assumption of viscously evolving disc, where the accretion rate is uniform across the disc. While this α-disc model provides a good framework of viscous processes and angular momentum transport within accretion discs, the wind-driven model is increasingly favoured for its ability to explain the efficient removal of angular momentum, as well as for being consistent with direct observations of jets and outflows in accretion discs.

The focus of our study is the examination of disc wind efficiency's impact on planetary system formation. Building upon the foundational α-disc model by Shakura and Sunyaev [1], our investigation adopts the expanded α-disc model introduced by Tabone et al. 2022 [2]. This model incorporates the effect of magnetic disc winds in driving accretion and angular momentum extraction, highlighting a dual alpha parameterisation: α_{DW} for wind-driven accretion and α_{SS} for local disc turbulence. Our simulations focus on the variability introduced by the wind efficiency parameter λ, exploring its influence on disc accretion rates and surface mass density profiles.

The findings reveal significant implications of wind-driven disc for planet formation and migration. Specifically, discs with lower λ values, which correspond to flatter surface mass density profiles, exhibit reduced planetary migration speed. Furthermore, planetary systems where the planets vary by two orders of magnitude in mass can be formed in such discs.

Looking forward, the research aims to further bridge the gap between theoretical models and observational evidence, enriching our understanding of the complex processes that underlie planetary system formation. By integrating a broader range of observational data and introducing planet-planet interactions, we aspire to offer deeper insights into the diverse architectures of planetary systems and the dynamic processes that drive their evolution.

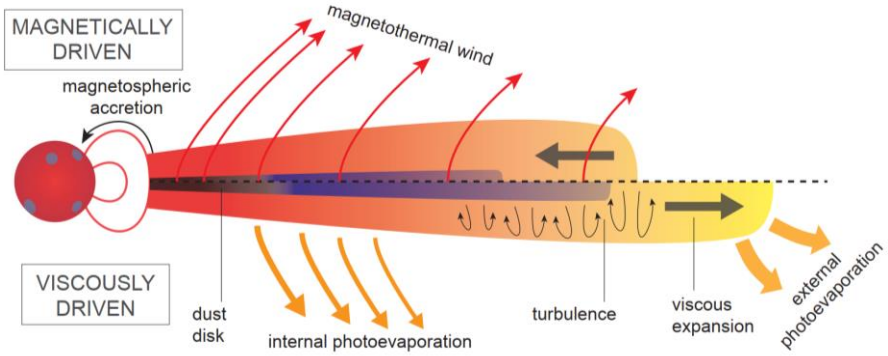

Schematic illustration of disk evolution under the two models: a viscous model, and a wind driven model (Manara et al. 2022)[3]

References

[1] Shakura, N. I., & Sunyaev, R. A. (1973). Black holes in binary systems. Observational appearance. *Astronomy and Astrophysics, Vol. 24, p. 337-355*, *24*, 337-355.

[2] Tabone, B., Rosotti, G. P., Cridland, A. J., Armitage, P. J., & Lodato, G. (2022). Secular evolution of MHD wind-driven discs: analytical solutions in the expanded α-framework. *Monthly Notices of the Royal Astronomical Society*, *512*(2), 2290-2309.

[3] Manara, C. F., Ansdell, M., Rosotti, G. P., Hughes, A. M., Armitage, P. J., Lodato, G., & Williams, J. P. (2022). Demographics of young stars and their protoplanetary disks: lessons learned on disk evolution and its connection to planet formation. *arXiv preprint arXiv:2203.09930*.

An explainable model for solar active regions

Martin Sanner[1], Dr. Karen Meyer[2], Prof. Stephen McKenna[3]

[1] School of Science and Engineering (Mathematics), University of Dundee, 2472597@dundee.ac.uk
[2] School of Science and Engineering (Mathematics), University of Dundee, kmeyer001@dundee.ac.uk
[3] School of Science and Engineering (Mathematics), University of Dundee, s.j.z.mckenna@dundee.ac.uk

Abstract

Solar active regions are regions of intense magnetic fields on the sun, which are often linked with the emergence of space weather. Space weather events (such as coronal mass ejections or solar flares) can impact electronic systems the events encounter, so studying these regions and their evolution is important for the electronics safe and continued use on and around Earth.

However, active regions are not uniformly defined - different teams may look at different parameters, valuing some features over others, and applying different cutoffs for region definition. As active regions consist of multiple polarities, the simplest common option between these definitions is an analysis of regions as bipolar segments of high magnetic field strength. Employing bipolar active regions as objects of interest is thus a natural choice.

For accurate space weather prediction, accounting for all active regions present at a given time is vital. Such models need to have a correct listing of newly formed active regions. However, the active region emergence process is complex and detecting new regions can be difficult. Their detection is made possible by using solar surface rotation models.

We present a computer vision system for detecting newly forming bipolar active regions, based on their physical parameters (with magnetic flux and distance between polarities as primary measurements). Detections of newly forming active regions are reported alongside physical parameters, enabling them to be easily compared to databases created using a choice of the reported physical parameters.

With the resulting set of comparisons, applied metrics in the fields (covering both usage in heliophysics and computer vision) are considered, focussing on metrics such as precision and recall for the system's detection component. Experiments are reported on simulated synoptic magnetogram data (currently achieving an average precision of 83%), while historic synoptic magnetogram and full-disk magnetogram experiments are in preparation.

An eventual goal of the work is the prediction of active region parameter evolution through neural networks.

University of Dundee

Poster Presentations

(In order shown in Programme)

Synthetic high-quality Computed Tomography (CT) Image generation from low-quality Cone-Beam CT

Alzahra Altalib[1], Alessandro Perelli[2], Dr Chunhui Li[3]

[1,2,3]School of Science and Engineering, University of Dundee [1]2600129@dundee.ac.uk
[2]aperelli001@dundee.ac.uk
[3]c.li@dundee.ac.uk

Abstract

Cancer is a complex and fatal disease that requires complex treatment to combat its progression. The treatment of cancer often involves radiotherapy, where high-energy radiation is used to destroy cancerous tumours. To ensure precision in the radiation delivery while protecting the surrounding healthy tissues, a process called radiotherapy treatment planning is employed. Numerous advancements have been made in the planning process, such as the advent of 3D conformal radiotherapy and image-guided radiation therapy, which allow doctors to offer personalised treatment to patient's unique anatomy. However, challenges still exist in the distribution of radiation doses when the tumours are of an irregular shape [1]. Such irregularities can often lead the nearby critical organs to radiation exposure as well. To cater to this, advanced computing techniques such as deep learning (machine learning) and model-based learning (mathematical techniques) are being used. Such methods traditionally rely on the use of standard imaging techniques like Computed Tomography (CT); however, during radiotherapy treatment, it is crucial to have high-quality CT images to position (register) the patient correctly. Performing several CT scans leads to high X-ray dose issues.

The use of Cone Beam Computed Tomography (CBCT) is being explored for treatment planning and dose estimation to address the issue of high X-ray doses. CBCT provides fast 3D image generation with a single scan, potentially reducing radiation dose delivery and improving patient comfort. Yet it is subject to some inherent limitations as well. These include artefacts, poor soft tissue contrast, and geometric distortions that can hinder the overall efficacy of dose estimations. This is due to the relatively low resolution offered by CBCT images compared to CT images. The project aims to use low-dose CBCT scans to perform dose calculations by obtaining CT images synthetically. This will have a massive impact on healthcare protocols and reduce the X-ray dose during treatment planning.

The research involves developing a novel deep-learning method for the generation of synthetic CT images from CBCT data to calculate the dose given during the radiation therapy plan. The phantom scans are to be carried out for oncology planning that mimic human tissue and tumour characteristics. The corresponding CBCT images will be synthesized using the proposed approach while making a comparative analysis with high-quality CT scans carried out under the same configuration. This comparison is crucial for evaluating the efficacy of the developed method. Based on the synthesized images, the X-ray dose will be calculated to be delivered on a radiotherapy plan, and the results will be validated by comparing them to the dose that has been calculated using a high-quality CT scan for performance benchmarking. If the comparison is within a specific threshold, it could potentially reduce the radiation dose to the patient, where the core potential of this research resides. This will allow ease of measurements through CBCT while offering similar performance on dose estimation to CT high-quality images while keeping the radiation exposure at lower levels. The approach to the image quality problem is depicted in Figure 1.

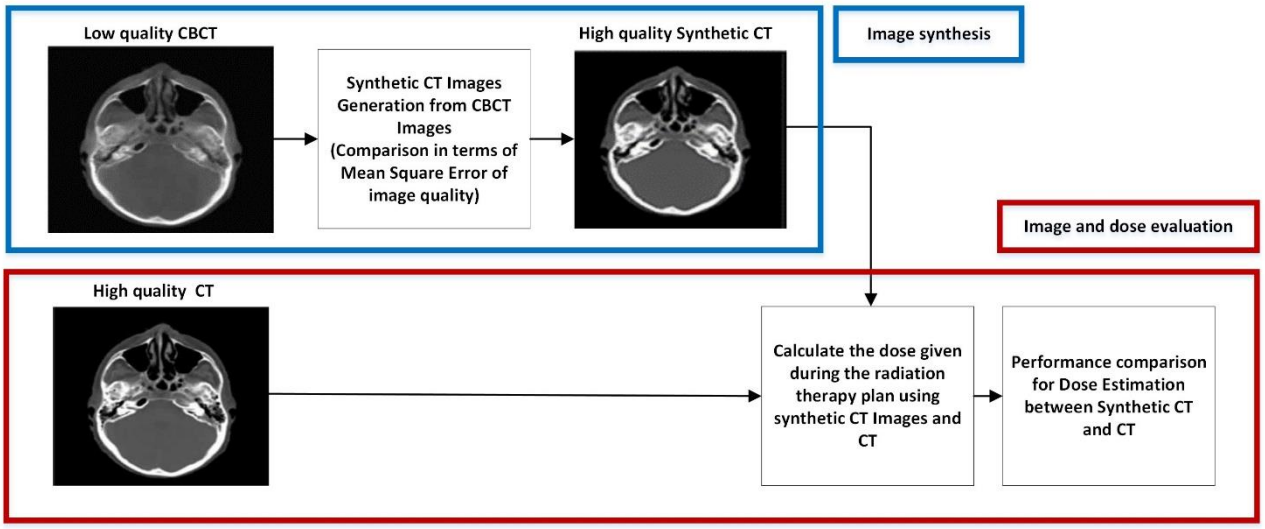

Figure 1: Synthetic CT Images Generation and Dose Estimation using CBCT data
CT and CBCT Scans Source. Adapted with permission from[2].

References

[1] Nuyts, S. (2007). Defining the target for radiotherapy of head and neck cancer. Cancer Imaging, 7(Special issue A), S50–S55. https://doi.org/10.1102/1470-7330.2007.9009

[2] Thummerer, A., Zaffino, P., Meijers, A., Marmitt, G. G., Seco, J., Steenbakkers, R. J., ... & Knopf, A. C. (2020). Comparison of CBCT based synthetic CT methods suitable for proton dose calculations in adaptive proton therapy.

Photoacoustic imaging with endogenous contrast (biomarkers)

Amirhossein Pourali, James Joseph , Ghulam Nabi

apourali@dundee.ac.uk
jjoseph001@dundee.ac.uk
g.nabi@dundee.ac.uk

Abstract

Photoacoustic imaging (PAI) with endogenous contrast as a biomarker has emerged as a promising modality for high-resolution imaging of deep biological tissues. This review explores the applications of PAI in medical imaging, particularly in the detection of biomarkers for disease diagnosis and therapy monitoring. The integration of PAI with other imaging methods, such as ultrasound, MRI, and positron emission tomography (PET), is discussed to enhance the sensitivity and specificity of biomarker detection. Additionally, the potential of deep learning algorithms in PAI and the challenges associated with their implementation are highlighted. The review also addresses recent advances in PAI, including the use of multifunctional nanoplatforms for diagnosing hepatocellular carcinoma and the potential of 2D nanomaterials as biomarkers for clinical applications. Furthermore, the capability of PAI to map tumour haemoglobin concentration and oxygen saturation levels non-invasively, without the need for exogenous contrast agents, is emphasized. The review concludes by discussing the classification of PAI systems, including photoacoustic microscopy (PAM), photoacoustic tomography (PAT), and photoacoustic computed tomography (PACT), and their respective imaging capabilities.

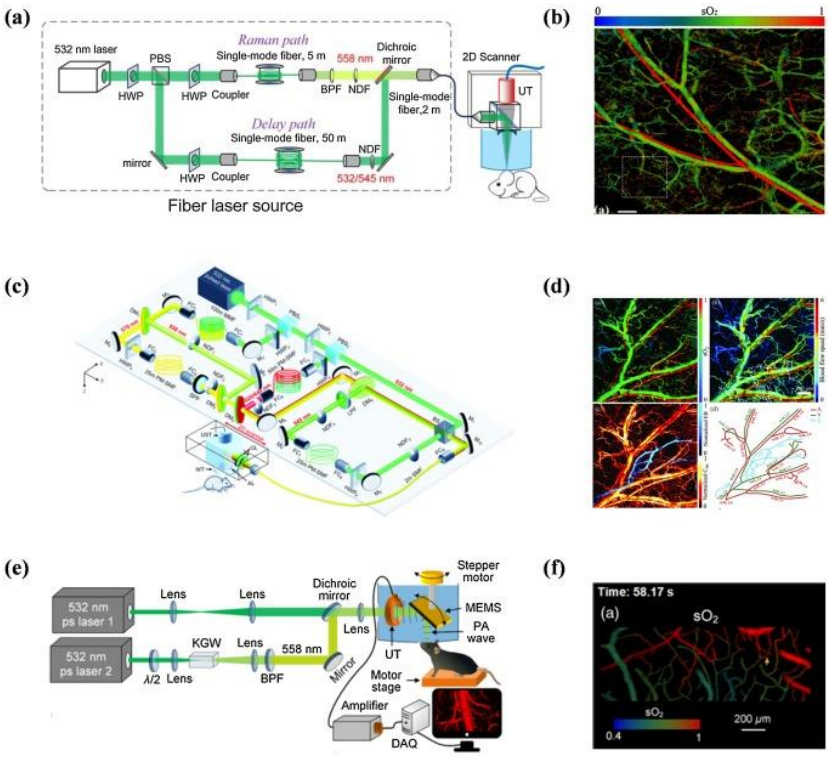

Fig. 1. (a) Schematic representation of the PAM system in which a stimulated-Raman-scattering-based multi-wavelength pulsed laser source is utilized. (b) In vivo imaging of oxygen saturation in the mouse ear [1]. (c) Schematic representation of five-wavelength OR-PAM. (d) A schematic image related to compensated sO_2, blood flow speed, and the blood and lymphatic vessels. (e) Schematic image related to the functional PAM (fPAM) system according to a Raman laser using KGW crystal as the Raman material. (f) sO2 images related to single-impulse electrical stimulation (2)(3)(23). ***(5) have utilized*** *PA microscopy to evaluate the initial dip in mouse brains and demonstrated the single-impulse-stimulated microvascular hemodynamics at single-vessel resolution (mouse brains as a case study). Fast label-free imaging of single-impulse response determined as outstandingbrain–computer interfaces in a real-time condition. Figure 2 shows a scheme from 532-nm picosecond-pulsed lasers used for a dual-wavelength fPAM system in Ref. (5).*

References

[1] John S, Hester S, Basij M, Paul A, Xavierselvan M, Mehrmohammadi M, et al. Niche preclinical and clinical applications of photoacoustic imaging with endogenous contrast. Photoacoustics. 2023;32:100533.

[2] Liu C, Chen J, Zhang Y, Zhu J, Wang L. Five-wavelength optical-resolution photoacoustic microscopy of blood and lymphatic vessels. Advanced Photonics. 2021 Jan 4;3

[3] Liang Y, Jin L, Guan BO, Wang L. 2 MHz multi-wavelength pulsed laser for functional photoacoustic microscopy. Opt Lett [Internet]. 2017;42(7):1452–5. Available from: https://opg.optica.org/ol/abstract.cfm?URI=ol-42-7-1452

[4] Wang K, Li C, Chen R, Shi J. Recent advances in high-speed photoacoustic microscopy. Photoacoustics [Internet]. 2021;24:100294. Available from: https://www.sciencedirect.com/science/article/pii/S2213597921000549

[5] Yun He a, b JS b KIM b RC b and LVW c. Wave of single-impulse-stimulated fast initial dip in single vessels of mouse brains imaged by high-speed functional photoacoustic microscopy. J Biomed Opt. 2020;25(6).

Sonodynamic Therapy for glioblastoma

Danial Kordbacheh[1], James Joseph[2], Sourav Banerjee[3]

[1]School of Science and Engineering, School of medicine, 2436650@dundee.ac.uk
[2]School of Science and Engineering, jjoseph001@dundee.ac.uk
[3]School of Medicine, s.y.banerjee@dundee.ac.uk

Abstract

Sonodynamic therapy (SDT) represents a promising approach in cancer treatment, utilizing ultrasound in conjunction with sonosensitizers to eradicate tumor cells. Through the activation of sonosensitizers by low-intensity ultrasound, SDT triggers the generation of reactive oxygen species (ROS) within the tumor microenvironment, instigating oxidative stress and consequent apoptosis in cancer cells. Notably, SDT offers advantages such as reduced invasiveness, precise tumor targeting, and minimal systemic side effects compared to conventional therapies. Its capacity to selectively eliminate cancerous tissues while preserving healthy cells highlights its potential as a groundbreaking therapeutic strategy in oncology, paving the way for more effective and tolerable cancer treatments.

The current investigation has developed and validated an automated in vitro system tailored specifically for sonodynamic therapy (SDT), revolutionizing the precision of treatment application. This sophisticated system allows for meticulous adjustment and mapping of focused ultrasound fields across diverse exposure conditions and setup configurations. By finely tuning parameters including ultrasound frequency, intensity, plate base material, thermal effects, and the integration of live cells, this study ensures optimized experimental conditions for SDT. Notably, when coupled with a sonosensitizer, the focused ultrasound triggers apoptotic cell death in primary patient-derived glioma cells while concurrently amplifying intracellular levels of reactive oxygen species (ROS). Furthermore, the remarkable reduction in 3D growth observed in primary glioma stem neurospheres post-SDT exposure underscores the profound potential of this approach in combating cancer stem cells, thereby advancing our understanding and application of SDT in cancer therapy.

In my PhD project, I aim to design a new setup that enhances ultrasound field mapping accuracy and enables experiments with mice. This new approach to testing Sonodynamic Therapy (SDT) in lab-based disease models could facilitate comparison with existing treatments. Understanding the physical properties affecting precise determination and application of focused ultrasound (FUS) dose to cells is vital for in vitro SDT experiments. Many current systems prioritize investigating specific properties like standing waves over cell testing. Further research is necessary to refine setups and tumor models for swift parameter optimization. This understanding could guide the development of optimal FUS parameters for clinical SDT applications.

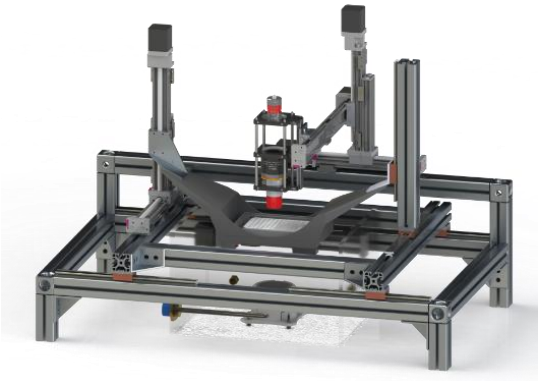

Figure 3

Assessing and quantifying the relationship between spasticity, proprioception, and movement post-stroke

Jasmine Usher[1,2], Dr. Alejandra Aranceta-Garza[1,2], Dr. Jacqui Morris[3]

[1] Biomedical Engineering, j.j.usher@dundee.ac.uk
[2] Centre for Medical Engineering Technology, aarancetagarza001@dundee.ac.uk
[3] School of Health Sciences

Abstract

Introduction: *Stroke causes a range of motor and sensory impairments including muscle weakness, spasticity, and changes in proprioception that in turn influence functional performance and independence in activities of daily living.* These changes negatively impact independence yet, little is known about their interactions and impact on recovery post-stroke. Therefore, this research aims to understand and quantify the relationships between post-stroke complications including spasticity, proprioception deficits and motor function changes over the first 6 months of rehabilitation.

Methods: This research is split into two parts: assessment of current literature and acquisition of new evidence through a longitudinal clinical research trial. To complete the first, a systematic literature search was conducted on Scopus, PubMed, and Web of Science using the key terms: stroke; movement; proprioception; spasticity; rehabilitation; and upper limb. For inclusion, papers must have assessed two of spasticity, proprioception, or motor function post-stroke. Demographic data; relationships assessed; number of assessment timepoints; prescription of anti-spasticity medication; and outcome measures used were extracted from each eligible study. Random effects model meta-analyses were carried out to i) investigate variable changes in time, and ii) assess the overall strength of correlations between variables.

Results: To date, the results obtained are pertinent to the first stage of the research. A total of 8,701 studies were identified, with 52 (including clinical trials, observational and longitudinal studies) meeting the criteria for inclusion. The mean age [range] and time since stroke at the start of studies of participants was 61 [44.9-76.0] years and 23 [0.10-97.2] months, respectively. From the meta-analyses, it was found that spasticity increased ($OR = 0.5$, $p = 0.0475$) in time, proprioception impairment decreased ($OR = 3.15$, $p < 0.0001$), as did motor function impairment ($OR = 3.21$, $p < 0.0001$). The overall correlation between spasticity and proprioception was weak ($r = 0.33$, $p = 0.0283$), between proprioception and motor function was moderate ($r = 0.45$, $p < 0.0001$) and between spasticity and motor function was moderate ($r = 0.55$, $p < 0.0001$).

Discussion: Understanding associations between post-stroke complications is vital in the development of personalised rehabilitation programs to improve the quality of life of those affected by stroke. Results of the meta-analyses found both spasticity and proprioception were moderately correlated with motor function, highlighting the importance of quantifying these during motor rehabilitation. Spasticity and proprioception were found to be weakly correlated with each other, although only three studies were found to study and quantify this relationship. Little evidence regarding the changes in variables over time was available with only two, four and six studies included in the spasticity, proprioception, and motor function change in time analyses, respectively. To build upon current evidence, the clinical research trial will involve collecting spasticity, proprioception, and movement (including motor function and kinematics using a 5-camera system) data at four timepoints from up to 120 participants after their first-ever stroke. Relationships of obtained data with various clinical measures and demographic data at each of the four time points will then be explored.

Skull Exposure to Various Ultrasound Wave Propagation

Saeed Charbenny[1], Zhihong Huang[2]

[1] School of Science and Engineering (Biomedical Engineering), 2403602@dundee.ac.uk
[2] z.y.huang@dundee.ac.uk

Abstract

Focused ultrasound (FUS) is desirable in medical applications for its safety and accuracy and is a non-invasive treatment option. Such advantages to FUS have led researchers to investigate its effect on various medical conditions, including neurons. There was various research on the effect of ultrasound on the brain and how such effects can be harnessed to treat different brain conditions, such as tremors. FUS has two main branches: Low-Intensity Focused Ultrasound (LIFU) and High-Intensity Focused Ultrasound (HIFU). The lattercauses tissue ablation. LIFU, on the other hand, focuses on lower intensities, which are accompanied by small, neglectable temperature rises that do not cause tissue damage. An investigation between a continuous and pulse signal was carried out to record the thermal change of the outer and inner skull.

The simulation ran using Sim4Life, an existing treatment transducer replicated for simulation purposes with an aperture of 90mm and a diameter of 71.5mm. The transducer was placed on the top-front right side of the human head, which is similar to an ongoing treatment method [1]. The skull was subjected to different ultrasound beams. The first is a continuous ultrasound wave for 30 seconds, and the second is a pulsed signal that has a Pulse Repetition Frequency (PRF) of 100 Hz, a Duty Cycle of 1%, and a gap of 2 seconds between each pulse for 30 seconds in total. Inner and outer skull temperatures were monitored.

The result of the rise in thermal skull temperature under the two different ultrasonic approaches was that the effect of having a continuous wave, the outer skull had a temperature rise of 37.00102°C from 37°C, an increase of 0.00102°C after 7.34 seconds. Meanwhile, the inner skull temperature rose from 37°C to 37.0107°C, an increase of 0.0107°C after 34.28 seconds, after which a drop of temperature started. With pulses, there was a rise in outer skull temperature from 37°C to 37.00099°C, an increase of 0.00099°C. In contrast, the inner part of the skull increased in temperature from 37°C to 37.01039°C, an increase of 0.01039°C. The temperature difference between continuous and pulses is an increase in the outer skull temperature of 0.00003°C while there was a difference of 0.00031°C increased temperature of the inner.

It is also worth noting the time of heating. The difference in temperature rise between the outer and inner is that the outside is at room temperature of 25°C, which counters the temperature rise due to ultrasound. In comparison, the inner is affected by the closed-loop average body temperature of 37 °C, which leads to a higher temperature increase.

The difference between continuous and pulse input shows the importance of choosing the right treatment option. It also shows that pulse has the potential to deliver the same desired clinical outcome with less chance of causing permanent damage to the cells.

In conclusion, the pulse showed a lower risk of tissue damage than continuous waves, especially if the treatment requires extended exposure to ultrasound.

Figure 1: Ultrasound transducer setup in head

References

[1] Martin M. Montia,b,c, Caroline Schnakers, Alexander S. Korb, Alexander Bystritsky, Paul M. Vespab. Ultrasonic Thalamic Stimulation in Disorders of Consciousness after Sever Brain Injury: A First-in-Man Report. *Brain Stimulation,9*(6): P940-941 Available at: Accessed April 15, 2024. https://www.brainstimjrnl.com/article/S1935-861X(16)30200- 5/fulltext.

Oral Soft Tissue Angiography Imaging Using a Hand-held Intraoral Probe

Tianyu Zhang[1], Simon Shepherd[2], Zhihong Huang[1], Michaelina Macluskey[2], Chunhui Li[1,*]

[1] Centre for Medical Engineering and Technology, University of Dundee, Dundee DD1 4HN, UK, txzhang@dundee.ac.uk
[2] School of Dentistry, University of Dundee, Dundee DD1 4HN, UK
[*] c.li@dundee.ac.uk

Abstract

Early detection of oral potentially malignant lesions and cancers is associated with improved outcomes and prognosis. The gold standard of biopsy is invasive with associated cost and morbidity. Optical coherence tomography-based angiography (OCTA) has a non-invasive high resolution imaging capability, making it a promising tool for oral soft tissue lesion screening. This study aimed to evaluate a hand-held OCTA probe on the buccal mucosa and labial mucosa of 10 healthy volunteers to determine the normal vascular signature of this site. In this study, a Swept-Source Optical Coherence Tomography (SSOCT) system with a centre wavelength of 1300 nm utilizing an intraoral scanning probe was used to acquire data. The probe with lateral and axial resolutions of 39.38 µm and 33.37 µm has a field of view of up to 9mm in diameter, while its imaging depth is around 1.7mm. To minimize motion artifacts and scanning time, all datasets underwent processing using the windowed Eigen-decomposition algorithm. Quantitative assessment was performed using adaptive thresholding and Hessian filtering. Angiography quantitative analysis in buccal mucosa revealed an average vessel density of 62.96% (σ=2.99%), an average vessel diameter of 80.94 (σ=6.71) µm and an average weighted tortuosity of 1.29 (σ=0.036), while the angiography in labial mucosa had an average vessel density of 65.67% (σ=2.80%), an average vessel diameter of 87.28 (σ=5.64) µm and an average weighted tortuosity of 1.29 (σ=0.027). These findings indicate that hand-held intraoral OCTA probe imaging could be used for the early diagnosis of premalignant lesions by identifying specific and detailed vascular signature differences. Therefore, this probe design could revolutionize oral mucosal diagnostic imaging and alert clinicians to areas that may merit further investigation. In conclusion, although further research with larger datasets of both normal tissue and pathologies would be required, preliminary evidence indicates that investment in OCTA probe evolution and allied software design may contribute to the development of clinically useful intra-oral diagnostic imaging.

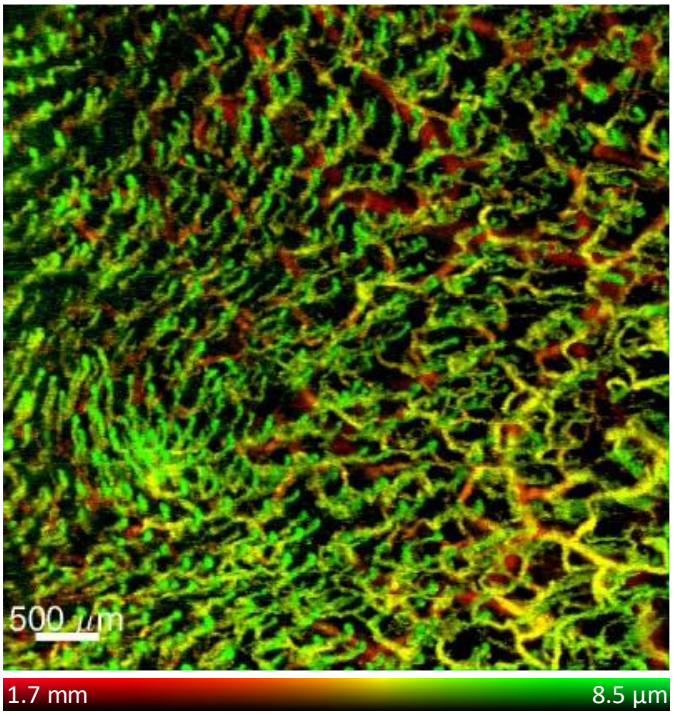

Figure 1: The depth-encoded angiography projection of buccal mucosa. (Scale bar: 500 µm on both axis; Color bar: the hue changing from green to red represents the change of depth from 8.5 µm to 1.7 mm, while the intensity of each hue value represents the OCTA intensity.

Multi-Functional Imaging Optical Coherence Tomography (OCT) for Monitoring Acne Development in Human Facial Skin In-Vivo

Zhengshuyi Feng[1], Prof. Zhihong Huang[1], Dr. Chunhui Li[1]

[1] Centre of Medical Engineering and Technology, 180021128@dundee.ac.uk

Abstract

Skin acne is the most common skin disease in adolescents but can involve all age groups with an estimated global prevalence of 9.4%. However, the current clinical diagnosis of facial acne relies on objective methods, i.e., clinicians' observation and dermoscopy. Optical coherence tomography (OCT) is a non-invasive imaging modality. Functional OCT imaging includes both optical coherence elastography (OCE) and optical coherence tomography based on angiography (OCTA) provide useful information to analyse and characterise the skin pathological conditions.

Although the development of each OCT function has been widely published, there is no study to combine structural image, angiography and elastography of in-vivo tissue from a single scanning. In this study, a multi-functional OCT system is developed to provide above mentioned functional imaging from one single scan.

This study obtained an approval letter from the School of Science and Engineering Research Ethics Committee of the University of Dundee. Facial acnes from 5 volunteers were scanned, the acne development processes are monitored at the same site for 15 days. For the functional OCT system, a swept source OCT system operated on a 1300 nm central wavelength with a sweeping rate of 400 kHz was utilised. The handheld probe included a piezoelectric actuator with an angle of 45° for SAW generation on the facial surface for elastography function. The actuator was driven by a chirp signal with a frequency range from 0.1 to 7 kHz. The elastography could be reconstructed based on the phase velocity dispersion curve and penetration depth. For angiography function, the *en-face* structural and angiography projections could be generated to show the vessel network within the facial acne region. The total acquisition time would last 15 seconds.

Figure a and b show day 1 and day 15 of acne developments from one volunteer. Based on the cross-sectional elastography, the maximum Young's modulus of the facial acne development stage demonstrated a decreasing trend (49.5%). As days increased, from the vascular projection map, it is noticeable that there is a significant change in the density of blood vessels around acne and the size of acne. In summary, the multi-functional system could demonstrate fully functions including structure, elastography and angiography, which is benefit for clinical dermatology research, i.e., drug treatment monitor in the future.

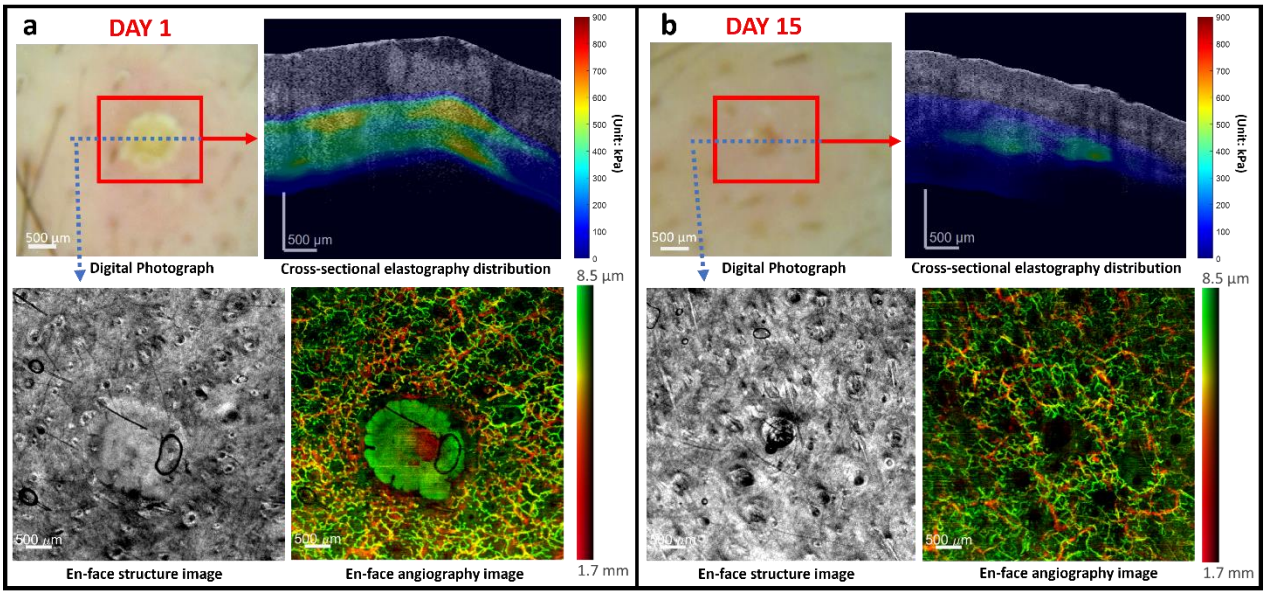

University of Dundee

Novel sensor development for an improved muscle movement detection and classification

Nicholas Ged Deane[1], Dr. Ale Aranceta-Garza[1], Dr. Alessandro Perelli[1], Dr. Mario Ettore Giardini[2]

[1] Biomedical Engineering, Centre for Medical Engineering and Technology, 130025430@dundee.ac.uk
[2]Department of Biomedical Engineering, University of Strathclyde, Glasgow.

Abstract

As embedded and wearable technologies have gotten more advanced, their capabilities have grown exponentially. In recent years, this has resulted in wearable technology, like smartwatches being able to track the wearer's heart rate (Pasadyn, Soudan et al. 2019); lightweight wearable patches that can calculate blood-sugar levels without drawing blood (Nakagawa, Hirota et al. 2022); conductive threads that can be layered in a wearable capable of monitoring muscle atrophy (Rice and Kiourti 2023); and even sportswear that reacts to movement to provide haptic feedback (Rudolf, Stjepanovič et al. 2022).

With the rapid advancement in electronic components, current mobile medicine devices can perform tasks much faster allowing their use in real-time applications. Tasks which were previously reserved for terminal computer systems, such a diagnostic ultrasound scan, can now be performed and immediately uploaded to a cloud-based program which then relies to a mobile device for a real-time diagnosis (Clarius 2024). This boost to performance has also allowed for multiple sensors to be used in tandem to further enhance performance and allow for new functionalities, such as using wireless monitoring systems in clinical settings, which allow for a mobile use whilst being user friendly, allowing those able to engage with normal daily activities whilst being user observation (Cosoli, Spinsante et al. 2021).

The aim of this research project is the development of a new generation of sensors to track muscle movement. For this, I will firstly perform a systematic literature review of the current state of technology for detection and assessment of muscle movement using two main technologies: optomyography (OMG) and surface-electromyography (sEMG). This review will allow for the assessment of current principles involved in both technologies which will lead to the second stage of my research: the development of novel sensors for muscle movement assessment. It is envisioned that this novel technology will address current challenges in muscle movement assessment seen in current detection methods, such as motion artifacts, sweat, environmental noise, signal-to-noise ratio, amongst others. While this technology has a wide range of potential applications from a medical monitoring and diagnostic tool to a commercial virtual reality interface, however the scope of this project will focus on the implementation of a wireless muscle activity detection system in a clinical setting for the express purpose of providing robust and reliable information for assessing, monitoring, and tracking skeletomuscular issues via monitoring of upper limb muscle activity.

The latter stage of the research will be achieved through the use of neural net based artificial intelligence alongside traditional pattern recognition techniques (such as structural or fuzzy based models) during its initial prototyping phase. Using a deep learning model validation will be done using data acquired during the course of this project, this information will comprise of a known hand position, sEMG signal and OMG signal all correctly timestamped to provide the AI with all the tools needed to determine gesture. This approach will be taken to assess the suitability of using AI tools to identify and correct any interference or artifacts commonly seen in current sensors, and embedding new pattern recognition algorithms that can be implemented to improve movement detection and gesture control when compared with other currently used models of multidimensional arrays.

References

Clarius (2024). "Mobile Ultrasound Clarius." Accessed 08/04/24 Available at: https://clarius.com/

Cosoli, G., et al. (2021). "Wireless ECG and cardiac monitoring systems: State of the art, available commercial devices and useful electronic components." Measurement **177**: 109243.

Jiang, S., et al. (2021). "Emerging wearable interfaces and algorithms for hand gesture recognition: A survey." IEEE Reviews in Biomedical Engineering **15**: 85-102.

Muhammed, H. H. and J. Raghavendra (2015). "Optomyography (OMG): A novel technique for the detection of muscle surface displacement using photoelectric sensors." measurements **10**: 13.

Nakagawa, Y., et al. (2022). "Accuracy of a Professional Continuous Glucose Monitoring Device in Individuals with Type 2 Diabetes Mellitus." Clinical Journal of the American Society of Nephrology : CJASN **68**(1): E5-e10.

Pasadyn, S. R., et al. (2019). "Accuracy of commercially available heart rate monitors in athletes: a prospective study." Cardiovascular Diagnosis and Therapy **9**(4): 379-385.

Rice, A. and A. Kiourti (2023). "A Stretchable, Conductive Thread-Based Sensor Towards Wearable Monitoring of Muscle Atrophy." IEEE Transactions on Biomedical Engineering **70**(8): 2454-2462.

Rudolf, A., et al. (2022). Review of Smart Clothing with Emphasis on Education and Training. International Symposium "Technical Textiles - Present and Future". Edition 2021**:** 219-226.

Building & optimizing light-sheet microscope to analyse the coordination & control of critical cell behaviours driving gastrulation in the chick embryo.

S. Mubarak[1], C. J. Weijer[2], M. MacDonald[3]

[1] School of Life Sciences, University of Dundee, 2474488@dundee.ac.uk
[2] c.j.weijer@dundee.ac.uk
[3] School of Science and Engineering (Physics), m.p.macdonald@dundee.ac.uk

Abstract

Gastrulation signifies a key stage in early embryonic development of vertebrate embryos, where the embryo reorganizes from a one-dimensional epithelial layer into a complex multi layered structure. This involves the coordination of cell divisions, cell differentiation, cell shape changes, and highly organised large-scale movements of hundreds and thousands of cells in the embryo. During chick gastrulation, the prospective mesendoderm forms a crescent-shaped area at the posterior edge and the mesendoderm precursor cells move toward the midline of the epiblast to form a structure known as the primitive streak, from which cells ingress into the embryo and migrating out creating the inner layers. The tissue motions driving the formation of the primitive streak are caused by apical contraction and elongation along the opposite direction which leads to ingressions, and directional intercalations. The directional intercalations within the mesendoderm are related to extensive supracellular cables of phosphorylated myosin light chain (Rozbicki et al., 2015, Serrano Nájera et al., 2020).

To investigate these cell behaviours, state-of-the-art techniques are employed including recently developed fluorescently labelled transgenic chick lines, created in collaboration with the Roslin Institute, Edinburgh, alongside custom-built Digital Scanned Laser Light-sheet Microscopes (DSLM) which allows imaging in vivo for extended time periods with minimum light-induced damage coupled with sophisticated computational tools for image analysis.

The DSLM system, controlled by sophisticated software, consists of laser, an AOTF works as a high dynamic shutter that can control up to 8 wavelengths simultaneously, a scanner which generates the light-sheet and a high-sensitivity CMOS camera. Objectives are positioned at a 45-degree angle from the stage, and an automatic height adjustment done along the z-axis ensures continuous focusing on the uneven embryo surface (Figure 1). The AOTF is controlled by the camera, through a hardware connection minimizes photodamage by deviating the laser beam when the camera is not exposed, while the scanner triggers the camera and controls exposure time. This light-sheet microscopy technique allows optical sectioning of fluorescently labelled cells, producing volumetric images with high spatial and temporal resolutions. Chick embryos' transparency enables light penetration up to approximately 25 µm of tissue with minimal scattering, absorption, and optical aberrations before image quality diminishes.

The primary objectives of these investigations are two-fold: firstly, to understand the coordination of key cell behaviours in the epiblast through chemical and mechanical cell-cell signalling, utilizing chick embryos labelled with Actin reporter lifeact and MyosinIIA GFP knockin (ACTM1); secondly, to explore the mechanisms underlying cell ingression from the primitive streak and the signals regulating this process, employing chick embryos labelled with Actin reporter and nuclei (ACTN). Embryos are cultured according to Chapman et. al, 2001 and mounted in a dedicated chamber for overnight imaging (Weijer et al., 2015). The DSLM microscope scans the sample forward in laser of one colour (channel 1) and scanned back with the other colour (channel 2) for the same position (Figure 2). These investigations promise to deepen our understanding of embryonic development and open avenues for further exploration into characterizing myosin intercalations and nuclei ingressions during gastrulation.

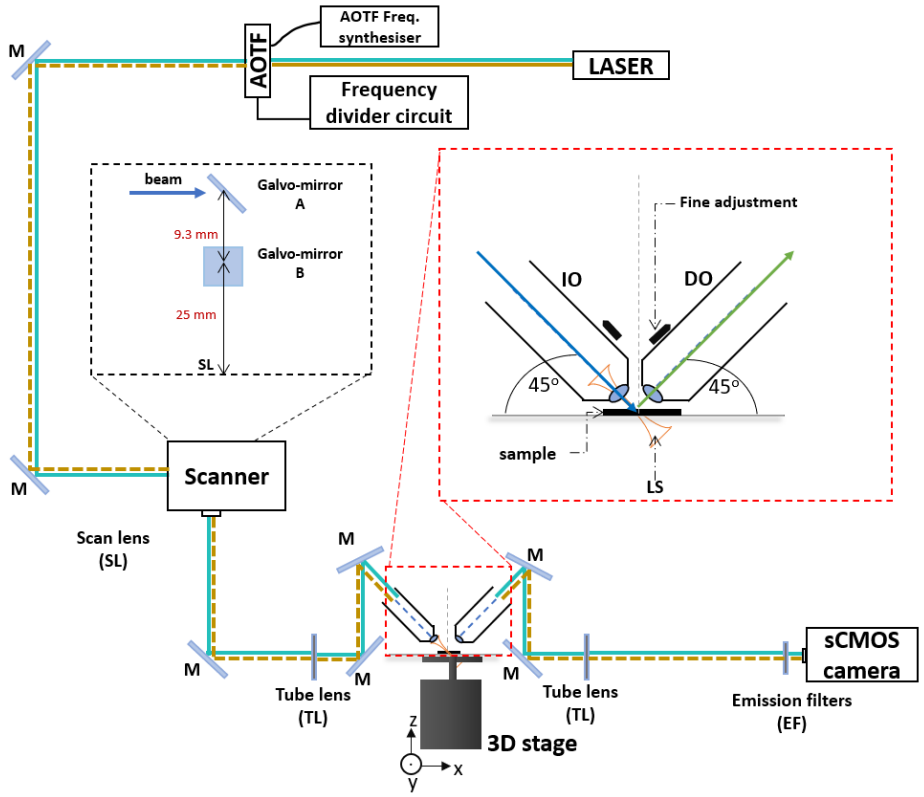

Figure 1: Labelled diagram of the dual colour DSLM (top view); sample and objectives (side view); the laser is dual-colour (488 nm and 561 nm); the AOTF works as a shutter controls up to 8 wavelengths simultaneously; frequency divider circuit is connected to the AOTF for an alternating clock-like signal.; M – Mirror; Scanner (consist of two galvo-mirrors scanning the beam along X and Z directions to generate the light-sheet); IO – Illumination Objective; DO – Detection Objective; 3D stage to position and move the sample

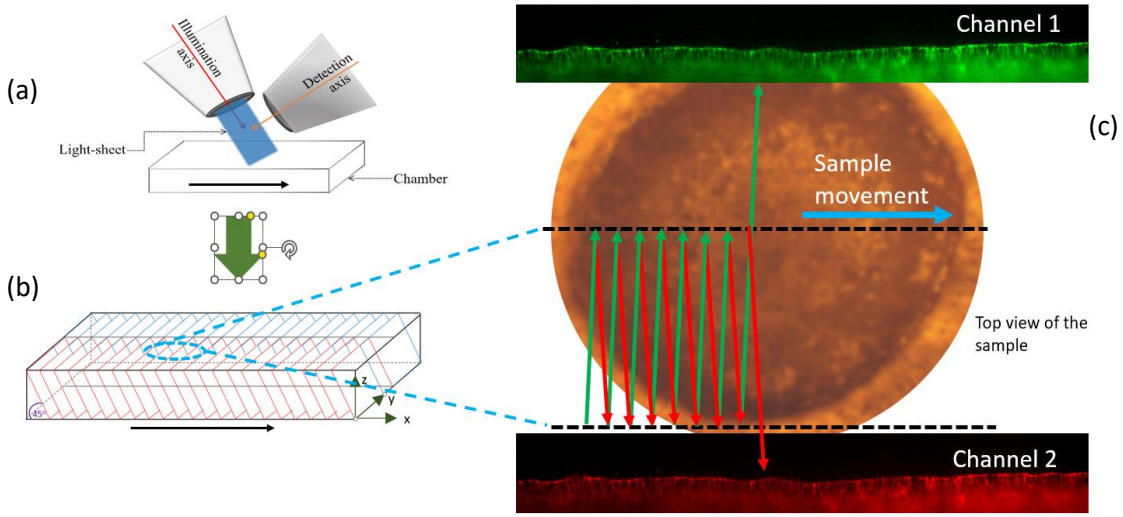

Figure 2: (a)Illumination of the light sheet. (b) Two overlapping scans (red and blue) cover the surface of the embryo. The raw images are 45° aligned. After the acquisition, images are transformed from 45° to 90°. (c) The sample is scanned forward in laser of one colour (channel 1) and scanned back with the other colour (channel 2) for the same position.

References

Chapman, S., Collignon, J., Schoenwolf, G. and Lumsden, A. (2001). An improved method for chick whole-embryo culture using a filter paper carrier. Developmental Dynamics, 220(3): pp.284-289.

Serrano Nájera, G. and Weijer, C. (2020). Cellular processes driving gastrulation in the avian embryo. Mechanisms of Development, 163: p.103624.

Rozbicki, E., Chuai, M., Karjalainen, A., Song, F., Sang, H., Martin, R., Knölker, H., MacDonald, M. and Weijer, C. (2015). Myosin-II-mediated cell shape changes and cell intercalation contribute to primitive streak formation. Nature Cell Biology, 17(4): pp.397-408.

Weijer, C., Rozbicki, E., Chuai, M. and Weijer, C., (2015). Technique for Liquid Culture of Early Chick Embryos Suitable for Long Term Live Imaging. Protocol Exchange.

Antimicrobial ZnO nanoparticle embedded Polyethersulfone synthesis using green chemistry

Yuhang Dong[1], Qi Zhao[2], Thomas Jones[3]

[1] Mechanical and Electronic Engineering, 2494951@dundee.ac.uk
[2] q.zhao@dundee.ac.uk
[3] t.d.a.jones@dundee.ac.uk

Abstract

The functionalisation of membranes by the embedding of nanoparticles (NP) can induce desirable properties such as antimicrobial activity, corrosion resistance and antifouling. In this study, we aim to make chemical sensing through the release of DNA via cell lysis possible by embedding antimicrobial ZnO NPs into polyethersulfone (PES).

The phase inversion method is a common technique in the processing of polymer-NP, however it uses costly and toxic solvents such as N-Methylpyrrolidone (NMP). Alternative, non-solvent phase inversion processing (NIPS) has been investigated to negate the use of these detrimental chemicals. Of particular interest is the use of dimethylacetamide (DML), which is typically used as a fertiliser, and has recently been demonstrated in the formation of PES membranes(C. Kahrs et al., 2020).

In this study, we used the non-toxic solvent DML instead of the traditional toxic solvents NMP during PES synthesis whilst incorporating antimicrobial ZnO nanoparticles into polyethersulfone. We characterized the antimicrobial properties of the synthesized polymers against Gram-positive S. aureus and Gram-negative antimicrobial E. coli using the bacterial staining method and spread plate method. Figure 1 shows typical fluorescence microscope images of live and dead E. coli on different surfaces after 1-hour co-culture.

A significant increase in the proportion of dead bacteria (stained red) on the surface of samples with added ZnO, was observed while the proportion of live bacteria (stained green) decreased noticeably. This demonstrates that the addition of ZnO nanoparticles enhances the antimicrobial performance of the polymer, indicating the successful embedding of ZnO nanoparticles into the PES membrane. Additionally, the results from both methods indicate that PES-ZnO polymer synthesized using DML exhibits excellent antimicrobial properties, validating the feasibility of using DML as a substitute for NMP.

In the next step, I plan to explore the optimal concentration of ZnO nanoparticles and embed other antimicrobial nanoparticles.

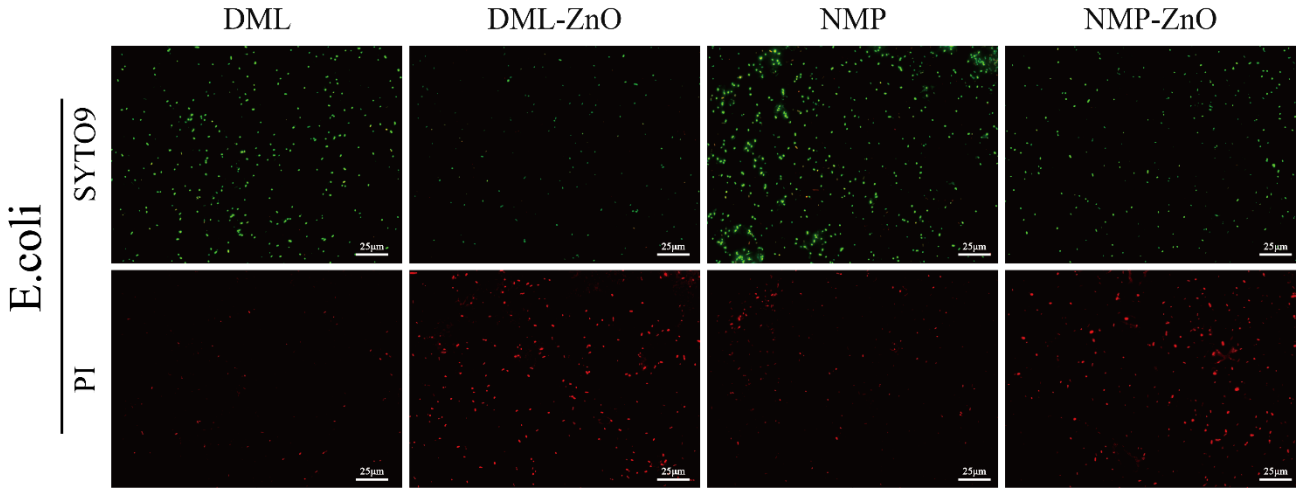

Figure 1: Typical fluorescence microscope images of live and dead E. coli after 1 hour coculture.

References

C. Kahrs, J. Schwellenbach, Membrane formation via non-solvent induced phase separation using sustainable solvents: A comparative study, Polymer (Guildf). 186 (2020) 122071.

North PHASE observation of the young cluster Tr37

Ferdinand Hollauf[1], Aurora Sicilia Aguilar[2]

[1] School of Science and Engineering, University of Dundee, Nethergate, Dundee DD1 4HN, 2616070@dundee.ac.uk
[2] SUPA, School of Science and Engineering, University of Dundee, Nethergate, DD1 4HN, Dundee, UK, a.siliciaaguilar@dundee.ac.uk

Abstract

The North-PHASE Legacy Survey is using the T80 telescope from the Javalambre Observatory (Spain) to study variability in several young clusters in the northern hemisphere. It produces time-resolved observations that enable us to 'use time to map space', identifying young variable stars and the processes that cause their variability, such as stellar spots, accretion variations, and occultations by circumstellar material. I will present the initial results for the cluster Tr37, which will be the subject of my PhD, having started in January 2024.

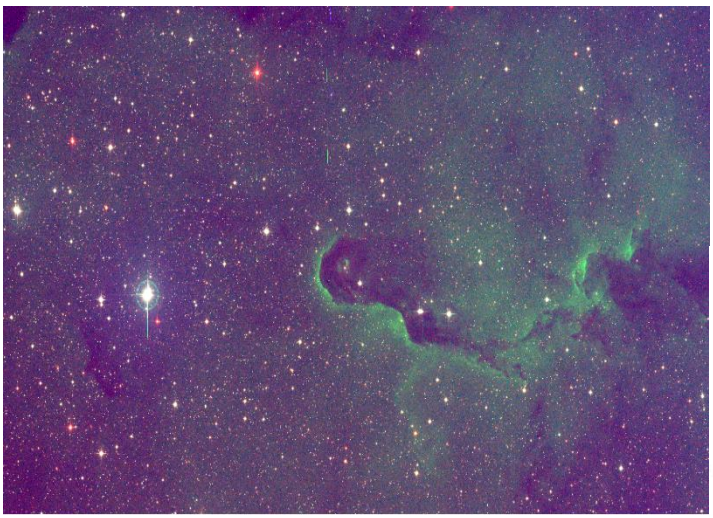

Figure 1: Part of the Trumpler 37 cluster,a region dominated by young stellar objects.This is a RGB image formed by combining images from filters rSDSS-r band wavelength(blue)),J0660-Hα band(green) and zSDSS-z band(red).On the left is a logo of the North PHASE legacy survey

University of Dundee

How can subtitled media be adapted for People with Aphasia?

Zihao You[1], Michael Crabb[2], Jacky Visser[3]

School of Science and Engineering (Computing), University of Dundee, Dundee, UK.
[1] 2565278@dundee.ac.uk
[2] m.z.crabb@dundee.ac.uk
[3] j.visser@dundee.ac.uk

Abstract

Recently, consuming media has become a vital part of people's daily lives under the rapid development of technology. Subtitles (i.e. white text on a black background located at the bottom centre of the screen as depicted in Figure 1) offer an alternative method for people to access the media's audio content, for the purpose of avoiding loud environments (S4C & RNID Cymru, 2001, p. 6) and assisting in secondary language acquisition (Perez et al., 2013, p. 720; Reynolds et al., 2022, p. 134). However, subtitled media consumptionis deemed to be more challenging for people with accessibility needs including blind and visually impaired (BVI) people (Nevsky et al., 2023, p. 94) and deaf and hard of hearing (DHH) people (Black, 2021, p. 82; Nevsky et al., 2023, p. 94; Reynolds et al., 2022, p. 134; S4C & RNID Cymru, 2001, p. 6; Ward & Shirley, 2019, p. 585). The community this research pinpoints is People with Aphasia (PWA), who also face significant challenges in consuming subtitled media, necessitating tailored solutions to improve their engagement and understanding.

Aphasia is a language and communication impairment caused by a stroke that affects understanding, speaking, reading, writing, and using numbers (Sherratt, 2023, p. 2). According to the Stroke Association, at least 350,000 people in the UK have aphasia (Stroke Association, n.d.). They struggle to regain a meaningful level of participation at home and the workplace (Dalemans et al., 2008, p. 1072; Parr, 2001, p. 274), which leads to social isolation (Ross & Wertz, 2003, p. 356) and depression (Hilari et al., 2010, p. 181). Researchersin recent years have been striving to develop solutions that support their communication (i.e. using augmentative and alternative communication (AAC) strategies to add to/replace the ordinary impaired communication methods) (Millar & Scott, 1998, p. 3; Moorcroft et al., 2018, p. 710) and language understanding (i.e. using eye-tracking technology to investigate eye movements) (Sharma et al., 2021, p. 1008).

Despite the number of works carried out in the domains of subtitled media adaptation to various communities of focus and communication support for PWA, none have attempted to address the intervention of subtitled media adaptation being used with the communities of aphasia (Nevsky et al., 2023, pp. 102-103). This doctoral work begins by conducting a systematic literature review that explores the challenges that different communities of focus face when consuming subtitled media and the works been carried out to mitigate against this (i.e. by altering the subtitles' position, location, content, or style). To better understand the needs of the community (PWA) the research is targeting, volunteering in a local charity (Chest Heart & Stroke Scotland) and participating in weekly workshops have been planned. The additional drop-in at workshops (Straight Talking Group sessions) run by the AAC research group within the department adds the benefits of the user-centred design phase later on, in which they will potentially get involved (e.g. via surveys, focus groups, etc.) in the design, development and evaluation of accessibility interventions that meet their requirements.

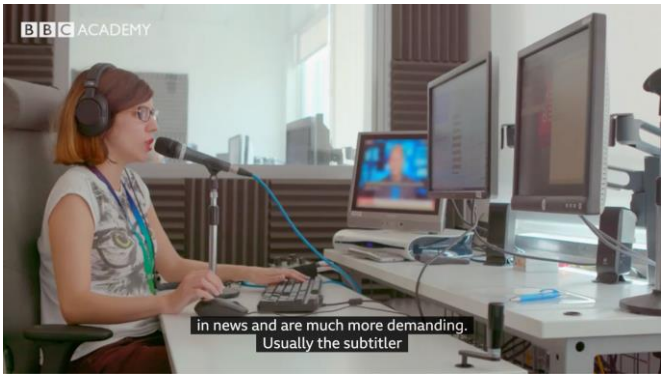

Figure 1: Traditional subtitle display on BBC.

References

S4C & RNID Cymru. (2001). Research Into the Demand for Welsh Language Subtitling in Wales, 6.

Perez, M. M., Van Den Noortgate, W., & Desmet, P. (2013). Captioned video for L2 listening and vocabulary learning: A meta-analysis. *System*, *41*(3), 720.

Reynolds, B. L., Cui, Y., Kao, C. W., & Thomas, N. (2022). Vocabulary acquisition through viewing captioned and subtitled video: A scoping review and meta-analysis. *Systems*, *10*(5), 134.

Nevsky, A., Neate, T., Simperl, E., & Vatavu, R. D. (2023). Accessibility Research in Digital Audiovisual Media: What Has Been Achieved and What Should Be Done Next?. In *Proceedings of the 2023 ACM International Conference on Interactive Media Experiences* (pp. 94, 102-103).

Black, S. (2021). The potential benefits of subtitles for enhancing language acquisition and literacy in children: An integrative review of experimental research. *Translation, Cognition & Behavior*, *4*(1), 82.

Ward, L., & Shirley, B. G. (2019). Personalization in object-based audio for accessibility: A review of advancements for hearing impaired listeners. *Journal of the Audio Engineering Society*, *67*(7/8), 585.

Sherratt, S. (2023). People with aphasia living alone: A scoping review. *Aphasiology*, 2. Stroke Association. (n.d.). *Aphasia awareness and the communications access symbol*. https://www.stroke.org.uk/stroke/effects/aphasia/aphasia-awareness

Dalemans, R. J., De Witte, L. P., Wade, D. T., & Van den Heuvel, W. J. (2008). A description of social participation in working-age persons with aphasia: A review of the literature. *Aphasiology*, *22*(10), 1072.

Parr, S. (2001). Psychosocial aspects of aphasia: whose perspectives?. *Folia phoniatrica et logopaedica*, *53*(5), 274. Ross, K., & Wertz, R. (2003). Quality of life with and without aphasia. *Aphasiology*, *17*(4), 356.

Hilari, K., Northcott, S., Roy, P., Marshall, J., Wiggins, R. D., Chataway, J., & Ames, D. (2010). Psychological distress after stroke and aphasia: the first six months. *Clinical rehabilitation*, *24*(2), 181.

Millar, S., & Scott, J. (1998). What is augmentative and alternative communication? An introduction. *Augmentative communication in practice: An introduction*, 3.

Moorcroft, A., Scarinci, N., & Meyer, C. (2018). A systematic review of the barriers and facilitators to the provision and use of low-tech and unaided AAC systems for people with complex communication needs and their families. *Disability and Rehabilitation: Assistive Technology,* 710.

Sharma, S., Kim, H., Harris, H., Haberstroh, A., Wright, H. H., & Rothermich, K. (2021). Eye tracking measures for studying language comprehension deficits in aphasia: A systematic search and scoping review. *Journal of Speech, Language, and Hearing Research*, *64*(3), 1008.

Investigating the degree of inclusion of educators in the development of Adaptive Learning system

Nawaf Alajlani[1], Micheal Crabb[2], Ian Murray[3]

[1] School of Science and Engineering, 2429039@dundee.ac.uk
[2] School of Science and Engineering, m.z.crabb@dundee.ac.uk
[3] School of Science and Engineering, i.r.murray@dundee.ac.uk

Abstract

The development of Adaptive Learning (AL) often involve different stakeholders among which educators are fundamental. The inclusion of educators has enjoyed towards ensuring the optimisation and effective deployment of adaptive learning. The role of educators remains important because of their role in the overall education system. Over time, their involvement has been discovered to include curriculum design, content integration, personalisation, learning evaluation adaptability amongst others. With this array of responsibility, it because evident that their inclusion should be of uttermost importance in the AL implementation. This research is aimed at investigating the degree of inclusion of educators in the development and implementation of AL.

As a background of this research was conducted, a core systematic review background was formed for this basis. The systematic review aimed to understand the involvement of stakeholders in creating adaptive learning systems. We conducted a systematic literature review to determine which stakeholder groups are actively involved in different stages of system creation. We found out that educators have insignificant involvement in the design, implementation, and evaluation of ALS creation. This work was published in the Journal of Computers in Education (2023) (Alajlani et al., 2023). Additionally, a qualitative approach was adopted for this research. This approach is hinged on the need to retrieve rich contextual information that elaborate the subjectivity and underlines the basis for a particular opinion. In the implementation, interview\workshop was used for data collection with preference for semi- structured type. The choice of the semi- structured was based on the ability to draft core questions that guided the interviews and prevented the sessions from going out of scop. It allowed the editing of the questions that were in-between the interviews to further enrich the quality of findings. Overall, twelve participants were involved in the research from the University of Dundee. This number emerged from purposeful sampling which focused on selecting participants That are lecturers and have deployed AL in the classroom. Overall, this research is expected to provide new information will be obtained regarding the role that educators played and their and their involvement in the development of AL. A better knowledge of the similarities between educational patterns will be achieved as a result of the findings, which will allow for the successful implementation of ALS. The findings will establish the degree of involvement together with typology of involvement. Also, this research will further cement the depth of impact within the overall development lifecycle.

References

Alajlani, N., Crabb, M. & Murray, I. A systematic review in understanding stakeholders' role in developing adaptive learning systems. *J. Comput. Educ.* (2023). https://doi.org/10.1007/s40692-023-00283-x

A brief investigation into the relationships of macroscopic and microscopic cortical bone traits in the elderly clavicle.

Corrina Wilson[1], Julieta Gomez Garcia-Donas[2], Craig Cunningham[3]

[1] Centre for Anatomy and Human Identification, School of Science and Engineering, University of Dundee, Dundee, Scotland, UK, corrinaqwilson@gmail.com
[2] jgomezgarciadonas001@dundee.ac.uk
[3] c.a.cunningham@dundee.ac.uk

Abstract

To build a biological profile for the deceased, the age of the skeleton must be estimated. Currently, humans are living longer and healthier lives than ever before. As age increases, various factors affect the skeletal system (such as health, disease, environment, etc.), and these factors will compound over time. Therefore, the older the individual is, the more difficult it is to assign age to the skeleton meaning that current aging methods tend to underestimate age in the elderly.

The most popular estimation methods are done macroscopically, with microscopic parameters mainly considered in very fragmented remains. A previous study showed there are age-related links between cortical and trabecular bone, but none have investigated the relationship between macroscopic and microscopic bone in the clavicle (Wilson, 2023). Thus, the aim of this study is to explore the combination of macro- and microscopic approaches in relation to age.

30 medial-end segments of the left clavicle were collected, cleaned, micro-CT scanned, examined, and made into slides. The three macroscopic parameters were measured from the surface of the sternal facet (Figure 1) following Falys and Prangle (2015). Micro-CT scans of the trabecular bone were assessed three-dimensionally through 5 parameters in two volumes of interest in the medial end (one superior, one inferior). 14 parameters were recorded from the cortical bone by following standard practices in the literature. Osteon frequency related variables were measured from 8 periosteal sampling areas on the histological sections, while cortical area related parameters were measured from the entire cross-section (Figure 2).

Significant correlations were found between the macro- and microscopic parameters, but none of the macroscopic parameters were linked to age. Surface porosity was significantly linked to OPD(I), On.Pm, Sup TB.N, and Sup Conn.D while osteophyte formation was linked to inferior Tb.N and Conn.D. The correlations were all weak to moderate (between 0.3 and 0.4). Surface topography was not significantly correlated to any other parameter.

The relationship between the macroscopic and trabecular parameters were all negative, suggesting that as the trabecular number and connectivity decreased, the overall porosity of the medial surface and the formation of osteophytes increased. As individuals age, bone quality decreases due to the deteriorating nature of senescence, meaning that the amount of bone present will decrease and become more porous. In the cortical bone, there was a positive correlation between macroscopic surface porosity and OPD(I) and a negative one between porosity and On.Pm. Increases in OPD, overall porosity, and decreased osteon perimeter are caused by the increased decoupled intracortical remodelling expected with age increasing. These parameters again align with the expected trends.

The results confirmed the expected age-related trends due to higher remodelling in bone in the elderly, although no correlation to age was reported for the macroscopic parameters. Future work is necessary on this subject to confirm the outcome obtained here in view to provide further knowledge to the growing research on age changes in the elderly.

Figure 1: Sternal end of clavicle

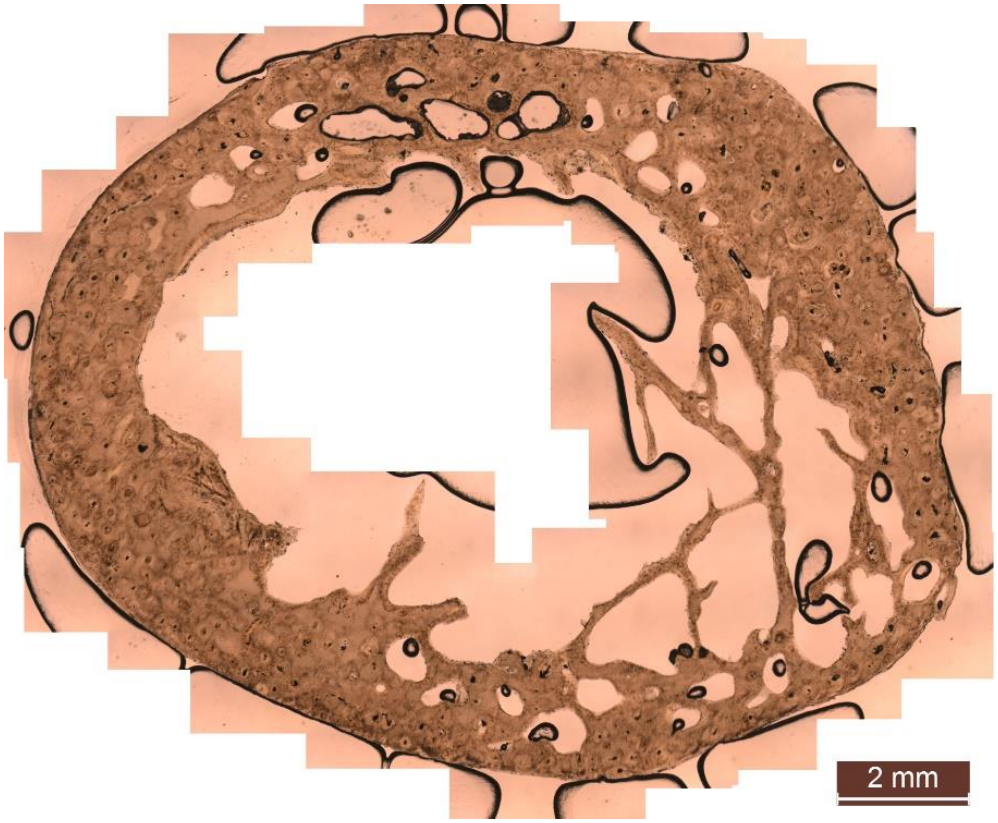

Figure 2: Stiched image of histological section (specimen 1509.3)

References

Falys, C.G. and Prangle, D. (2014) 'Estimating age of mature adults from the degeneration of the sternal end of the clavicle', *American Journal of Physical Anthropology*, 156(2), pp. 203–214. Available at: https://doi.org/10.1002/ajpa.22639.

Wilson, C.Q. (2023) *Exploring age-related trends in cortical and trabecular bone in an elderly Scottish sample: a pilot study on the clavicle*. Master of Science by Research. University of Dundee. Available at: https://dx.doi.org/10.15132/20000380.

Intracortical porosity in the clavicle of an elderly Scottish sample: exploring sampling areas within the cross-section

Kelly Watson[1], Dr Craig Cunningham[2], Dr Julieta G. García-Donas[3]

[1]Centre for Anatomy and Human Identification, School of Science and Engineering, University of Dundee, Scotland, UK, kmwatson@dundee.ac.uk, [2] c.a.cunningham@dundee.ac.uk, [3] jgomezgarciadonas001@dundee.ac.uk

Abstract

Cortical bone is the solid shell which surrounds the central marrow cavity and contains canals allowing the passage of vascular supply. Intracortical porosity is defined as the percentage of cortical bone occupied by pores (void spaces within the cortical area). Intracortical porosity can be affected by factors such as age, sex, biomechanics, and pathologies, which can lead to bone loss and ultimately fracture. The aim of this study is to determine any differences in intracortical porosity and related parameters between sampling areas of the clavicular cross-section, accounting for sex and intra-skeletal variability. This research was conducted on an elderly Scottish sample to provide further information on a population sample which has not yet been explored with regards to intracortical porosity, and an age-group that is underrepresented in literature and increasing in size globally.

Thirty Scottish individuals (15 males and 15 females) from the Centre of Anatomy and Human Identification were used (age range: 67-97 years). Thin sections were taken from the medial, midshaft and lateral segments of the clavicle. Ninety thin sections were processed, and photomicrographs were taken of all areas in each slide and stitched together to produce one complete image (Figure 1). Cross-sections were split into four quadrants for analysis which was carried out using Pore Extractor 2D to explore 5 parameters: cortical area (CA), total pore number (TPN), mean pore area (MPA), mean pore circularity (MPC) and cortical porosity (CP) (Figure 2). After data collection, statistical tests were used to compare sex and anatomical segment differences between quadrants.

Statistically significant sex differences were found between quadrants for all parameters in ≥1 of the anatomical segments. The mean rank values for males were usually higher than that of females except for a few locations. Regarding anatomical segment differences, laterally, significant differences between ≥3 quadrants were observed for all parameters in males, whereas in females, these differences were only observed in CA, TPN and MPA. In the medial segment, females produced no significant differences between quadrants. However, in males, significant differences were observed between quadrants for CP. In the midshaft, significant differences were found between quadrants for both sexes in CP and TPN.

Results produced by this study further contribute to knowledge on intracortical porosity in the clavicle with regards to sex and biomechanical forces applied along and within anatomical segments. The sex differences observed are likely due to factors including hormones, physical exercise rates and skeletal element size variation. Differences between segments are potentially explained by differences in biomechanical forces acting on different areas of the clavicle, as both medial and lateral segments have muscle attachments and articulations, however, these are absent in the midshaft segment.

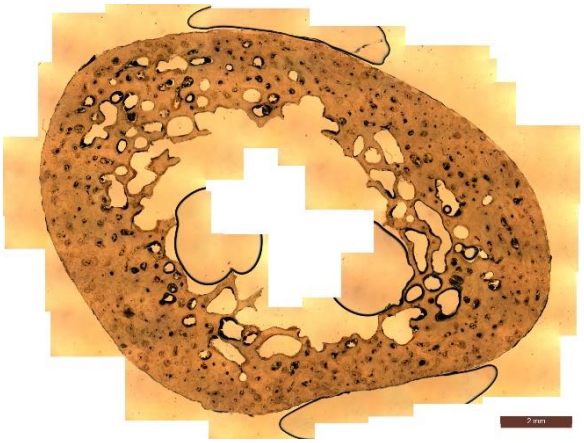

Figure 1: Stitched image of clavicular cross-section.

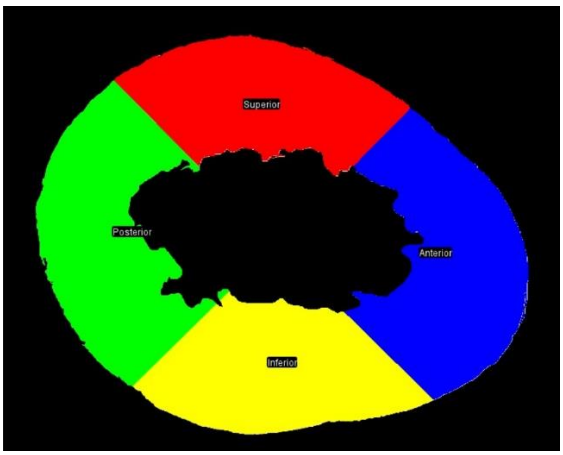

Figure 2: Clavicular cross-section separated into quadrants.

Electropolymerized InZnSe@PtAg quantum dots@molecularly imprinted polymer on screen-printed carbon electrodes for the ultrasensitive detection of NS1 dengue virus protein with smartphone-based sensing in saliva

Kirstie Isla Gray, Oluwasesan Adegoke

Leverhulme Research Centre for Forensic Science, University of Dundee, Dundee, DD1 4HN, UK,
KIG: 2606465@dundee.ac.uk
OA: o.adegoke@dundee.ac.uk

Abstract

Dengue virus (DENV) is still one of the most prolific diseases affecting many tropical parts of the world today. Current methods of DENV detection are slow, arduous, and not sensitive enough to detect low concentrations present in real samples. Electrochemical lab-on-a-chip biosensors have attracted much attention for disease detection in recent years due to their high sensitivity and selectivity. The use of semiconductor quantum dots (QDs) is very attractive in electrochemical biosensors due to their enhanced electrochemical behaviour compared to bulk materials.

The QDs can be deposited onto the surface of the electrode, increasing the electrochemical output, and creating a more sensitive biosensor. In this project, we used InZnSe@PtAg QDs in an electrochemical assay for DENV detection. This is a novel QD that does not contain Cadmium, which is common in synthesised QDs and is toxic, leading to a less biocompatible system. The ability of the newly synthesised InZnSe@PtAg QDs to increase the electrochemical signal of the electrode was validated.

For the biosensor to have affinity for DENV non-structural 1 (NS1) viral protein, this study synthesised a molecular imprinted polymer (MIP) using o-Phenylenediamine (OPD) as the monomer. The MIP was designed to have DENV NS1 shape specific cavities, to allow for a more selective biosensor. The difference between the electrochemical signal with and without the presence of the viral protein can be quantified to determine the concentration of viral protein in the sample. This is represented in Figure 1.

To improve the accessibility of the nanoprobe, it was developed on screen-printed carbon electrodes (SPCEs) and recovery studies were performed using smartphone-based technology. These recovery studies involved spiking saliva samples with the viral protein and measuring the electrochemical output. This shows that the developed biosensor is able to be used in complex biological samples and results can be easily accessed through the smartphone-based electrochemical system.

The developed assay was optimised and proven to be selective and sensitive for DENV NS1 VP using differential pulse voltammetry (DPV). The linear range of this developed nanoprobe was 1 fg/ml to 100 pg/ml and the calculated limit of detection was 1.36 pg/mL). The developed electrochemical nanoprobe demonstrates its suitability for point-of-care diagnosis of DENV.

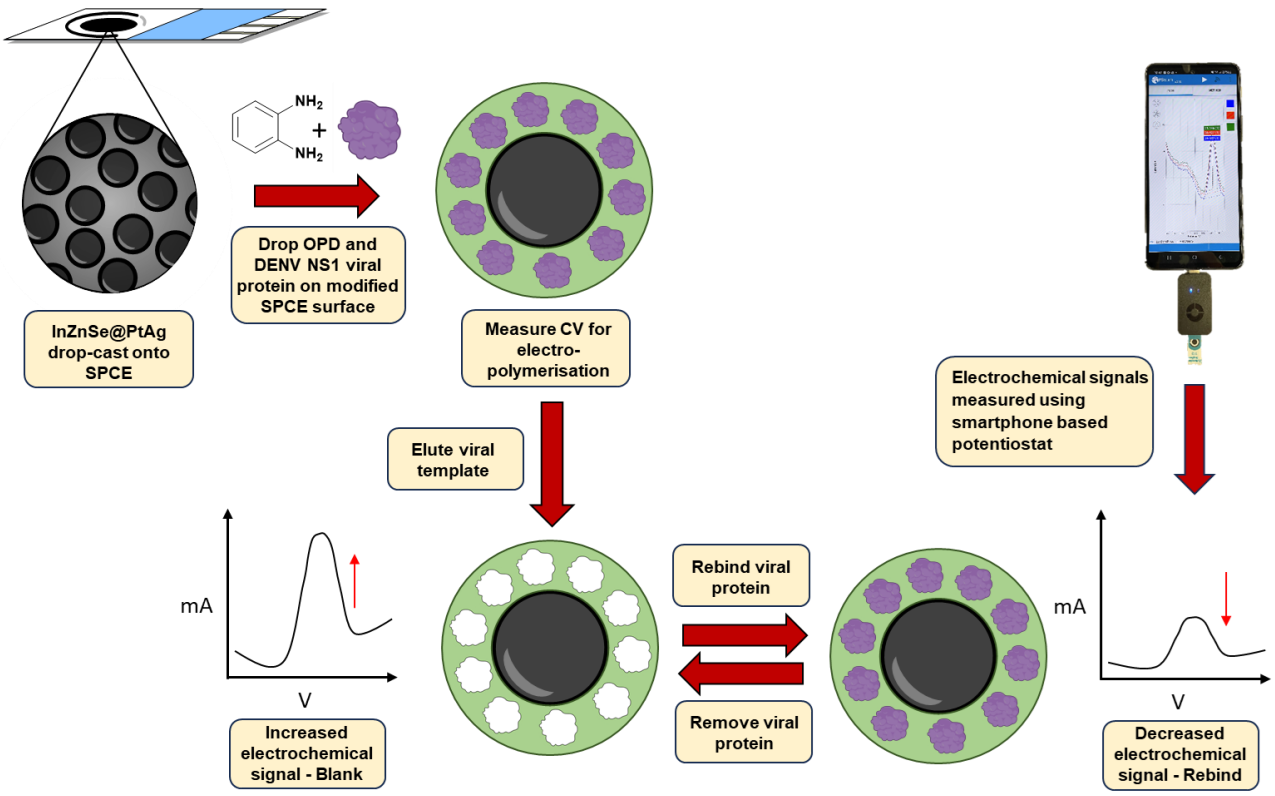

Figure 1: Graphical abstract of dengue virus detection using smartphone-based screen printed electrode technology

The Metabolic Profile of the Synthetic Cannabinoid Receptor Agonist ADB-HEXINACA using Human Hepatocytes, LC-QTOF-MS and Synthesized Reference Standards

Steven Baginski[1], Lorna Nisbet[2], Craig McKenzie[3], Henrik Gréen[4]

[1] Leverhulme Research Centre for Forensic Science, 2470295@dundee.ac.uk
[2] lnisbet001@dundee.ac.uk
[3] Leverhulme Research Centre for Forensic Science, University of Dundee; Chiron AS, craig.mckenzie@chiron.no
[4] Department of Biomedical and Clinical Sciences, Linköping University; Department of Forensic Genetics and Forensic Toxicology, National Board of Forensic Medicine, henrik.green@liu.se

Abstract

Forensic toxicology involves the detection and quantitation of drugs in biological samples and interpretation of the results, for legal purposes. Synthetic cannabinoid receptor agonists (SCRAs) are compounds that bind to and activate the cannabinoid receptors similarly to Δ^9-tetrahydrocannabinol (Δ^9-THC), the main psychoactive constituent of cannabis. However, SCRAs are substantially more potent and have been implicated in intoxications and deaths worldwide. Increasing our systematic understanding of SCRA metabolism supports clinical and forensic toxicology casework, facilitating the timely identification of analytical targets for toxicological screening procedures and confirmatory analysis. This is particularly important as new SCRAs continue to emerge on the illicit drug market. In this work, the metabolism of ADB-HEXINACA (ADB-HINACA, *N*-[1-amino-3,3-dimethyl-1-oxobutan-2-yl]-1-hexyl-1*H*-indazole-3-carboxamide), which has increased in prevalence in the United Kingdom and other jurisdictions, was investigated using *in vitro* techniques. The (*S*)-enantiomer of ADB-HEXINACA was incubated with pooled human hepatocytes over 3 hours to identify unique and abundant metabolites using liquid chromatography–quadrupole time-of-flight mass spectrometry (LC-QTOF-MS). In total, 16 metabolites were identified, resulting from mono-hydroxylation, di-hydroxylation, ketone formation (mono-hydroxylation then dehydrogenation), carboxylic acid formation, terminal amide hydrolysis, dihydrodiol formation, glucuronidation and combinations thereof. The majority of metabolism took place on the hexyl tail, forming ketone and mono-hydroxylated products. The major metabolite was the 5-oxo-hexyl product (M9), while the most significant mono-hydroxylation product was the 4-hydroxy-hexyl product (M8), both of which were confirmed by comparison to in-house synthesized reference standards. The 5-hydroxy-hexyl (M6) and 6-hydroxy-hexyl (M7) metabolites were not chromatographically resolved, and the 5-hydroxy-hexyl product was the second largest mono-hydroxylated metabolite. The structures of the terminal amide hydrolysis products without (M16, third largest metabolite) and with the 5-positioned ketone (M13) were also confirmed by comparison to synthesized reference standards, along with the 4-oxo-hexyl metabolite (M11). The 5-oxo-hexyl and 4-hydroxy-hexyl metabolites are suggested as biomarkers for ADB-HEXINACA consumption.

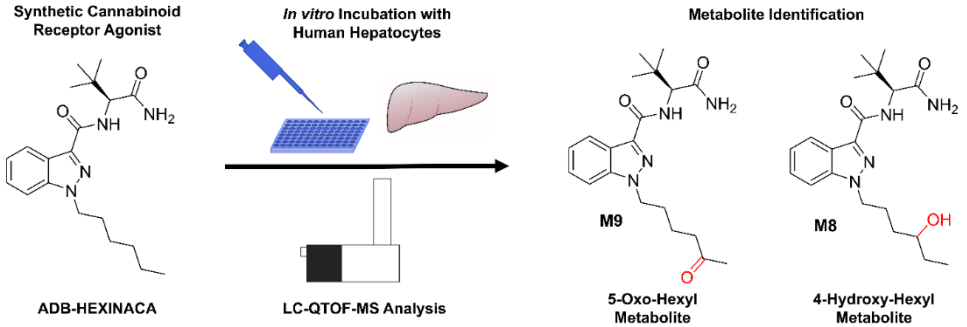

Figure 1: The two major metabolites produced following incubation of ADB-HEXINACA with human hepatocytes

Reference

Baginski SR, Rautio T, Nisbet LA, Lindbom K, Wu X, Dahlén J, McKenzie C, Gréen H. (2023). The metabolic profile of the synthetic cannabinoid receptor agonist ADB-HEXINACA using human hepatocytes, LC–QTOF-MS and synthesized reference standards. *Journal of Analytical Toxicology,* 47(9): 826–834.

Experimental study on the effects of installation parameters on vibratory driving performance of monopiles

Liqun Fang[1], Michael Brown[2], Matteo Ciantia[3]

[1] Geotechnical Engineering, 2497353@dundee.ac.uk
[2] M.J.Z.Brown@dundee.ac.uk
[3] m.o.ciantia@dundee.ac.uk

Abstract

The global offshore renewable energy provision is expected to grow from 8.8GW in 2022 to 35.5GW in 2027. Monopiles are a common foundation type for offshore wind turbines. In Europe in 2020, over 280 monopiles were installed, constituting more than 80% of the newly installed offshore wind turbines. The conventional installation method for monopiles is impact-driving where hammer blows are applied to the pile top periodically. This dynamic process may cause significant noise emissions and steel fatigue damage. Compared with the traditional impact driving installation methods for monopiles, vibratory driving is a promising alternative with advantages of rapid installation, low acoustic noise emission and limitation of stresses during driving. During the installation, a vibratory hammer is clumped to the top of the pile and induces the vibration of the pile. This process leads to the rearrangement of the soil particles and reduces the shaft friction and the base resistance to achieve the piling. However, uncertainties over drivability assessment and the vibration parameter effects on driving performance may lead to pile refusal before reaching target depth and low penetration velocities. This knowledge gap may prove a barrier to widespread adoption of purely vibration-based installation.

A series of preliminary 1g reduced scale tests were conducted to drive an instrumented model pile in dry medium-dense and dense sand. This research presents preliminary 1g model test results of an experimental model investigation into these uncertainties. A mini vibration unit with exchangeable eccentric masses was used to install the pile. The frequency and the force generated by the vibratory driver can be controlled by changing the eccentric masses and electrical power supplied, in which the driving performance under different vibration controls was recorded. The preliminary results indicate that the ultimate installation depth and the driving velocity are influenced by the combined factors of frequency and driving force, and it appears that frequency plays a more significant role in determining installation performance. The results of this study will be used to assist in the development and design of on-board centrifuge vibro-driving systems (in high g-level), further study in discrete element modelling (DEM) will apply the results as verification.

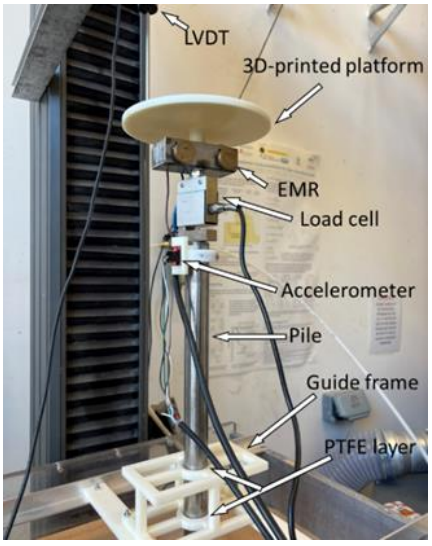

Figure 1: Experimental setup used for pile installation.

University of Dundee

Fluid-Solid Flow Transition in Mixed (Sand-Mud) Sediment: Enhanced Modelling of Sedimentation in Estuarine and Coastal Waters

Yi Yuan[1], Alan Cuthbertson, Tom Eaves

[1] School of Science and Engineering (Civil Engineering), University of Dundee, 2394028@dundee.ac.uk

Abstract

Sedimentation processes in natural estuarine or coastal sediment systems are normally divided into two regimes: (1) the hindered settling regime, where volumetric concentrations of polydisperse settling particles generate return flows and interactions through the faster-settling particles (e.g. sands) affecting the settling rates of other slower-settling particles (e.g. clays, muds)[1]; and (2) the consolidation regime, where the deposited sediment bed layers are compressed by the overburden at the top of the settling unit due to gravity[1]. Understanding of sedimentation processes has significant implications for improving predictions of mixed (i.e. sand-mud) sediment transport dynamics, as particularly crucial to maintaining navigation channels, ports, and harbours, understanding morphological evolution in affected coastlines, and preserving and enhancing sensitive habitats (e.g. mudflats).

In the simplest case, we can consider a well-mixed monodispersed suspension (i.e. cohesive clay suspension) settling within a vertical column under the assumption that (1) column side wall effects on sedimentation are negligible; (2) the two-phase (water-clay) suspension settles and compacts vertically in one-dimension; and (3) the initial clay concentration is lower than its gelling point ($\phi_0 < \phi_g$) at which a bed deposit layer structure begins to form. The full sedimentation process for a monodisperse suspension is shown schematically in *Figure 4*. At the initial time, the clay particle concentration is distributed evenly within the column [*Figure 4* (i)]. Throughout the sedimentation process [*Figure 4*: (ii)], the column region in which the hindered settling regime occurs progressively reduces in thickness as the interface separating the supernatant (clear water) layer from the settling suspension reduces in elevation, while the interface separating the hindered settling and consolidation regimes gradually increases in elevation from the bottom of the column. This increasing interfacial height, due to the deposition of clay particles from the hindered settling regime, is to some extent counteracted by compaction processes in the consolidation regime. Once the sedimentation processes has finished, the consolidated bed layer structure has a single interface separating from the upper clear water layer and the compacted clay deposit at the bottom [*Figure 4* (iii)]. The spatial and temporal transitions between these hindered settling and consolidation regimes are not currently well-understood or modelled, particularly when considering the sedimentation behaviour of bi-disperse and poly-disperse mixtures of cohesive (i.e. mud) and non-cohesive (i.e. sand) sediments. The aim of this project is therefore to develop a new integrated hindered settling – compaction model for multifractional sediments, accounting for polydisperse hindered settling and flow-driven compaction. This model development is informed and supported by laboratory experiments, conducted in a bespoke settling column, with the aim of improving the physical understanding and representation of hindered settling and compaction, and particularly the crucial fluid-solid regime transitions, for natural sediment mixtures during the sedimentation process.

Preliminary comparison of the monodispersed compaction model predictions and experimental measurements are presented in *Figure 5* for selected parametric runs. It is clearly shown that the model predictions correlate well with experimental measurement of the upper fluid-suspension interface for runs with lower initial settling heights ($h_0 \leq 0.165m$). However, the model slightly underpredicts the deposit height variations during the consolidation regime, including the final consolidated height, for runs with higher initial settling heights ($h_0 \geq 0.255m$). The main reason for this discrepancy is that characteristic physical parameters [i.e. gel point ϕ_g and permeability $k(\phi)$] of the clay suspension are calibrated based on the measurements with relatively low initial heights, meaning that the gravitational loading on the evolving layer structure is less than for runs with higher initial settling height. This may suggest that the calibrated linear behaviour between yield stress $\sigma_y'(\phi)$ and concentration ϕ near the gel point is only valid in the low-ϕ limit, with a non-linear relationship [$\sigma_y'(\phi) \sim \phi^2$] valid for higher fractional concentrations ϕ, the relation for which can be referenced from previous studies[2].

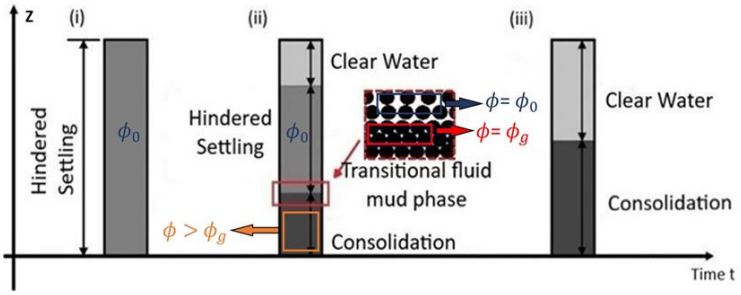

Figure 4: Geometry arrangements of well-mixed monodisperse suspension (low ϕ_0) settling with time lapses driven by gravity: (i) beginning of the settling (ii) intermediate state of the sedimentation process (iii) final deposit structure.

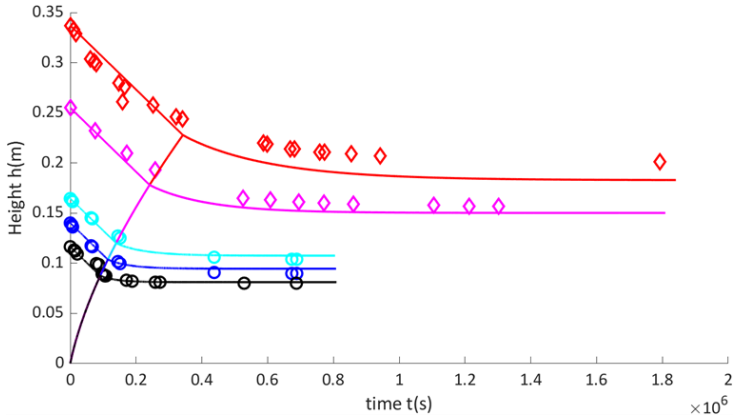

Figure 5: Model predictions (solid line) and experimental measurements (hollow points) of the fluid-sediment interface height over time using a suspended mixture of clays settling at different initial heights ($\phi_0 = 0.094$).

References

[1] TE SLAA, S., VAN MAREN, D. S., HE, Q. & WINTERWERP, J. C. (2015). Hindered Settling of Silt, Journal of Hydraulic Engineering, Vol. 141, No. 9.

[2] PATERSON, D. T., EAVES, T. S., HEWITT, D. R., BALMFORTH, N. J. & MARTINEZ, D. M. (2019). Flow-driven compaction of a fibrous porous medium," Physical Review Fluids, 4, Article 074306.

Feasibility of Polyvinyl Chloride's as a breast ultrasound phantom

Wadhhah Aldehani[1]

[1] School of Medicine & Biomedical Engineering, School of Science and Engineering

Abstract

Ultrasound phantoms are tools that mimic biological tissues, which allow the study of their reactions with ultrasound waves. Phantoms provide a controlled environment in which to test the performance of imaging modalities and to develop new methods. They can also be used to simulate different tissue types, allowing for more accurate testing. A standard biological breast soft tissue has a speed of sound of 1450 to 1540 (m/s) and an attenuation coefficient of 0.3 to 0.7 (dB/cm/MHz), while breast glandular tissue has a speed of sound 1430 to 1630 (m/s) and attenuation of 0.5 to 1.0 (dB/cm/MHz)[1,2].

Aim

This study aims to evaluate polyvinyl chloride (PVC) tissue mimicking material for breast phantoms in ultrasound B-mode.

Methods

A breast phantom was constructed from tissue mimicking material and analysed using ultrasound to assess its image quality. Various samples of PVC material were fabricated, each of which contains a different concentration of PVC and an additive. The process is split into two stages: lesion fabrication and background fabrication. In the lesion fabrication stage, the lesion is created with 8 x10^2 (PVC 8 and DOP 100), to simulate isoechoic pattern with 0% GP, hypoechoic pattern with 0.1% GP, and hyperechoic pattern with 2% and 4%. Whereas, to simulate the background, it was mimicked using 8 x10^2with 0.5% GP. The silicone mould is used to shape the lesions.

Results

Breast tissue samples was tested based on speed of sound, attenuation, acoustic impedance. Sample with 0.1% GP mimics breast glandular tissues with speed of sound of 1454 (m/s) and attenuation of 0.45 (dB/cm/MHz), while sample with 0.5% mimics breast fatty tissues with speed of sound of 1502 (m/s) and attenuation of 0.64 (dB/cm/MHz). However, samples with 2 and 4% GP mimic various types of breast lesions, with sound speed of 1578.11 and 1645.76 (m/s) and attenuation of 1.21 and 1.76 (dB/cm/MHz), respectively.

Conclusion

We have demonstrated that it is possible to fabricate ultrasound phantoms that reproduce the image characteristics of fatty breast tissue and typical breast lesions using low-cost materials that are widely available and stable at room temperature.

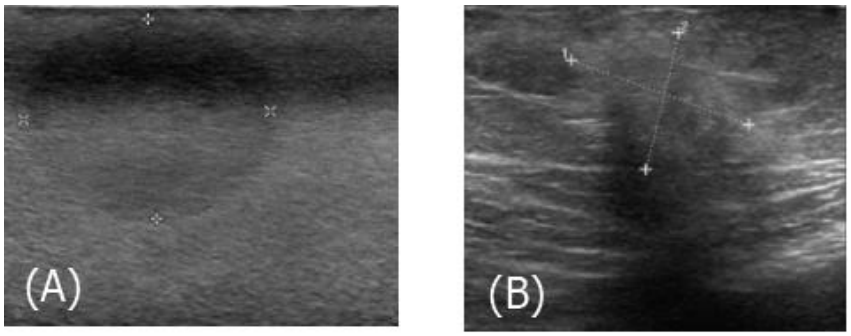

Figure 1. Comparison of phantom and real tissue images. (A) An ultrasound image of the simulated mammary glandular tissue produced with graphic powder at 0.1% concentration; (B) a real ultrasound breast image (hypoechoic area)*[3]*. A linear 5MHz transducer was used to acquire both images.

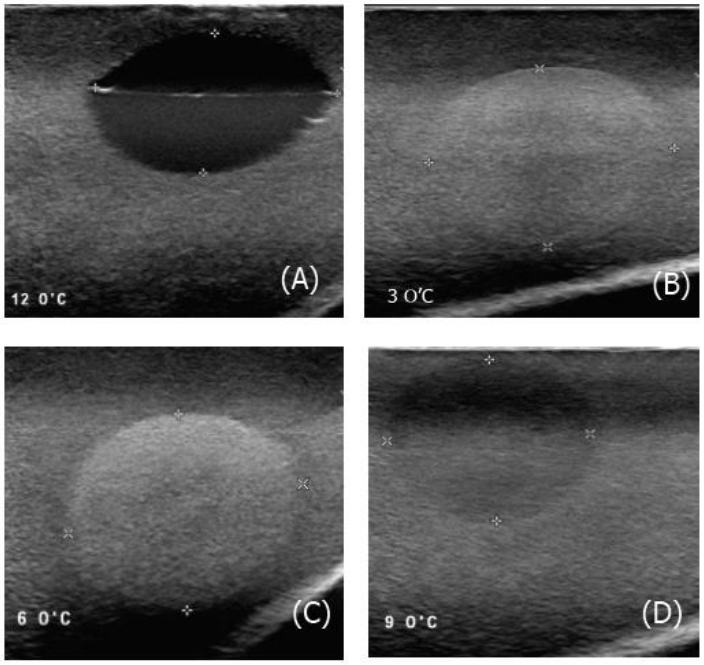

Figure 2. Ultrasound images of simulated lesions. These images were acquired with a 5 MHz linear transducer in samples with graphite powder concentrations of 0% in (A); 2%(B); 4% (C); and 0.1(D).

References

1. Fish, P. *Physics and Instrumentation of Diagnostic Medical Ultrasound*; Wiley: Chichester, 1990; ISBN 978-0-471-92651-1.
2. *Diagnostic Ultrasound*; Rumack, C.M., Levine, D., Eds.; Sixth edition.; Elsevier: Philadelphia, PA, 2023; ISBN 978-0-323-87797-8.
3. Ai, S.; M, R.; Ms, S.; B, N.; A, M. The Normal Types of Ultrasound Breast Morphology (Glandular Tissue and Fat Lobules) among Women of Different Age Groups in Golden Horses Health Sanctuary. *OMICS J Radiol* **2016**, *05*, doi:10.4172/2167-7964.1000243.

Advancing Prostate Cancer Treatment: The Role of Focused Ultrasoundand Sonodynamic Therapy

Muteb Alrashdi[1,3], Ghulam Nabi[1,3], James Joseph[2,3]

[1] Division of Imaging Sciences and Technology, School of Medicine, University of Dundee, Ninewells Hospital, Dundee,UK, 2439018@dundee.ac.uk

[2] Department of Biomedical Engineering, School of Science and Engineering, University of Dundee,UK

[3] Centre for Medical Engineering and Technology, University of Dundee, Dundee, UK

Abstract

Prostate cancer (PCa) is the most commonly diagnosed cancer in males worldwide and is thefifth leading cause of cancer-related deaths in men. Globally, this disease accounted for 1,414,249 newly diagnosed cases and 375,000 fatalities in 2020 (1).

Objectives

This poster will explore the therapeutic mechanisms, effectiveness, and potential clinicalintegration of focused ultrasound (FUS) and sonodynamic therapy (SDT) for PCa treatment.

Methods

Using the MEDLINE database, we review the literature and recent studies focusing on theapplication and outcomes of FUS and SDT in PCa.

Results

FUS is a procedure using focused ultrasound pulses to thermally ablate tissue at a focal point, causing temperature increases from 70 to 80°C. This can cause necrosis, cavitation, thermal tissue coagulation, and heat stress (2). SDT's therapeutic effect depends on activating the sonosensitizer via low- intensity focused ultrasound, which catalyzes reactive oxygen species production. The exact mechanism is unknown (3).

Recent meta-analyses highlight the therapeutic potential of Full Transurethral Urethral Surgery FUS in PCa. Whole-gland FUS, when combined with TURP, has shown satisfactory functional outcomes, including reduced prostate volume and improved urinary status (4). FUS is preferred over prostatectomy for urinary and sexual functions, with partial-gland FUS offering a safer profile and similar oncological effectiveness (5). Focal FUS therapies for intermediate-risk PCa have lower adverse effects on erectile, urinary, and bowel functions without compromising cancer control (6).

On the other hand, SDT has emerged as a targeted treatment with high selectivity for inducing apoptosis in PCa cells. The therapy's specificity stems from the preferential accumulation of sonosensitizers within cancercells, leading to the targeted generation of reactive oxygen species upon ultrasound activation and confiningcytotoxic effects to the tumour microenvironment. This selective mechanism minimises off-target effects and spares healthy tissue (7).

Preclinical research has validated the efficacy of SDT across various cancer types, including PCa, highlightingits versatility and potential as a broad-spectrum anticancer treatment. A notable study demonstrates SDT's capability to enhance chemotherapeutic sensitivity in paclitaxel-resistant PCa cells, potentially offering a new avenue for overcoming drug resistance by modulating the PI3K/Akt/mTOR pathway (8).

Conclusion

FUS and SDT represent promising advancements in PCa treatment. They offer targeted, less- invasive options with the potential to improve quality of life by minimising the side effects typical of more aggressive treatments. Preliminary evidence suggests that FUS and SDT may provide comparable oncologicaloutcomes with fewer complications, making them compelling alternatives in the management of PCa. Ongoing research is essential to confirm their efficacy and establish their role in clinical practice.

References

1. Leslie SW, Soon-Sutton TL, R IA, Sajjad H, Skelton WP. Prostate Cancer. StatPearls. Treasure Island (FL):StatPearls Publishing, Copyright © 2024, StatPearls Publishing LLC.; 2024.
2. Alkhorayef M, Mahmoud MZ, Alzimami KS, Sulieman A, Fagiri MA. High-Intensity Focused Ultrasound (HIFU)in Localized Prostate Cancer Treatment. Pol J Radiol. 2015;80:131-41.
3. Pan M, Hu D, Yuan L, Yu Y, Li Y, Qian Z. Newly developed gas-assisted sonodynamic therapy in cancertreatment. Acta Pharm Sin B. 2023;13(7):2926-54.
4. Pan Y, Wang S, Liu L, Liu X. Whole-gland high-intensity focused ultrasound ablation and transurethral resection of the prostate in the patients with prostate cancer: A systematic review and meta-analysis. Front Oncol.2022;12:988490.
5. He Y, Tan P, He M, Hu L, Ai J, Yang L, et al. The primary treatment of prostate cancer with high-intensityfocused ultrasound: A systematic review and meta-analysis. Medicine (Baltimore). 2020;99(41):e22610.
6. Javier-DesLoges J, Dall'Era MA, Brisbane W, Chamie K, Washington III SL, Chandrasekar T, et al. The state offocal therapy in the treatment of prostate cancer: the university of California collaborative (UC-Squared) consensus statement. Prostate Cancer and Prostatic Diseases. 2023:1-3.
7. Tong T, Lei H, Zhang S, Jiang D, Guan Y, Xing C, et al. Effective Sonosensitizer Delivery by Redox Sensitive Nanoparticles for Prostate Cancer Sonodynamic Therapy via Amplifying Oxidative Stress and Peroxidation. Adv Healthc Mater. 2022;11(23):e2201472.
8. Wu Y, Liu X, Qin Z, Hu L, Wang X. Low-frequency ultrasound enhances chemotherapy sensitivity and induces autophagy in PTX-resistant PC-3 cells via the endoplasmic reticulum stress-mediated PI3K/Akt/mTOR signaling pathway. Onco Targets Ther. 2018;11:5621-30.

University of Dundee

Other abstract submissions

(Not Presented at Symposium)

Generating Chest Radiology Report Findings using a Multimodal Method

Chenyu Wang[1], Stephen McKenna[2], Vladimir Janjic[3]

[1] School of Science & Engineering, 2410984@dundee.ac.uk
[2] s.j.z.mckenna@dundee.ac.uk
[3] vjanjic001@dundee.ac.uk

Automating radiology report generation from chest x-ray (CXR) images has attracted increasing interest due to its potential to improve clinical efficacy and efficiency, and alleviate the pressures faced by radiologists. Previously reported methods [1][2][3] tend to be unimodal, relying solely on the extraction of visual information from images to generate radiology report text. These techniques, while innovative, overlook the potential benefits of incorporating available textual data in a multi-modal approach.

The indications section of a radiology report is written before the CXR is acquired; it describes the referring clinician's reasons for requesting the CXR along with relevant aspects of the patient's history. We propose to use multi-modal deep learning, leveraging both radiology images and indication text, for generation of radiology report findings text. We extend two existing methods, R2Gen [2] and CvT2DistilGPT2[3], using this approach. As shown in Figure 1, the model architecture comprises three primary components: an image encoder, a text encoder, and a text generator. The image encoder is tasked with extracting visual features from radiology image(s). The text encoder focuses on extracting textual features from the indication text. The text generator utilizes a transformer-based architecture to generate the final report findings. It is fine-tuned, conditioned on the extracted visual and textual features.

We evaluated methods on two publicly available datasets, MIMIC-CXR [4] and IU X-ray [5]. Experimental results demonstrate that the incorporation of indications text in our multi-modal approach enhances the performance. Furthermore, our extension of CvT2Distil-GPT2 exceeds the performance of all the reported unimodal methods.

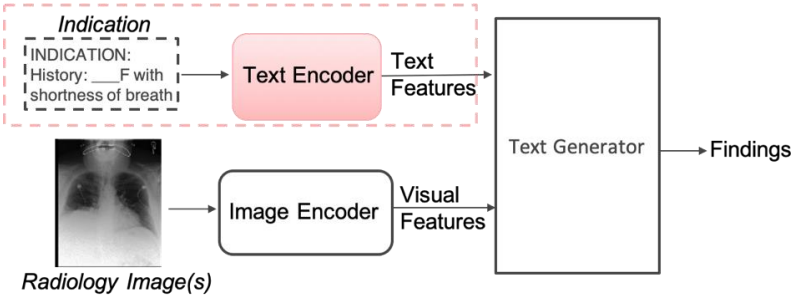

Figure1: Proposed multi-modal framework for automatic radiology report generation.

References

[1] Mingjie Li, Bingqian Lin, Zicong Chen, Haokun Lin, Xiaodan Liang, and Xiaojun Chang. Dynamic graph enhanced contrastive learning for chest x-ray report generation. In Proc. IEEE/CVF Conf. Computer Vision and Pattern Recognition, 3334–3343, 2023.

[2] Zhihong Chen, Yan Song, Tsung-Hui Chang, and Xiang Wan. Generating radiology reports via memory-driven transformer. In Proc. Conf. Empirical Methods in Natural Language Processing (EMNLP), 1439–1449, 2020.

[3] Aaron Nicolson, Jason Dowling, and Bevan Koopman. Improving chest x-ray report generation by leveraging warm starting. In Artificial Intelligence in Medicine, volume 144, page 102633. Elsevier, 2023.

[4] Alistair EW Johnson, Tom J Pollard, Nathaniel R Greenbaum, Matthew P Lungren, C Deng, Yifan Peng, Zhiyong Lu, Roger G Mark, Seth J Berkowitz, and Steven Horng. MIMIC-CXR-JPG, a large publicly available database of labeled chest radiographs. arXiv–1901, 2019

[5] Dina Demner-Fushman, Marc D Kohli, Marc B Rosenman, Sonya E Shooshan, Laritza Rodriguez, Sameer Antani, George R Thoma, and Clement J McDonald. Preparing a collection of radiology examinations for distribution and retrieval. In J. Am. Medical Informatics Assoc., volume 23, pages 304–310. Oxford University Press, 2016.